PHYSIOLOGY AND

PHARMACOLOGICAL STUDIES OF INSECT CALCIUM CHANNELS

a thesis presented by

HUGH ANTHONY PEARSON

for the degree of Doctor of Philosophy in the University of
London.

Department of Pharmacology, Royal Free Hospital School of
Medicine.

May 1990

ProQuest Number: 10611096

ProQuest 10611096

ABSTRACT

In this study the physiology and pharmacology of insect Ca^{2+} channels has been investigated using two preparations. In a skeletal muscle preparation from larvae of the moth _Plutella xylostella_, all or none action potentials were studied in the presence of TEA. These action potentials were Ca^{2+}-dependent as was shown by the decline in amplitude and maximum rate of rise of the action potential when the extracellular Ca^{2+} concentration was reduced, abolition in Ca^{2+}-free saline and block by inorganic Ca^{2+} channel blocking agents. Furthermore, TTX had no effect on the action potential.

Removal of Cl^- ions from the external medium resulted in a decrease in the maximum rate of rise of the action potential, suggesting the involvement of inward Cl^- currents. However, the Cl^- channel blocker ethacrynic acid was without effect.

The organic Ca^{2+} channel antagonists of all 3 classes had no effect on the action potential suggesting that L-type channels were not involved. Furthermore, Lambert-Eaton myasthenic syndrome IgG had no effect on the action potential suggesting antigenic differences to L-type calcium channels. Ryanodine greatly prolonged the action potential possibly due to a decrease in release of Ca^{2+} from intracellular stores, while the antihelminthic agent avermectin, although causing changes in the passive properties of cells had no effect on the action potential indicating a lack of action on insect calcium channels.

To investigate neuronal Ca^{2+} channels, cells from

thoracic ganglia of the locust _Schistocerca gregaria_ were studied under whole cell patch clamp. Using 10mM Ba^{2+} or Ca^{2+} as the charge carrier, large biphasic currents were stimulated by depolarisation from a holding potential of -80mV. These currents were unaffected by replacement of external Na^+ with choline and thus were not carried by TTx-insensitive Na^+ currents. The two current components (sustained and transient) showed the same steady state inactivation kinetics, but could be separated by $10\mu M$ Cd^{2+} which selectively blocked the sustained current. For the organic antagonists, verapamil inhibited both components of current while nitrendipine was without effect. Single channel recordings of Ca^{2+} channels proved to be difficult, the only channel seen appearing to have transient characteristics. These data suggest that the channels in both skeletal muscle and nerve of insects do not readily fit into the pharmacological classification of L-, N- and T-type Ca^{2+} channels used in many vertebrate systems.

Finally, ryanodine, avermectin and the pyrethroids S-bioallethrin and deltamethrin were found to have no effects on Ca^{2+} channels in locust neurones.

CONTENTS

    a) Insect Calcium Channels

    b) Vertebrate calcium channels

    c) Role of calcium channels in excitation-contraction
coupling in skeletal muscle.

    d) Calcium channel structure

    e) Pharmacology of calcium channels

    a) Preparation of Plutella muscle fibres for
intracellular recording.

    b) Salines used with Plutella

    c) Electrophysiological recordings

    d) Drug and antibody preparation and application

    e) Analysis of action potentials

    f) Presentation of data

LIST OF TABLES

choline substitution on calcium channel currents

Table 4.2   Summary of properties of calcium channels in Plutella muscle and locust neurone.

LIST OF ILLUSTRATIONS

9

CHAPTER 1

GENERAL INTRODUCTION

The work presented in this thesis describes experiments aimed at investigating the physiology and pharmacology of calcium channels in insect skeletal muscle and neurones. As a potential target site for rational pesticide development, calcium channels have so far been overlooked, and the exploitation of differences between insect and vertebrate calcium channels may give rise to the development of more specific pesticides than we already posess.

Insect calcium channels

Two preparations were used in this study; a skeletal muscle preparation from larvae of the moth <u>Plutella xylostella</u>, and a neuronal preparation from the thoracic ganglia of the locust <u>Schistocerca gregaria</u>.

As far as this study is concerned, an important difference between vertebrate and insect skeletal muscle is the ionic basis of the muscle action potential. In vertebrates, nerve stimulation leads (via transmitter release) to depolarisation of the postsynaptic muscle fibre. Voltage dependent sodium channels which can be blocked by tetrodotoxin (TTx) are activated by this depolarisation and the resulting increase in sodium conductance gives rise to an 'all-or-none' action potential which is propagated throughout the skeletal muscle membrane. In contrast, action potential propogation in a number of insect species is not thought to involve voltage-dependent sodium channels.

Although stimulation of excitatory nerves results in an electrical response that is similar throughout the muscle fibre due to its multiple innervation, direct stimulation of the same fibre results in graded responses that do not propagate throughout the muscle fibre (Belton, 1969, Deitmer, 1977b). This graded response can be converted to an all-or-none, propagating action potential when potassium channel blockers such as tetraethylammonium (TEA) are used (Fukuda and Kawa, 1977, Ashcroft, 1981, Miyamoto et.al., 1984, Washio, 1972), suggesting the existence of a high density of rectifying potassium conductances in the muscle membrane. Removal of sodium ions from the bathing medium or the presence of TTx have little effect on action potentials (in the presence of TEA) in insect muscles (Fukuda et al.,1977, Washio, 1972, Deitmer and Rathmeyer, 1976, Ashcroft, 1981). However, when calcium is removed, action potentials are abolished, while a reduction in the extracellular calcium concentration results in changes in the amplitude and rate of rise of action potentials similar to those predicted by the Nernst equation assuming that the muscle cell membrane becomes permeable to calcium during the action potential (Fukuda et al., 1977, Washio, 1972, Miyamoto et al., 1984, Deitmer and Rathmeyer, 1976, Ashcroft, 1981). This suggests that Ca^{2+} channels underly these action potentials in insects. Further evidence for this is suggested by block of the action potentials by Ca^{2+} channel antagonists such as Co^{2+}, Cd^{2+} and La^{3+} (Deimer and Rathmeyer, 1976, Ashcroft,1981) and the fact that these action potentials can be triggered in salines where Ca^{2+} has

14

been replaced by Ba^{2+} or Sr^{2+} (Fukuda et al.,1977, Washio, 1972, Deitmer and Rathmeyer, 1976, Ashcroft,1981). Voltage clamp studies of insect skeletal muscle fibres have also confirmed the existence of Ca^{2+} channels in a number of species (Ashcroft and Stanfield, 1982a,1982b, Yamamoto et al., 1981, Yamamoto and Washio, 1981, Salkoff and Wyman, 1983). For instance, the inward current seen in Carausius morosus muscle fibres (Ashcroft & Stanfield, 1982a, Ashcroft & Stanfield, 1982b) was found to be activated at test potentials positive to approximately -40mV from a holding potential of -60mV. Maximum inward current was seen at test potentials to approximately 0mV, above which potential the inward current declined, reversing at an apparent (since leakage currents were not subtracted) test potential of approximately +35mV. The current was increased by increasing the Ca^{2+} concentration in the external saline and was blocked by La^{3+} and Cd^{2+} indicating that it was indeed a calcium current. The current was also found to be inactivating during the course of a voltage step, this decay being attributed to Ca^{2+}-dependent processes. In contrast to Carausius where the calcium channel was found to be impermeable to sodium ions, the inward calcium current of Tenebrio molitor was found to show a small degree of Na+ permeability (Yamamoto et.al., 1981, Yamamoto & Washio, 1981). In this preparation the inward current was activated at a test potential of approximately -20mV, reaching a maximum at -5mV. This current was also seen to have two phases to its decay and was completely blocked by Co^{2+} at a concentration of 15mM. The dorsal flight muscle of

<u>Drosophila melanogaster</u> (Salkoff & Wyman, 1983) shows calcium currents which decay rapidly and completely when Ca^{2+} is used as the charge carrying ion and choline has been substituted for Na+ in the extracellular saline. If Na+ is also present in the solution however, two phases of current, one rapidly inactivating and one slowly inactivating are seen. With Ba^{2+} as the charge carrier the inward current is only very slowly inactivating, and resembles the L-type current seen in vertebrate neurones. The current in all cases activates at a test potential of approximately -50mV and reaches a maximum at -20mV. Thus the currents underlying Ca^{2+}-dependent action potentials in skeletal muscle fibres from a number of different insect species appear to be slightly different in some respects, but all show decay when Ca^{2+} is used as the charge carrier and activate over a similar test potential range.

The second preparation used to investigate insect Ca^{2+} channels in this study was the neuronal somata freshly dissociated from the thoracic ganglia of the locust, <u>Schistocerca gregaria</u>. Certain cell bodies from these ganglia produce action potentials that are carried by both Na+ and Ca^{2+} and which can be blocked by Co^{2+} (Goodman & Heitler, 1979). In peripheral neurosecretory neurones from <u>Carausius</u>, action potentials in the nerve cell body are carried solely by Ca^{2+} (Orchard, 1976). Byerley and Leung (1988) have recently described voltage dependent calcium channels in embryonic cultures of neurones from <u>Drosophila</u>. In the latter preparation calcium currents were found to be blocked by Cd^{2+} and reduced by high concentrations of

16

verapamil but were unaffected by dihydropyridines and benzothiazepines.

Calcium channels from brain membranes of <u>Drosophila</u> have been reconstituted into planar lipid bilayers resulting in Ba^{2+}-permeant channel activity that can be blocked by Co^{2+} (Pelzer et al., 1989a). Different types of Ca^{2+} channel are present in this preparation which are either insensitive to verapamil and dihydropyridines or sensitive to only one of these classes of Ca^{2+} channel antagonist.

Biochemical studies on the binding of organic calcium channel antagonists to these membranes from <u>Drosophila</u> brains reveal significant differences between the vertebrate and insect preparations. Drosophila brain membranes show very high affinity binding for phenylalkylamines which can be inhibited by benzothiazepines as in vertebrates (Pauron et al., 1987, Greenberg et.al, 1989). The dihydropyridines only bind weakly to such membranes and do not inhibit the binding of phenylalkylamines, suggesting perhaps that the binding site for dihydropyridines is on a different type of Ca^{2+} channel to that which binds the phenylalkylamines (Pelzer et al., 1989a).

Vertebrate calcium channels

Although insect Ca^{2+} channels have not been characterised in detail, more work has been done on Ca^{2+} channels in vertebrates (see e.g. W.-Wray et.al., 1989). There are at least 3 different types of calcium channels underlying the Ca^{2+} currents seen in both neurone and muscle for vertebrates. These channel types were first described by Nowycky, Fox and Tsien (1985a) in sensory neurones

cultured from chick dorsal root ganglia and have been designated L, N and T. This classification is based on activation thresholds, inactivation rate and sensitivity to antagonists. The properties of these channels are given in Table 1.1 and are discussed below.

The T-type current is activated by small depolarisations (to test potentials of -50mV) from strongly negative holding potentials (-70 to -100mV). It is transient in nature, with a time constant of inactivation of milliseconds. With stronger depolarisations (to e.g. 0 or +10mV) from the same holding potential, N- and L-type currents become activated. The N-type current is transient (but inactivates more slowly than the T-type current), while the L-type current is sustained in nature. With more positive holding potentials (e.g. -40mV) the L-type current can be seen in isolation from both N- and T-type currents which are inactivated.

The single channel basis of the whole cell currents has been investigated (Carbone and Lux, 1984, 1987a, Nowycky et.al., 1985a) and shows that each current type is mediated by distinct and separate calcium channels. Channels mediating T-type currents have a lower conductance than L-type, with N-type of intermediate conductance (Table 1.1). T- and N-type channels tend to open in bursts near the beginning of a voltage step giving rise to the transient whole cell current. L-type channels on the other hand are usually active throughout the duration of a voltage step and consequently give rise to sustained currents. The different channel types also differ in terms of the degree of block

Table 1.1

Channel Type	Approximate activation threshold (mV)	Inactivation Rate	Single channel conductance (110mM Ba^{2+})	Sensitivity to block by:		
				organic Ca^{2+} channel antagonists	Cd^{2+}	w-Conotoxin
L	0	slow	25pS	sensitive	sensitive	sensitive
N	+10	intermediate	13pS	insensitive	sensitive	sensitive
T	-50	fast	8pS	insensitive	resistant	insensitive

Properties of Ca^{2+} channel types in vertebrate neurones, taken from Nowycky et al, 1985a, McCleskey et al., 1987 and Narahashi et al, 1987. These properties vary slightly between preparations and species.

19

caused by inorganic cations (e.g. Co^{2+}, Cd^{2+}, see Table 1.1) and by the organic Ca^{2+} channel antagonists such as dihydropyridines, which selectively modulate L-type currents.

Calcium currents are modulated by a variety of mechanisms (for reviews see Reuter, 1983, Reuter, 1987, Tsien et al., 1988, Eckert and Chad, 1984, Kostyuk, 1980, Dunlap et al., 1987, Dolphin, 1987). As far as accurate measurement of calcium currents is concerned the most important modulatory influences are those which cause inactivation of currents either short-term during the voltage step which elicits them or more slowly during the course of an experiment ("run down"). Short term inactivation of Ca^{2+} currents is now believed to involve both the effects of voltage and of calcium ions which enter through the channels themselves (Eckert and Chad, 1984, Ganitkevitch et al., 1987, Kass and Sanguinetti, 1984, Lee et al., 1985). L-type channels are highly susceptible to run-down, i.e. inactivation over the long term, particularly when the whole cell patch clamp technique is used. This is caused by a loss of agents in the cytoplasm which phosphorylate the channel, phosphorylation being required for its normal functioning (Chad and Eckert, 1986, Kameyama et al., 1988). The effects of dephosphorylation can be overcome to some degree by the addition of cAMP, ATP and Mg^{2+} to the patch pipette (Fedulova et al., 1985). In cardiac muscle cells, this phosphorylating mechanism may represent a means of modulating the L-type calcium current via β-adrenoceptors coupled to cAMP-dependent protein kinase

20

systems (Osterrieder et al., 1982, Cachelin et al., 1983, Trautwein et al., 1987).

The role of Ca^{2+} channels in excitation-contraction coupling in skeletal muscle

The sarcoplasmic reticulum and transverse-tubules of vertebrate skeletal muscle play an important role in excitation-contraction coupling. When the t-tubule membrane is depolarised by the muscle action potential, calcium is released from the sarcoplasmic reticulum, the elevated intracellular calcium then gives rise to muscle contraction (e.g. Constantin, 1975). The regions of muscle cell membrane which form the t-tubules are rich in binding sites for the dihydropyridine class of compounds suggesting a high density of Ca^{2+} channels, and Ca^{2+} entering the cells through these channels might be expected to give rise to Ca^{2+} release from the sarcoplasmic reticulum (Meissner, 1984 and Meissner et.al., 1986). However, block of calcium entry through t-tubule calcium channels does not prevent contraction in vertebrate skeletal muscle (Gonzales-Serratos at.al., 1982 and Knudson et al., 1986), indicating that Ca^{2+} entry through these channels is not their main physiological function. The function of these channels could be as a 'voltage sensor' in the membrane so that an action potential in the t-tubule triggers Ca^{2+} release from the sarcoplasmic reticulum (Schneider and Chandler, 1973, Beam and Knudson, 1988, Beam et al., 1989, Schwartz et al., 1985). Studies on mice suffering from muscular dysgenesis show that excitation-contraction coupling is severely disrupted in these animals. Action potentials and the sarcoplasmic

uptake of Ca^{2+} in dysgenic muscle fibres are unaffected but sarcoplasmic release of Ca^{2+} does not occur. However, when the muscle fibres of dysgenic mice are made to express a subunit of the purified calcium channel using cDNA expression techniques excitation-contraction coupling is restored (Tanabe et al., 1988). It has therefore been suggested that the 'voltage sensor' is contained within the t-tubule calcium channel and is connected to the calcium release channel (the 'ryanodine receptor') in the sarcoplasmic reticulum (Beam et al., 1989).

Little is known about the role of the calcium channel in excitation-contraction coupling in insects. The insect sarcoplasmic reticulum is well developed, and is particularly dense in regions adjacent to the neuromuscular junction (Belton, 1969). The amount of sarcoplasmic reticulum present in a given muscle fibre appears to be dependent on the type of contraction (either phasic or tonic) that is elicited by prolonged K+ depolarisation in that fibre (Cochrane et al., 1972). It would therefore seem likely that the sarcoplasmic reticulum of insect skeletal muscle plays a similar role to that of vertebrate muscle in excitation-contraction coupling. Further evidence that suggests a role of insect sarcoplasmic reticulum in excitation-contraction coupling is provided by the actions of the plant alkaloid ryanodine on insect skeletal muscle (see below).

Calcium channel structure

Structural investigations of the L-type Ca^{2+} channel are aided by the high affinity of binding to the channel

seen with the dihydropyridines. Photoaffinity labelling and purification of the vertebrate channel using dihydropyridines and phenylalkalamines has revealed the channel to be an oligomeric structure made up of 5 distinct subunits (reviewed by Catterall et al., 1989). These subunits have been labelled α_1, α_2, β, γ and δ. The relative molecular mass of the intact calcium channel/dihydropyridine receptor complex has been estimated to be 416kDa and the masses of the α_1, α_2, β, γ and δ subunits to be approximately 175kDa, 140kDa, 60kDa, 30kDa and 26kDa respectively. cAMP-dependent phosphorylation sites are present on the α_1 and β subunits while the α_2, γ and δ subunits are heavily glycosylated. The binding sites of all the classes of organic calcium channel antagonists are believed to be situated on the α_1 subunit which also appears to contain the Ca^{2+}-permeable pore of the channel (Pelzer et al., 1989b, Perez-Reyes et al., 1989). In Drosophila brain membranes, the only insect preparation so far studied, the protein involved in high affinity binding of phenylalkylamines has been purified and has a relative molecular mass of approximately 135 kDa (Pelzer et.al., 1989a) which is somewhat less than that for the vertebrate α_1 subunit above.

The α_1 and α_2 subunits of the t-tubule calcium channel from rabbit skeletal muscle (Tanabe et al., 1987, Ellis et al., 1987) and the α_1 subunit of the rabbit cardiac calcium channel (Mikami et al., 1989) have now been cloned. There are slight differences in the primary structure between cardiac and skeletal muscle Ca^{2+} channels, although certain

23

areas are highly conserved (Mikami et al., 1989). The differences may give rise to the minor differences in channel properties seen between purified L-type channels from cardiac and skeletal muscle when they are reconstituted into planar lipid bilayers (Rosenberg et al., 1986, Pelzer et.al., 1989b, Perez-Reyes et.al., 1989).

Further differences between L-type channels in neurones, skeletal muscle and cardiac muscle of vertebrates are highlighted by the actions of omega Conus Toxin (w-CgTx). The effects of this 27 amino-acid polypeptide in a variety of tissues and species are varied (summarised by Yoshikami et al., 1989). In brief, w-CgTx blocks synaptic Ca^{2+} channels in neurones but has no effect on similar channels in skeletal or cardiac muscle (see e.g. McCleskey et al., 1987). The effects of w-CgTx are further complicated by the species specificity of the toxin. However it would appear that these effects of w-CgTx support the idea that there are significant differences between L-type channels in nerve and muscle which may be exploited therapeutically in the future.

Pharmacology of calcium channels

i) Organic Ca^{2+} channel antagonists

The organic Ca^{2+} channel antagonists and agonists fall into 3 major structural classes; the 1,4-dihydropyridines (e.g. nitrendipine, BAY K 8644), the phenylalkylamines (e.g. verapamil) and the benzothiazepines (e.g. diltiazem). In vertebrate tissues, all three compounds act by binding to the α1 subunit (see above) of the L-type Ca^{2+} channel at sites which modulate the gating behaviour of the channel.

Different binding sites exist for each class of compound and these sites are believed to interact with each other (e.g. Striessnig et al., 1986). The dihydropyridine class of compounds normally act as either antagonists (e.g nifedipine) or agonists (e.g. BAY K 8644) at L-type channels although it is now believed that many dihydropyridines also have partial agonist or partial antagonist effects (Brown et.al., 1986). The expression of agonist or antagonist behaviour by the dihydropyridines is thought to be a function of membrane potential (Brown et al., 1986, Bean, 1984), being agonists at hyperpolarised and antagonists at depolarised membrane potentials. Agonist responses are promoted when the channel is in the resting state (hyperpolarised holding potentials). The action of "antagonist" drugs from all 3 classes can be converted to an agonist response by the application of GTP analogues to the internal surface of cell membranes (Scott and Dolphin, 1987). This suggests that the channel protein can be stabilised in the conformation favouring agonist responses (resting state) by the association of an activated G protein. This effect is prevented by pertussis toxin, suggesting further that the G proteins involved are members of the Gi or Go families (Scott and Dolphin, 1987).

The mechanism by which modulation of the L-type channel is brought about by these compounds is not believed to be mechanical block of permeation as in the case of the inorganic antagonist ions (see below) but rather an effect on the gating characteristics of the channel. The L-type channel shows 3 distinct modes of channel gating. Mode 1 is

25

characterised by brief openings occurring in rapid bursts of activity and is the mode that is most commonly seen in single channel recordings in the absence of drug. Agonist modulation of the channel leads to a favouring of mode 2 behaviour where the openings become prolonged and hence raise the open probability of the channel. In mode 0 behaviour the channel becomes unavailable for opening and this mode is favoured by drugs acting as antagonists (Hess et al., 1984, Nowycky et al., 1985b).

An important difference between the different classes of Ca^{2+} antagonist is the use dependence of block. Block of the L-type current by phenylalkylamines requires the repeated opening of the channels by depolarisation before block can take place and a number of depolarisations are required before full inhibition is achieved. This is also seen to a lesser extent with diltiazem-like compounds, but not with dihydropyridines where the block is immediate and complete with the first depolarising step (Lee and Tsien, 1983).

The response of insect Ca^{2+} channels to the organic Ca^{2+} channel antagonists has not been well defined. In Carausius skeletal muscle, D-600, a derivative of verapamil, completely blocks Ca^{2+}-dependent action potentials (Ashcroft, 1981). In Drosophila neurones however only a weak blocking action is seen with D-600, and dihydropyridines have no blocking effect whatsoever (Byerly & Leung, 1988).

ii) Inorganic Ca^{2+} channel blocking drugs

Calcium channel currents in vertebrates are blocked by

inorganic cations such as Co^{2+}, Cd^{2+}, and La^{3+}. L- and N-type currents are usually more susceptible to block by Cd^{2+} than T-type currents (Nowycky et al., 1985a, Narahashi et al., 1987) and the N-type current is preferentially blocked by gadolinium (Gd^{3+}) ions (Docherty, 1988). Block of channels by these agents is thought to be by their high affinity binding to sites within the pore that are involved in the permeation of Ca^{2+}. Unlike Ca^{2+}, these ions will not pass through the channel, and by binding within the channel prevent the passage of Ca^{2+} (Lansman et al., 1986). Co^{2+}, Cd^{2+} and La^{3+} are generally found to block Ca^{2+}-dependent action potentials in insect skeletal muscle (Deitmer and Rathmeyer, 1976, Ashcroft, 1981). In insect neurones Ca^{2+}-dependent action potentials can be blocked by Co^{2+} (Goodman & Heitler, 1979, Orchard, 1976) and Ca^{2+} currents have been shown to be sensitive to Cd^{2+} (Byerly & Leung, 1988). No studies have so far been reported on the differential sensitivity of Ca^{2+} current components in either insect muscle or nerve to these drugs.

iii) LEMS antibody

Lambert-Eaton myasthenic syndrome (LEMS) is an autoimmune disorder characterised by muscle weakness. Unlike myasthenia gravis, where circulating antibodies are directed against the postsynaptic ACh receptor of the neuromuscular junction, LEMS antibody binds to, and causes the loss of, Ca^{2+} channels at the presynaptic motor nerve terminal causing reduced release of acetylcholine (Lang et al., 1987a). In the NG 108-15 cell line and bovine chromaffin cells, LEMS antibody has been found to cause loss

27

of function of the L-type calcium channel although it is without effect on the T-type channel (Peers et al., 1990, Kim and Neher, 1988). However, the calcium channnels involved in neurotransmitter release at the skeletal muscle motor nerve terminal where LEMS antibody acts do not appear to be L-type (Burges and W.-Wray, 1989). Furthermore, LEMS antibody is without effect on L-type channels in the heart (Lang et.al, 1988). Thus regions of antigenic similarity must exist between the calcium channels involved in neurotransmitter release and neuronal L-type channels, while there are antigenic differences between L-type calcium channels of heart and nerve.

iv) Pyrethroids

The pyrethroids are divided into two classes by their action on insects. Type I pyrethroids cause behavioural changes associated with hyperactivity in the nervous system, while type II pyrethroids are lethal at low doses but cause few behavioural effects (Hart, 1986). Both type I and type II pyrethroids act at the level of the voltage sensitive Na^+ channel where they cause an increase in channel open time (Narahashi, 1986). The different action of these two classes in vivo are brought about by the degree to which channel opening is prolonged. Type I pyrethroids produce a moderate increase in the open time of sodium channels. This leads to a prolonged sodium current during and after the action potential which in turn leads to repetitive firing in neurones. Sodium channel open times with type II pyrethroids are extremely prolonged, and give rise to large, prolonged depolarisations of the nerve membrane. This leads

to a depolarising block of nerve conduction causing
paralysis and death. In the N1E-115 cell line (mouse
neuroblastoma) a type I pyrethroid, tetramethrin, produced a
reduction in the T-type Ca^{2+} current but had little effect
on the L-type current (Narahashi, 1986). In insects there
are no reported studies of the action of pyrethroids on Ca^{2+}
channels and experiments have therefore been carried out in
this thesis to investigate this.

v) Avermectins

Avermectins (AVMs) are potent antihelminthic and
insecticidal agents. The mode of action of AVMs is still
not fully understood but an irreversible action at
GABA-ergic synapses has been postulated (Fritz et al.,
1979). At the lobster neuromuscular junction AVM was found
by Fritz et al. (1979) to produce similar effects to GABA.
This action could be blocked by picrotoxin, a Cl^- channel
blocking agent, or by the GABA antagonist bicuculline
(Mellin et al., 1983). AVM has been shown to induce the
release of GABA from mammalian brain synaptosomes (Pong et
al., 1980) and enhance GABA and benzodiazepine binding in
rat brain membranes (Paul et al., 1980). Since AVM does not
compete with GABA for binding to mammalian synaptosomes it
seems that the binding of AVM is not to the same site as
that occupied by GABA (Pong and Wang, 1980). AVM may
therefore act in any (or all) of three ways. Firstly, the
GABA-mimetic effects of AVM may be caused by the stimulated
release of GABA from GABA-ergic synapses. Secondly, AVM may
act directly on the GABA-receptor/Cl^- channel complex to
induce the opening of the Cl^- channel. Lastly, AVM may act

by promoting GABA binding to the GABA-receptor, so promoting opening of the channel. Direct effects of AVM not involving the GABA receptor have also been reported. In locust extensor tibiae muscle and neurones from Helix aspersa, membrane potential changes and chloride conductance increases are induced by AVM in cells that are insensitive to GABA and do not posess an inhibitory nerve supply (Duce and Scott, 1985, Bokisch and Walker, 1986). The postsynaptic effects of AVM and GABA in locust neurones have been compared using the noise analysis technique (Hart et al., 1986). Both AVM and GABA were found to produce inward currents at a -70mV holding potential, however the single channel conductance (and open time) of the channels opened by GABA were found to be significantly different from those opened by AVM. Furthermore, reversal potentials for the currents induced by AVM and GABA in these neurones were found to be different (Lacey, 1987). These data suggest that AVM and GABA act on different channels. The highly positive reversal potential for the AVM induced current together with the low conductance of the channels suggests that AVM may possibly modulate or activate Ca^{2+} channels. Some of the experiments described in this thesis were performed to investigate this possibility.

vi) Ryanodine

Ryanodine modulates excitation-contraction coupling in vertebrate skeletal muscle, cardiac muscle and vascular smooth muscle. In general the application of ryanodine to vertebrate skeletal muscle gives rise to a prolonged contracture, whilst in cardiac muscle and cardiovascular

30

smooth muscle a flaccid paralysis develops (Jenden and Fairhurst,1969, Sutko et al., 1985, Ito et al., 1986). In skeletal muscle it has been proposed that this effect is primarily due to an increase in Ca^{2+} release from the sarcoplasmic reticulum while in cardiac muscle and vascular smooth muscle Ca^{2+} release is inhibited (Sutko et al., 1979). Radiolabelled ryanodine has been used to isolate its 'receptor' from the sarcoplasmic reticulum which has been identified as the 'foot' structure that bridges the gap (of approximately 100A) between the sarcoplasmic reticulum and the t-tubule membrane (Lai et al., 1988). The ryanodine receptor consists of 4 identical polypeptides each with a relative molecular mass of approximately 400,000. Both the primary structure (Takeshima et al., 1989) of the subunits and the three-dimensional structure of the complex (Wangenknecht et al., 1989) have now been described. Reconstitution of this receptor into planar lipid bilayers reveals that it acts as an ionic channel permeable to Ca^{2+} with a slope conductance of approximately 90pS in 50mM Ca^{2+} (Lai et.al., 1988). This correlates well with the value of 100pS obtained from similar experiments in which the heavy density sarcoplasmic reticulum fraction (which contains the foot structure and hence the ryanodine receptor/Ca^{2+} release channel) of rabbit skeletal muscle was incorporated in planar lipid bilayers (Smith et al., 1986a, 1986b). In the presence of ryanodine this channel enters a lower conductance state of approximately 35pS (Imagawa et al.,1987) but becomes almost permanently open, leading in skeletal muscle to the contracture seen with ryanodine.

Similar effects may occur for cardiac sarcoplasmic reticulum Ca^{2+} channels, but the apparently opposite effect of ryanodine in this muscle may be explained by Ca^{2+} depletion from the sarcoplasmic reticulum stores (Fill and Coronado, 1988).

In locust skeletal muscle the application of ryanodine gives rise to a period of contracture followed by a flaccid paralysis. At the same time the electrical response to depolarisation in these fibres is converted from a graded to an all-or-none event (Usherwood, 1962). The change in the electrical response was interpreted by Usherwood to be due to a block or reduction in the potassium conductance of the muscle fibre by ryanodine. A similar change in the K^+ conductance following ryanodine treatment has been described in crab muscle but was interpreted as an effect secondary to the increased intracellular Ca^{2+} concentration caused by ryanodine (Goblet and Mounier, 1981). Thus it seems likely that for insect skeletal muscle, ryanodine also acts to alter intracellular Ca^{2+} levels suggesting an important role for the sarcoplasmic reticulum in excitation-contraction coupling in insects. The development of a flaccid paralysis in locust may indicate a similarity of insect excitation-contraction coupling mechanisms with those in vertebrate cardiac muscle. Also, as in vertebrate heart, Ca^{2+} may play an important part in action potential propogation and Ca^{2+} entry may trigger release of Ca^{2+} from the sarcoplasmic reticulum (Fabiato and Fabiato, 1979).

The experiments described in this study aimed to provide

information on the physiology and pharmacology of Ca^{2+} channels in two different insect preparations. In the first part of this thesis the properties of insect skeletal muscle Ca^{2+} channels were investigated by studying action potentials in larval muscle fibres. The second part of this thesis describes the investigation of Ca^{2+} channel currents in insect neurones using patch clamp techniques. Preliminary reports of the work presented here have been published (Barrett, Pearson and W.-Wray, 1988, Lees, Pearson and W.-Wray, 1988, Lees, Pearson and W.-Wray, 1989, Pearson, Newsom-Davis, Lees and Wray, 1989, Pearson, Lees and W.-Wray, 1990).

CHAPTER 2

EXPERIMENTAL METHODS

1. Methods for Chapter 3

a) Preparation of Plutella muscle fibres for intracellular recording

Larvae of the diamondback moth <u>Plutella xylostella</u> grow to a maximum size of approximately 1.5cm in their final instar. In these experiments, specimens of roughly 0.5cm were used, at which size we would expect them to be in their 4th or 5th instar.

Individual larvae were pinned by head and tail on a 30mm plastic dish with a sylgard base and immersed in a dissecting saline. A dorsal incision along the midline of the larva allowed the body wall to be opened up and pinned out flat. The viscera and fat body were then removed thus exposing the muscle fibres of the body wall. The dish was then transferred to the electrophysiological rig for recording.

b) Salines used with Plutella

Dissection of the Plutella larvae was carried out using a saline based on one described by Weevers (Weevers, 1966) for lepidoptera (see Table 2.1). The solution was adjusted to pH 7.0 using NaOH and to an osmolarity of 280 mosmol with sucrose.

Recordings of action potentials were performed in a similar saline which contained, in addition, 25mM

Table 2.1 Salines used with Plutella larvae.

	NaCl	KCl	MgCl₂	CaCl₂	NaHCO₃	NaH₂PO₄	glucose	TEABr	sucrose	pH	osmolarity (mosmol)
Dissecting	12	30	18	3	0.06	0.06	133	-	-	7.0	280
Recording	12	30	18	10	0.06	0.06	-	25	800	7.0	920

	Na -isethionate	K- ethyl sulphate	MgSO₄	CaSO₄	NaHCO₃	NaH₂PO₄	glucose	TEABr	sucrose	pH	osmolarity (mosmol)
Cl-free	12	30	18	5	18	0.06	0.06	-	25	800	7.0	920

Table 2.1

Values are concentrations in mM. Osmolarity for the dissecting saline was adjusted to the required level using sucrose. Values given for osmolarity of recording and Cl-free salines are approximate.

35

tetraethylammmonium bromide (TEA-Br) to block potassium conductances and convert the action potential from a graded to an all-or-none event (see Table 2.1). The concentration of $CaCl_2$ was raised to 10mM (except where stated otherwise) in order to aid resolution of action potentials. Instead of adjusting the osmolarity as above, the osmolarity of the saline was raised by replacing the 133mM glucose with 800mM sucrose. This prevented muscle contraction during stimulation of action potentials (Hodgkin et.al. 1957, Howarth 1958).

In some experiments, the calcium concentration was changed. No other changes were made to the salines to compensate for the alteration in the osmolarity since the osmotic differences between salines would be very small indeed when compared to the overall osmolarity of the solutions. In other experiments, the Cl^- ions in the saline were replaced with membrane impermeant salts (Table 2.1). The $CaSO_4$ used in this saline proved to be very difficult to dissolve in aqueous solution and was found to form a precipitate at concentrations higher than 5 mM. The calcium concentration used in these solutions was therefore measured directly using a calcium sensitive electrode, and the calcium concentration in the Cl^--containing control saline was adjusted to give the same concentration. All solutions were made up fresh on experimental days using deionised water, analytical reagent grade salts and a 1M $CaCl_2$ stock solution (BDH Chemicals).

c) Electrophysiological recordings

Recordings of action potentials were always made from

36

the same identified segmental muscle fibre in the 2nd abdominal segment (Fig 2.1), since this allowed better comparison of results between specimens. The dish containing the prepared specimen of Plutella was mounted under a light transmission microscope (Zeiss, x400 magnification), and the desired muscle fibre was identified. The bath was then perfused with recording saline. Intracellular recordings (using a Zeiss sliding-plate micromanipulator) were performed using glass microelectrodes made from thin-walled, fibre-filled capillary tubes (Clark's GC 150TF-15) pulled on a Kopf 720 electrode puller. Microelectrodes (5-15 MΩ) were filled with 3M KCl, mounted in a teflon holder (Clark's EH 45T/1.5) and were connected to the headstage of an Axoclamp-2A amplifier via an Ag-AgCl interface in the holder. Voltage and current outputs from the amplifier were passed to a Tektronix storage oscilloscope where they were connected to D.C.-coupled amplifiers (5A21N or 5A22N) in order to display signals from the microelectrode. The voltage signal was low pass filtered by the Axoclamp (3-5kHz) and passed via the oscilloscope to an F.M. tape recorder (Racal store 4) and a chart recorder (Gould BS 272) which was used to monitor resting potentials on a slow time base throughout the experiment.

Once the microelectrode had been immersed in the saline in the dish, 0.1nA square-wave current pulses (20ms duration, 1Hz) were passed through the microelectrode with the amplifier in bridge mode. Contact with the muscle fibre was seen as an increase in the amplitude of the square-wave

TRACHEAE

SEGMENTAL GANGLIA

AXOCLAMP

PLUTELLA XYLOSTELLA
4th INSTAR LARVA

Figure 2.1

see over for legend

38
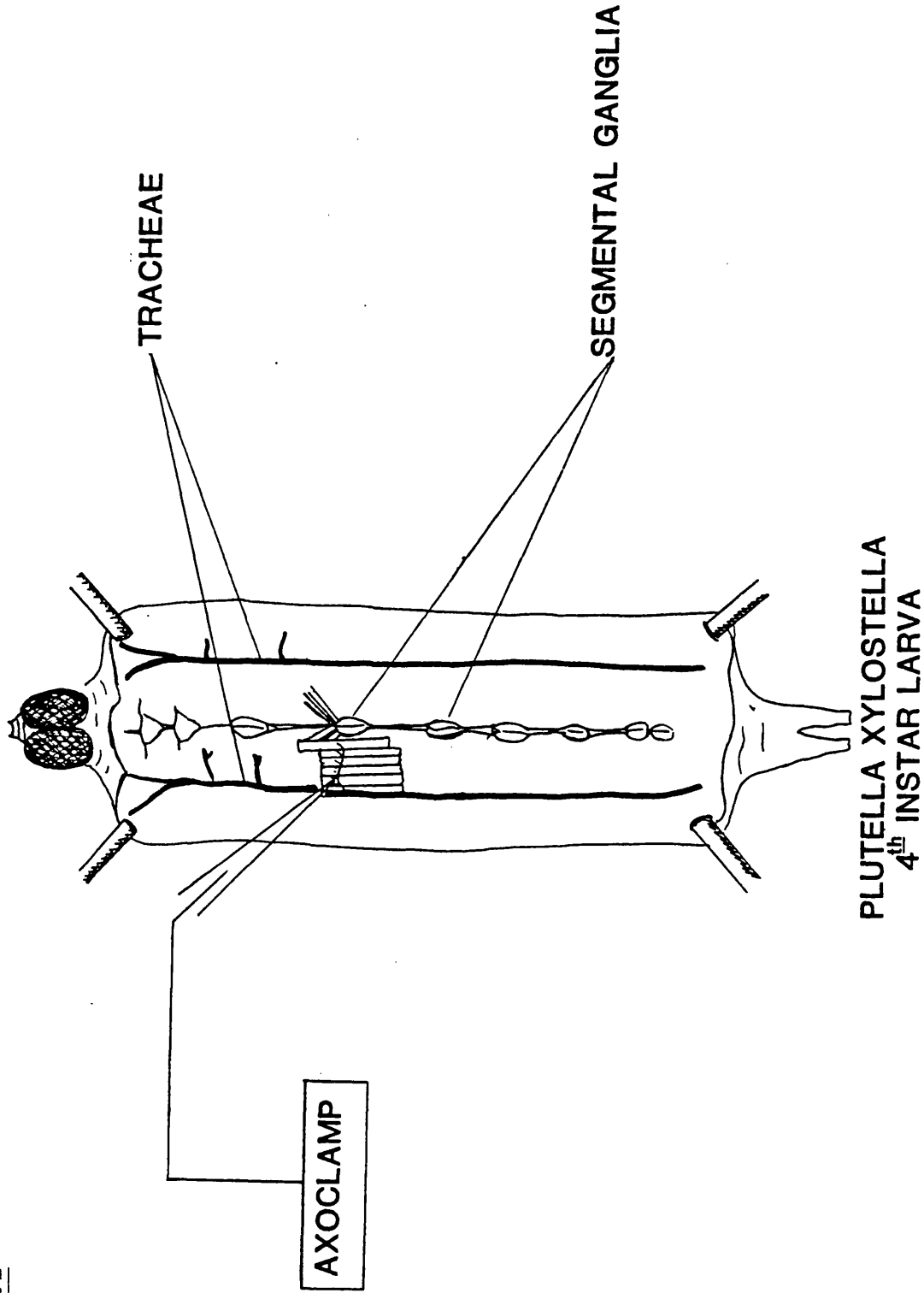
<u>Legend for Figure 2.1</u> Stimulation of action potentials in Plutella muscle fibres.

Diagram showing dissected specimen of Plutella xylostella ready for recording. Recordings were always made from the same identified segmental muscle fibre indicated in the diagram.

voltage response to current passage (i.e. an apparent increase in microelectrode resistance). Once contact was made with the muscle fibre, impalement was carried out by either advancing the microelectrode slightly further or by simply tapping the base plate of the microscope. Successful impalement of the muscle fibre was typified by a conversion of the voltage response from a square wave to a slowly rising (and decaying) waveform and observation of the cell's resting potential. After balancing of the bridge circuit to neutralise the resistance of the microelectrode the amplifier was switched to discontinuous current clamp (DCC) mode. Early experiments using bridge mode for the recording of action potentials were made more difficult by having to constantly balance the bridging circuit during experiments as small changes in the microelectrode's resistance occured. This is not a problem in the DCC mode since the DCC mode is independent of small changes in microelectrode resistance. After impalement and observation of a steady resting potential for 2-3 minutes, action potentials in the muscle fibre were stimulated by passage of square-wave current pulses through the microelectrode (40ms duration, every 10 seconds). The amplitude of the current pulses ranged from 8-20nA, the magnitude being adjusted so that the action potential peak occurred earlier than the end of the pulse.

Where drug application caused changes in membrane potential, the resting potential was kept constant at the resting potential of each cell by D.C. current passage, thereby allowing accurate comparison of control and test parameters for action potentials. Where this was necessary

it will be noted in the text. All experiments were carried out at room temperature (22-24°C).

d) Drug and antibody preparation and application

Drugs that were easily soluble in aqueous solutions (Cd^{2+}, Co^{2+}, La^{2+}, TTx, ryanodine and ethacrynic acid) were made up into stock solutions of 1mg/ml in recording saline. The stock solutions were then transformed by tenfold serial dilution to give solutions which could be added to 250ml of recording saline in manageable and appropiate quantities.

Drugs that were relatively insoluble in water were dissolved in either ethanol (diltiazem, verapamil and nitrendipine) or dimethylsulphoxide (avermectin) to give concentrations of 1mg/ml in the organic solvent. These stock solutions were also tenfold serially diluted in the solvent to give concentrations of drug that could be added to the recording saline such that the concentration of organic solvent was always less than 0.01% v/v. Where an organic solvent was used, the control saline had an equal concentration of the solvent added to it.

Analytical reagent grade chloride salts of Co^{2+}, Cd^{2+} and La^{3+} were purchased from BDH. TTx was purchased from Koch-Light Laboratories, diltiazem from Abbott Laboratories and ethacrynic acid and verapamil were purchased from Sigma. Nitrendipine was a gift from Bayer and avermectin B_1 was a gift from Merck, Sharpe and Dome. Ryanodine was purified from plant material at Wellcome Research Laboratories, Berkhamsted and was 98.5% pure.

Control and LEMS IgG fractions were prepared by Dr. B. Lang and Mr. A. Roberts of the Department of Neurology, Royal Free Hospital from human plasma using the Rivanol/ammonium sulphate method (Horejsi & Smetana, 1954). Fractions were 90-95% pure and after sterilisation by millipore filtration were stored frozen at -20°C in Hartman's solution. LEMS IgG was obtained from the plasma of a patient who had associated small cell carcinoma of the lung and whose IgG has been previously shown to crossreact with, and cause the loss of function of, presynaptic Ca^{2+} channels at the mouse neuromuscular junction (Lang et al, 1987a). Control IgG was prepared from the pooled plasma of normal control humans. Stock solutions of IgG, containing 17-20mg IgG/ml were dialysed against Plutella dissecting saline.

Muscles were perfused in the bath with control saline at a rate of 10-15ml/min using a gravity feed system and 15-25 action potentials stimulated. The perfusing saline was then switched to one containing the drug. Action potentials (15-25) were then again recorded in the presence of drug. Antibody application was made by incubating 10-15 unmounted, dissected specimens for 24 hours prior to recording with control or LEMS IgG, present in dissecting saline at a final concentration of 4mg/ml. During this time, the solutions were bubbled with 100% O_2 at room temperature (21-24°C). The insect muscles were then washed in recording saline and mounted in individual dishes for recording (i.e. in the absence of further antibody).

e) Analysis of action potentials.

Analysis of action potential data was performed using a Computer Automation computer with CED 701 interface using programmes written by the author in Fortran. Recordings of voltage were replayed from an F.M. tape recorder and stored on floppy disc after digitisation at 5kHz. Blocks of 512 data points (i.e. 102.4ms) were read by the computer, and blocks containing data which crossed above a preset discriminating cursor (i.e. those blocks which contained an action potential) were displayed on an oscilloscope screen. Blocks which contained action potentials were aligned on the screen so that the first point of the depolarising response to cross the discriminating cursor occurred at the 128th point on the display. This allowed several action potentials to be averaged. The first one hundred points of the display were averaged to give a value for the cell's resting potential just prior to stimulation of the action potential. Measurements of amplitude, overshoot and duration at half amplitude were made and the action potential measurements visually checked before acceptance by means of displayed cursors. The voltage trace was then differentiated to allow measurements of the maximum rate of rise and maximum rate of fall of the action potential to be made (Fig 2.2). Each action potential and its differentiated trace were plotted on a Bryans X-Y plotter as were the averaged traces at the end of analysis. Values for each of the measured parameters were also averaged by the program and standard errors for each parameter obtained.

43

Figure 2.2

MAX. RISE

MAX. FALL

MAX. FALL

dV/dT

20 V.s^{-1}

0 mV

AMP

OS

T$_{1/2}$

RP

V

20 mV

I

20 nA

20 ms

see over for legend

44
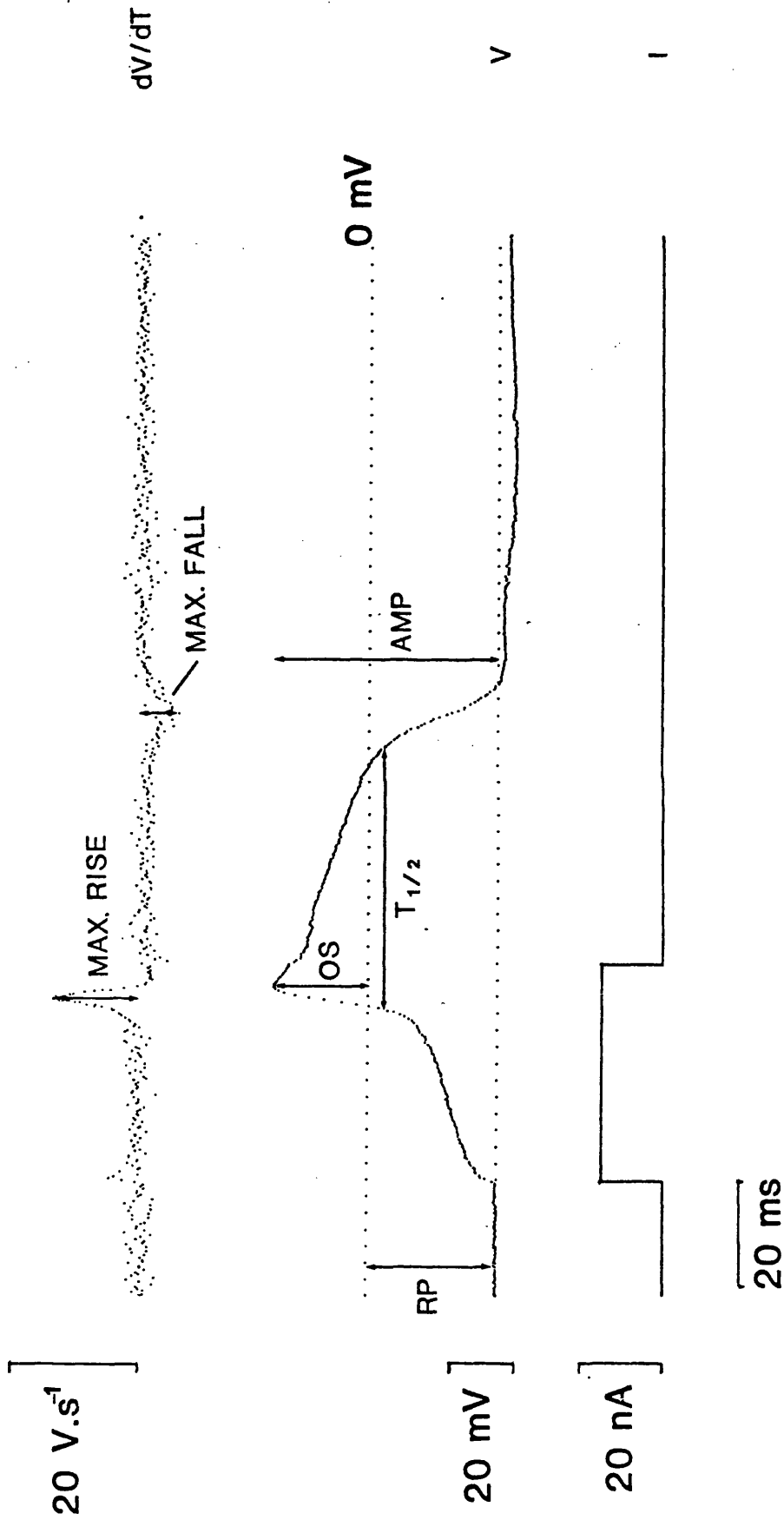
<u>Legend for Figure 2.2</u> Measurement of action potentials in Plutella muscle fibres.

Diagram showing measurements made from muscle fibre action potentials. Action potentials were stimulated by passing square wave current pulses through the recording electrode (bottom trace). The computer program used for analysis measured cell resting membrane potential (RP) and action potential overshoot (OS), amplitude (AMP), and the duration for which the action potential remained above half the maximal value ($T_{1/2}$) from the voltage trace (middle). From the computer-differentiated voltage trace (upper trace) the maximum rate of rise (MAX. RISE) and maximum rate of fall (MAX. FALL) were also measured by the computer program.

f) Presentation of data

All measured parameters are presented as the mean ± standard error averaged over each group of cells in control or test salines. Measurements made of the effect of LEMS IgG were compared using the two tailed Student's t-test. Values for application of all other test substances were compared using the paired Students t-test. The value of significance was set at $p < 0.05$

2. Methods for chapter 4

a) Preparation of cells from locust thoracic ganglia for patch clamp recording.

Cell bodies of neurones from the desert locust _Schistocerca gregaria_ were prepared from the three thoracic ganglia which run down the midline of the ventral body wall of the thorax. After removal of the head, two paramedian incisions approximately 2-3mm either side of the midline allowed the part of the thoracic wall containing the ganglia to be bent away from the rest of the thorax. The thoracic wall was then removed by an incision at the junction between thorax and abdomen and was then immmersed in a dish containing dissecting saline. The thoracic ganglia were then removed from the wall and cleaned of fat and connective tissue. The connective nerves between the three ganglia were severed and the ganglia from 4-5 locusts were then placed in dissecting saline containing 1mg/ml trypsin

46

(bovine pancreatic trypsin, BDH). The ganglia were allowed
to digest for 10-15 minutes at 30°C to allow dispersion of
individual cell bodies when the sheaths were later removed
and to remove any adherent debris or glial cells from cell
surface membranes. The ganglia were then placed in a
solution of 2mg/ml bovine serum albumin (Sigma chemicals)
for approximately one minute to inactivate the trypsin and
were then thoroughly washed in fresh dissecting saline. The
fine membranous sheaths surrounding the ganglia were removed
and individual nerve cell bodies were isolated by repeatedly
passing the ganglia through a narrow bore (1-1.5mm) glass
pipette. The cell suspension was filtered through a $50\mu m$
nylon mesh to remove the remains of ganglia and larger
debris, and the filtrate was then repeatedly (4-5 times)
spun down and washed in dissecting saline which contained
penicillin (200 U/ml) and streptomycin(200 U/ml) to reduce
the risk of bacterial or fungal infection of the cells.
Cell suspensions were prepared on the day of the experiment
and stored (at 4°C) for no longer than 16 hours.

b) Salines used for locust ganglia cells.

i) Dissecting saline

Dissection of the ganglia and isolation of cell bodies
was performed using a standard locust dissecting saline
(Table 2.2). The pH of the solution was adjusted to 7.4
using Tris and the osmolarity to 390 mosmol with sucrose.

ii) Salines used for whole cell recordings

The composition of the saline in which the cells were
bathed for whole cell recording is given in Table 2.2. The

47

Table 2.2

Salines used for whole-cell and cell-attached patch recordings with cells isolated from locust thoracic ganglia.

	NaCl	CsCl	Choline-Cl	KCl	$MgCl_2$	$CaCl_2$	$BaCl_2$	HEPES	TEABr	TTX	EGTA	pH	Osmolarity (mosmol)
Dissecting Saline	185	-	-	5	-	4	-	10	-	-	-	7.4	390
Recording Saline 150 (whole cell)	150	-	-	5	2	-	10	10	25	.0025	-	7.4	390
Choline Saline (with Ba^{2+} as charge carrier)	-	-	155	-	2	-	10	10	25	.0025	-	7.4	390
Choline Saline (with Ca^{2+} as charge carrier)	-	-	155	-	2	10	-	10	25	.0025	-	7.4	390
Pipette Saline (whole cell)	-	160	-	-	2	0.1	-	10	20	-	1.1	7.4	370
Pipette Saline (cell attached)	-	-	-	-	-	-	110	10	25	.0025	-	7.4	390

Values are concentrations in mM. The osmolarity of salines was adjusted to the required level with sucrose.

48

pH of the recording saline was adjusted to 7.4 with Tris and the osmolarity to 390 mosmol with sucrose. In some experiments cells were bathed in solutions in which all cations other than the charge carrying ion (Ba^{2+} or Ca^{2+}) were replaced with choline (Table 2.2). The osmolarity and pH of these solutions were adjusted to the values given above using the same methods.

The patch pipette was filled with a saline shown in Table 2.2. The pH of the saline was again adjusted to 7.4, this time with CsOH and the osmolarity was adjusted to 370 mosmol with sucrose. Pipette salines were filtered through a 0.22μm pore filter (Millipore) before being used to back-fill patch pipettes. The slight hypotonicity of the pipette saline appears to aid seal formation and rupture of the patch when the whole-cell configuration is attempted (Carbone and Lux, 1987a). EGTA was present in the pipette solution to buffer intracellular levels of calcium (Carbone and Lux, 1987a).

The pipette and bath salines were designed to block potassium and other conductances which would otherwise contaminate the calcium current in these cells. Thus TEA blocks delayed rectifier, calcium-activated, inward rectifier and 'A'-current potassium channels when applied to both the inside or the outside of cell membranes (Hille, 1984). Furthermore, Cs^+, present on the inside of the cell from the patch pipette solution, blocks all potassium channels (Stanfield, 1983). Sodium currents were eliminated by the addition of TTx to the outside of the cell. The use of Ba^{2+} as the charge carrying ion in these experiments was

because Ba^{2+} has been shown to have a higher conductance through some Ca^{2+} channel types (Nowycky et.al., 1985a), and since Ba^{2+} also minimises the run-down of the calcium current (Eckert & Chad, 1984). Furthermore, Ba^{2+} is also a blocker of K+ channels (Stanfield, 1983).

iii) Salines used for cell attached patch recordings

For experiments in which cell-attached recordings were made, the cells were bathed in dissecting saline (see above). The patch pipette was filled with a saline of composition shown in Table 2.2. The pH of the saline was adjusted to 7.4 with Ba(OH)$_2$ and the osmolarity was adjusted to 390 mosmol with sucrose. The pipette saline was filtered before being used to back-fill patch pipettes (as above). High levels of Ba^{2+} in the pipette when recording single calcium channel currents are necessary because of their low conductance which leads to a low signal to noise ratio. TEA and TTx were also present as above.

Many workers use bathing solutions designed to zero the cell resting potential when performing cell-attached recordings (see e.g. Hess et.al., 1984). In the cells used in this thesis however, it was found that such solutions caused rapid deterioration of cell appearance and it became difficult to obtain good pipette seals. It was therefore necessary to use other means to ascertain absolute values for the transmembrane potential during experiments (see section d) iii), below).

c) Patch pipette preparation

Pipettes used for patch clamping were pulled on either

a BB-CH Mecanex horizontal puller or a Kopf 720 microelectrode puller adapted for pulling patch pipettes. Glass capilliary tubes were mounted in the puller and heated by a platinum-iridium foil element. As the glass melted a tapering waist was pulled on the tube. A second pull produced pipettes that were steeply tapering with a blunt end and a resistance of 4-8 MΩ for whole-cell pipettes, 5-10 MΩ for cell-attached pipettes. Whole-cell pipettes were pulled using thin walled capilliaries (Clark's GC150TF-15) and cell-attatched pipettes using thick walled capillaries (Clark's GC150F-15). Pipette tips were coated in Sylgard resin which was heat cured in a microforge consisting of 3 turns of nichrome wire through which a current was passed. The coating of the pipette tips in Sylgard markedly reduces pipette capacitance (Hamill et. al., 1981). Fire polishing of pipettes was carried out by advancing the pipette tip very close to a heated, glass-coated loop of nichrome wire. This smoothed the end of the tip and also burned off any Sylgard which may have flowed to the very end of the pipette.

d).Electrophysiological recordings.

Cells were transferred to 35mm tissue culture dishes (Corning) by dropping 0.1-0.2ml of cell suspension onto the centre of a dish from a glass pasteur pipette. They were left for 3-4 minutes to allow settling and adherance of the cells to the bottom of the dish, and then washed with recording saline. The fluid height in the dish at the end of washing was left at approximately 2-3mm (volume 1-1.5ml

of saline); the low level of saline helps measurements by reducing pipette capacitance and probably also vibration of the meniscus due to air currents. The dish was then mounted on a microscope (Zeiss, Nikon TMS or Nikon TMD) and viewed with either phase-contrast or Nomarski optics. Small, spherical, smooth and phase-bright cells (10-30μM diameter), were selected for recording.

The patch pipette was mounted in a teflon holder (Clark's PC S3) and connected to the headstage of an amplifier (Axoclamp 2A, List EPC-7 or Axopatch 1C) via an Ag-AgCl wire in the pipette holder. Return to earth was provided via an Ag-AgCl wire immersed in the bath. The pipette was manipulated using a 3-plane hydraulic manipulator (Narishige MO 103M). Voltage and current outputs from the clamp amplifier were fed to a Tektronix storage oscilloscope with D.C. coupled amplifiers (either 5A21N or 5A22N) and, after amplification by these, to an F.M. tape recorder (Racal Store 4). The current output from the oscilloscope was also fed to a chart recorder (Gould BS272) on a slow time base to monitor baseline clamp current throughout the experiment. For whole cell experiments, signals were low-pass filtered at 3kHz by the clamp amplifier and switching characteristics for the Axoclamp were monitored throughout by a second oscilloscope. During cell attached recordings, the current signal was low-pass filtered at 1kHz by an 8-pole Bessel filter before being passed to the oscilloscope.

i) Whole cell recording

<u>Axoclamp</u>

The majority of whole cell recordings were carried out using the Axoclamp 2A amplifier. With the pipette immersed in the bath a repetitive current pulse was applied (1Hz, 0.1nA, 20ms) with the amplifier in bridge mode. The pipette was advanced until the tip touched the surface of the cell. This was seen on the oscilloscope as an increase in the voltage response to the current pulse (i.e. an apparent increase in the electrode resistance) and under the microscope as a slight dimpling of the cell surface. Slight, steady suction was then applied to the pipette via the side-arm in the pipette holder. Formation of a seal was characterised by an increase in the resistance of the electrode and suction was sustained until a seal of greater than 5 GΩ was achieved. At this point the deflection of the voltage trace in response to the current pulse was around 0.5V. Rupture of the cell membrane was achieved by application of short, sharp pulses of suction to the pipette and successful rupture was seen on the oscilloscope as a reduction in resistance and an increase in the rise time of the voltage change, corresponding to the cell's resistive and capacitative properties. The amplifier was then switched to the discontinuous single electrode voltage clamp (dSEVC) mode. In this mode the amplifier switches between sampling and current injection modes at a frequency that can be set by the user (8-15kHz in the case of these cells). The amplifier was made to pass 10mV voltage steps (1Hz, 20ms duration) while the gain of the holding circuit was increased as much as possible so that the voltage waveform became square and the waveform on the monitoring

oscilloscope showed that sampling of the membrane voltage occured at a point when the voltage transients had decayed completely. Further minor increase in the gain was possible with the imposition of small amounts of phase lag, and in this way the optimum clamp conditions for cells were obtained.

List or Axopatch amplifiers

When the List or Axopatch amplifiers were used, sealing of the pipette to the cell membrane was seen as a reduction in amplitude of the current response to an applied 1mV pulse with a duration of 20ms at a frequency of 1Hz. Once a seal of 5GΩ or better had been obtained, brief suction pulses were again used to rupture the membrane under the patch. Successful rupture was seen as a large increase in the capacitance transients at the beginning and end of the voltage pulse and a fall in resistance. Increasing the amplitude of the voltage step to 10mV allowed better resolution of the capacitance transients in the current trace which were reduced using the capacitance neutralisation controls of the amplifier. Correct adjustment of these controls allowed accurate measurement of the cell's capacitance which could be read directly from the dials on the amplifier.

Experimental protocol

The following experimental protocol was used for cells clamped with either the Axoclamp or the List/Axopatch amplifiers. The cell was clamped at a holding potential of -80mV and a series of 30-35 voltage pulses to test potentials of 10mV either positive or negative to the

54

holding potential were made (200ms duration, 0.4Hz). These
were used during analysis for leakage and capacitance
subtraction. Cells were left at a holding potential of
-80mV for 30 seconds before applying voltage pulses to test
potentials of -90mV up to potentials of +60mV in 10mV
increments (or occasionally 5mV increments) in order to
construct I-V curves. When different holding potentials
(other than -80mV) were used on the same cell, a period of
90 seconds was allowed before the above procedure was
repeated to allow time for any steady state inactivation of
channels to become complete.

The frequency and duration of pulses were always
controlled using a Grass S48 stimulator. Pulse amplitude
was set using the inbuilt voltage/current generators in the
Axopatch and Axoclamp and by the Grass stimulator when the
List amplifier was used.

ii) Cell capacitance

Because the Axoclamp amplifier had no provision for
direct measurement of cell capacitance it was necessary to
make measurements of cell capacitance after the above
experiments. This was achieved by switching the amplifier
to discontinuous current clamp mode and depolarising the
cell to a steady potential of +40 to +60 mV by steady D.C.
current passage of +0.5 to +0.1nA. Current pulses of
0.1-0.03nA (duration 200-400ms) were then superimposed at
0.4Hz. The charging of the cell membrane in response to the
current pulse is expected to be exponential, the time
constant of which is dependent on the cell's passive
resistive and capacitative properties, enabling calculation

55

of cell capacitance (see Analysis of recordings, below).
Depolarisation of these cells to steady positive potentials
(+40 to +60mV, see above) was necessary because at the
resting potential of these cells in the recording saline
(approximately 0mV), hyperpolarising current pulses gave
voltage responses that showed apparent regenerative phases
(Fig. 2.3). Posssibly, voltage dependent channels may be
tonically active at the resting potential which would become
progressively inactivated by hyperpolarisation. Indeed, at
the end of the hyperpolarising current pulse an action
potential appeared to be initiated. Holding the cell at
hyperpolarised potentials was found to be very difficult
since, with few channels active at these potentials, the
cell resistance was very high and large fluctuations in
holding potential occurred.

iii) Cell attached recording.

Recordings of single calcium channel currents were
performed using the List EPC 7 patch amplifier on cells
bathed in the locust dissecting saline. The protocol for
forming seals on the cell membrane was the same as that
given above, with the exception that the patch membrane was
not ruptured when a GΩ seal was formed. Because the cell
resting potential was not "zeroed" (i.e. made equal to 0mV)
using high potassium salines it was necessary to obtain
values for resting potentials of cells by other means.
Measurement of resting potential was achieved by impaling
the cell with an intracellular microelectrode either before
a seal was formed or immediately after an experiment. After
making a seal with a resistance of better than 15-20GΩ the
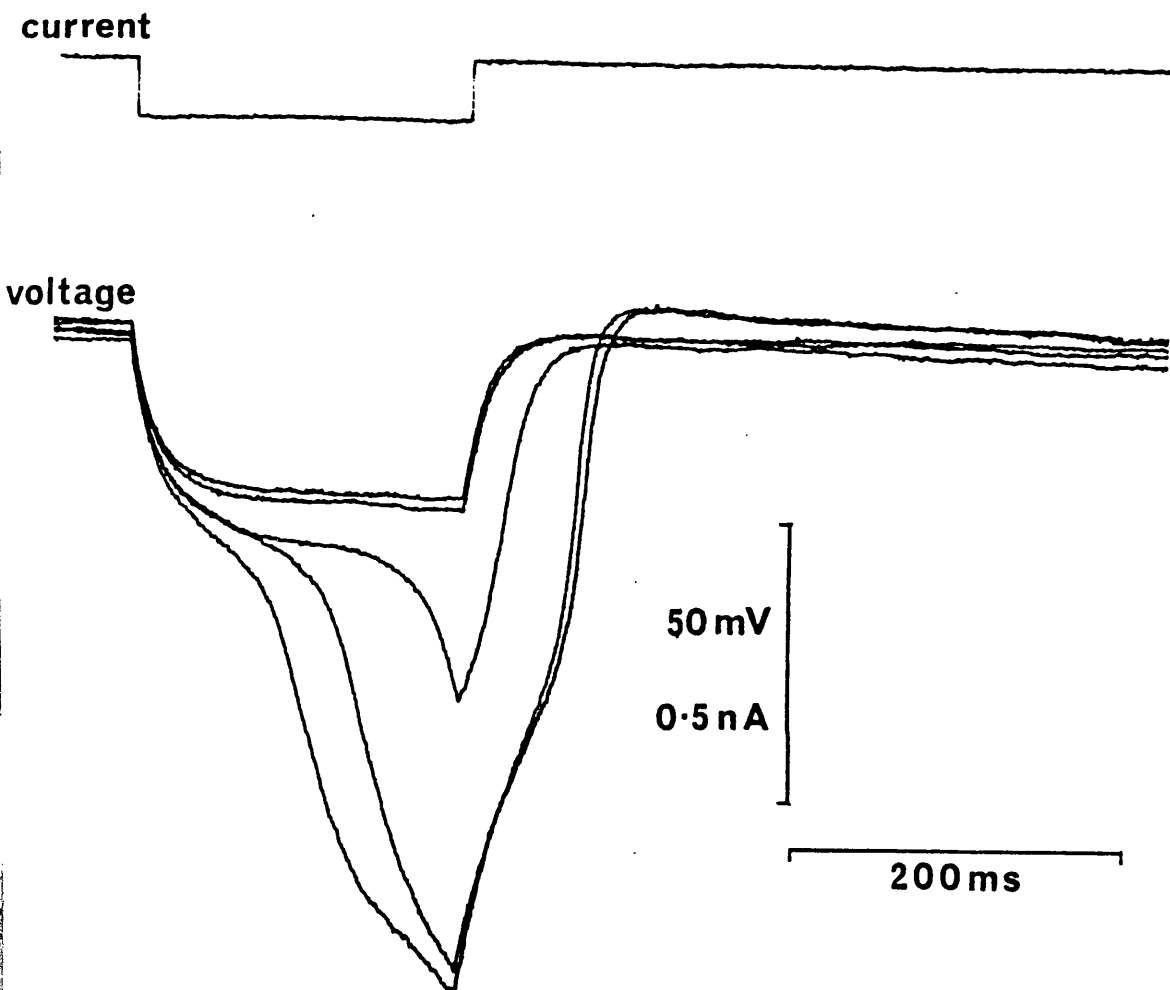
Figure 2.3 Regenerative responses seen in cells from locust thoracic ganglia.

Current (top) and voltage (bottom) traces from a cell under current clamp conditions. Repeated (0.5Hz) injection of 0.1nA of hyperpolarising current results in the observation of rebound action potentials in three of the five sequential voltage traces.

pipette potential (Vpip) was raised to a holding potential of approximately +40mV to give a transmembrane potential across the patch of -80mV. From this holding potential, Vpip was stepped to transmembrane test potentials of -30, -20, -10, 0 and +20mV (duration 200ms, frequency 0.1Hz). For each test potential, 20-30 steps were recorded for subsequent analysis. In cases where no channel activity was seen in the patch, other more hyperpolarised holding potentials were used (giving transmembrane holding potentials of between -90 and -200mV). Also, at each of these holding potentials, larger test potential steps were made (to give test transmembrane potentials of between -50 and +100mV), but no further channel activity was ever seen.

e) Drug preparation and application.

As in the experiments with Plutella muscle, drugs that were easily soluble in aqueous solutions (Cd^{2+} and ryanodine) were made up into stock solutions of 1mg/ml in recording saline, and stock solutions were then transformed by tenfold serial dilution to give solutions which could be added to 250ml of recording saline in manageable quantities. Drugs that were insoluble in water were dissolved in either ethanol (verapamil and nitrendipine) or dimethylsulphoxide (S-bioallethrin, deltamethrin and avermectin) to give concentrations of 1mg/ml in the organic solvent. These stock solutions were tenfold serially diluted in the solvent to give concentrations of drug that could be added to the recording saline such that the concentration of organic solvent was always less than 0.01% v/v. Where an organic

58

solvent was used the control saline had an equal concentration of the solvent added to it.

Drugs were obtained from the same sources as those used with the Plutella muscle fibres. Additionally, S-bioallethrin and deltamethrin (99% pure) were supplied by Wellcome Research Laboratories, Berkhamsted.

For application of all test salines other than those containing ryanodine, deltamethrin and S-bioallethrin, cells were perfused in the culture dish with control saline at a rate of 5-10ml/min using a gravity feed system. Firstly, control I-V curves were obtained as described above. Then from a holding potential of -80mV, 200ms depolarising pulses to a test potential of -10mV were applied every 10-20 seconds. Some cells showed 'rundown' (i.e. a progressive decline in the Ca^{2+} channel current with time), but cells were selected which showed little or no rundown. After obtaining a steady baseline for inward current, perfusion was switched to the test saline while continuing to apply the depolarising test pulses as above. When the Ca^{2+} channel current reached a steady level with the test saline, an I-V curve was again obtained as described above. For ryanodine, deltamethrin, S-bioallethrin and some of the experiments with nitrendipine, cells were not treated with both control and test solutions; instead dishes of cells (plated at the same time) were bathed in either control or test saline and a single I-V curve from each cell was obtained.

For the light-sensitive compounds (verapamil and nitrendipine) all experiments and drug handling were carried

out in darkened rooms illuminated by a sodium vapour lamp.

f) Analysis of patch recordings.

i) Whole cell recordings.

Data from recordings were stored on magnetic tape and analysis was carried out using a Computer Automation computer with CED 701 interface using programs written in Fortran. Voltage and current analogue data were simultaneously replayed from a tape recorder and after digitisation at 5kHz, stored on floppy disc. Data from the disc was read by the computer in blocks of 2048 data points (i.e. 409.6ms/block). A preset discriminating cursor identified blocks of data in which the cell voltage was stepped to another potential. The voltage steps were aligned so that the first point on the voltage trace above the cursor (i.e. the beginning of a pulse) occured at the 256th data point in a block. Baseline current and voltage values were calculated from the first 220 data points (44ms) in the block. The value of the potential during the voltage pulse was calculated by averaging 300 data points in the centre of the step. Leak and capacitance subtraction was performed by averaging together the 20-30 10mV steps made at the beginning of each experiment (see above). The averaged current trace so obtained was then scaled up to the size it would have been for each test voltage step (i.e. x step voltage/10) and subtracted from the current traces for the appropriate test potential. The parameters measured on the current trace after leak and capacitance subtraction were as follows; the maximum current seen during the pulse, the

(sustained) current obtained by averaging the data points during the last 10ms of the step and the time taken by the current trace to reach its maximum (see also Fig.2.4). The difference between peak and sustained currents was also calculated. All of the parameters measured on both current and voltage traces were displayed on the oscilloscope by means of horizontal and vertical cursors and checked by eye. Currents could be manually measured in cases where artefacts made computer calculations inaccurate.

ii) Single channel recordings.

As for the above experiments, data from single channel experiments were also stored on magnetic tape and digitised at 5kHz by the computer before being stored on floppy disc. Data were again read in 409.6ms blocks, and voltage pulses again identified and aligned using a discriminating cursor on the voltage trace. Leak and capacitance subtraction was performed by averaging together test steps to the same potential in which no channel activity occured and then subtracting this average from all of the steps to the same potential. After subtraction, 256 ms of current data containing the step were plotted out using a Bryans X-Y plotter. These hard records were then analysed by hand. Parameters measured were channel amplitude, open time and first latency.

iv) Measurement of cell capacitance.

As mentioned above, direct measurement of cell capacitance was possible with the List and Axopatch amplifiers, but a different approach was required when the
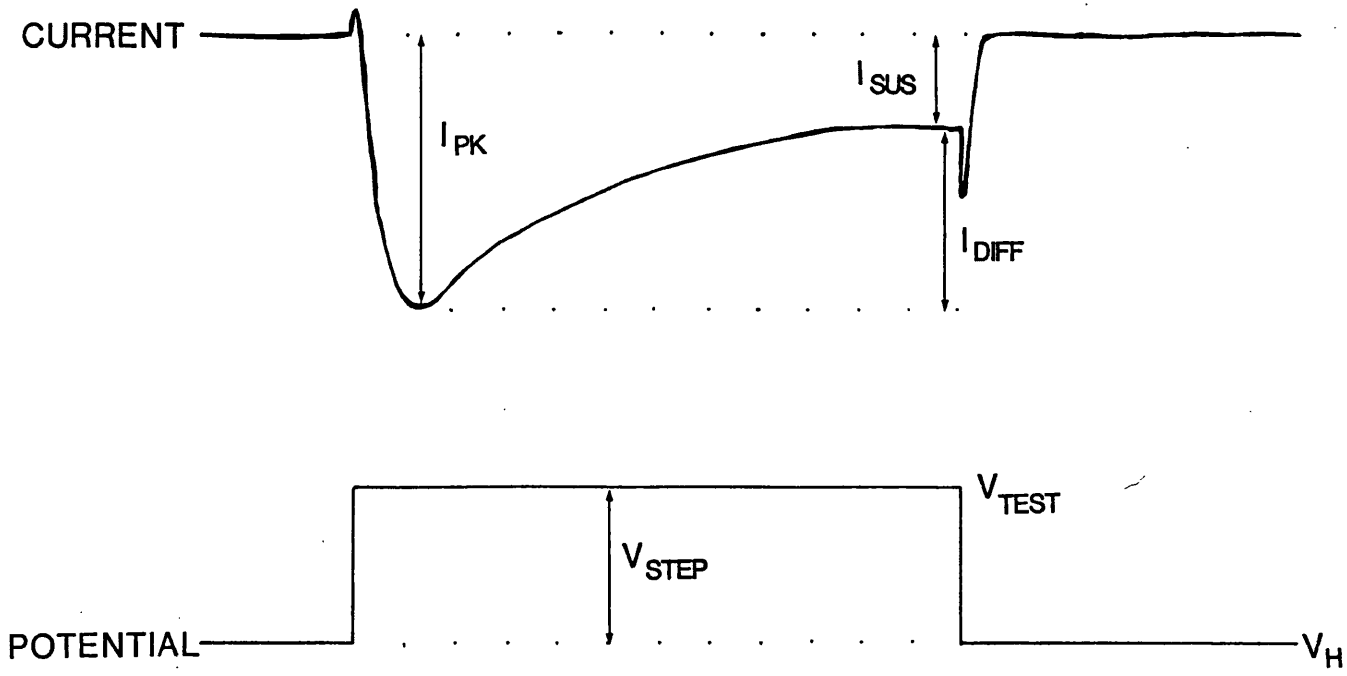
<u>Figure 2.4</u> Measurement of whole cell currents in locust neuronal cell bodies.

The diagram shows the current response to a step in potential from the holding potential (V_H) to a test potential (V_{TEST}). Current values measured were the maximum inward current (I_{PK}), the residual current remaining at the end of the voltage step (I_{SUS}) and the current that had inactivated during the course of the potential step (I_{DIFF}). I_{DIFF} is the difference between the I_{PK} and I_{SUS} measurements. When the current reversed at the highly positive test potentials I_{PK} was measured as the maximum outward current.

Axoclamp amplifier was used.

The passive resistive and capacitative characteristics of the cell membrane cause the voltage of the cell membrane to change in an exponential manner to square-wave current injection, the relationship between voltage change and time being given by the relation;

$$V_{(t)} = V_{max} (1-e^{-t/\tau})$$

where $V_{(t)}$ is the voltage change at a time t after the beginning of the pulse, V_{max} is the maximum potential change reached and τ is the time constant for charging of the cell membrane. The above was converted by taking natural logarithms to obtain;

$$\ln (V_{max}-V_{(t)}) = \ln V_{max} - t/\tau$$

and τ was then obtained by linear regression. The time constant, τ, is related to the capacitance (C) and the resistance (R) of the cell by;

$$\tau = RC$$

Since R was calculated by dividing V_{max} by the amplitude of the current pulse, and having calculated τ, C can therefore be obtained.

A number of assumptions are inherent in using this method. Firstly, the above equation is for a spherical cell, the membrane of which acts as a simple resistor/capacitor in parallel. Cells with long axon stumps and longer, narrower cell bodies show voltage changes that can not be described in the above simple manner (Katz, 1966). Therefore cells that were spherical as possible were chosen for recording. Secondly, the above calculation is for passive changes only and the presence of voltage

activated channels in the cell membrane would lead to erroneous results. Accordingly, small voltage changes only were used (10-15mV) at a holding potential chosen so that the membrane potential changes did not appear to cause opening and closing of channels and so that good exponential fits were obtained. Thirdly, the resistance of the seal between pipette and cell membrane must be much greater than the resistance of the cell to avoid errors in measuring cell resistance and this was always the case. Fourthly, current pulses must be longer than several time constants, since charging of the cell membrane would not be complete by the end of the pulse. Therefore pulses were always longer than 5 time constants, so that membrane charging was more than 99.4% complete. Data for capacitance calculation was stored on magnetic tape and voltage and current records digitised at 3kHz to floppy disc. Data blocks of 2048 points (676ms) were read from disc, and when points on the current trace crossed a preset discriminating horizontal cursor, were displayed on an oscilloscope screen. Baseline current and voltage values were measured by averaging the 100 data points immediately preceding the pulse and current amplitude was obtained by averaging 100 data points in the centre of the pulse and subtracting the baseline value from it. V_{max} was calculated by averaging 50 data points at the end of the pulse together and subtracting the baseline value from that value, and hence cell input resistance was calculated as above. Horizontal cursors were set on the calculated baselines and maximal values by the computer so that measurements could be checked by eye and discarded if they

were incorrect. The computer then plotted a graph of ln $(V_{max}-V_{(t)})$ against t and fitted a straight line to the data by linear regression to obtain τ and hence capacitance as described above. Values for input resistance and capacitance were averaged for 15-20 pulses from the same cell to obtain a mean value for input resistance and cell capacitance.

g) Presentation of data.

Data from whole cell experiments is presented as both absolute values for current in a set of cells and as values normalised for cell capacitance. All data is presented as the mean ± the standard error for cells in control or test salines, averaged over values for each cell. Values were compared using Student's two tailed t-test or paired t-test where appropriate with the level for significance set at $p < 0.05$.

CHAPTER 3

RESULTS

a) Introduction

The experiments described in this chapter were aimed at determining the role of Ca^{2+} channels in action potentials stimulated in skeletal muscle fibres from larvae of the moth Plutella xylostella and to investigate their pharmacology. Action potentials were stimulated by passing current pulses through an intracellular microelectrode which was also used for recording purposes. The effects of varying Ca^{2+} and Cl^- concentrations, TTX, organic and inorganic Ca^{2+} channel antagonists, ethacrynic acid, ryanodine, avermectin and LEMS IgG were tested on this preparation.

b) Properties of action potentials in muscle fibres of Plutella xylostella.

All experiments were carried out at the resting potential of the cells which ranged from -27 to -56mV, with a mean value of 41.6 ± 0.7mV (n=74 cells). In the absence of TEA, a graded action potential was stimulated by depolarisation of the cell, with a higher amplitude following stronger depolarisation. When TEA was applied, however, the action potential was converted to an all or none event that had the same amplitude despite stronger depolarising current pulses once suprathreshold stimulation had been achieved (see Figs 2.2 and 3.1a for typical action potentials). Action potentials in the presence of TEA had

mean amplitudes of 62.5 ± 1.3mV, and mean overshoots (maximum positive potential achieved during the action potential) of 21.0 ± 1.2mV (n=74 cells). The rising phase of the action potential had maximum rate of rise of 11.9 ± 0.6Vs^{-1}. The values for resting potential, amplitude, overshoot and maximum rate of rise of the action potentials of a given cell remained fairly constant over a time of 1-2 hours. On the other hand, the duration of the action potentials was far more variable, quite frequently changing considerably between consecutive events in a single cell and varying over a wide range between different cells making statistical analysis of data difficult. The duration at which the action potential was above the half-maximal level ranged in the 74 cells measured from 13ms to 3.34 seconds with a mean of 90.03 ± 44.75 ms.

c) Effect of altering the calcium concentration on action potentials.

Experiments described in this section were aimed at determining the involvement of Ca^{2+} ion movements during action potentials in Plutella muscle fibres. To do this cells were first perfused with saline containing 10mM Ca^{2+} and 20-30 action potentials were recorded. The perfusing saline was then switched to one containing either 5 or 2.5mM Ca^{2+} and a further 20-30 action potentials recorded. For cells perfused with 5mM Ca^{2+} the muscles were then perfused with a saline in which Ca^{2+} had been removed completely and again 20-30 action potentials were recorded. Following this, cells were again perfused with 10mM Ca^{2+} and a final

67

group of 20-30 action potentials recorded. For cells perfused with 2.5mM Ca^{2+} perfusion with the Ca^{2+}-free saline was omitted and perfusion was returned to the 10mM Ca^{2+} saline for the final recording of action potentials.

The effects of reducing the calcium concentration to 5mM are summarised in Table 3.1. There was a reduction in amplitude and overshoot of the action potential, but this did not attain statistical significance. The maximum rate of rise of the action potential was, however, significantly reduced ($p<0.05$) to approximately half its original value. The action potential duration was not significantly different from controls.

When the calcium was removed altogether no regenerative response was seen even when the current pulse amplitude was increased (Fig 3.1).

Because the possible reduction in amplitude did not attain significance with 5mM calcium, it was decided to repeat the experiment using a test concentration of 2.5mM Ca^{2+}. In 8 different cells where the calcium concentration was reduced from 10 to 2.5 mM, the amplitude in all cells was reduced. The maximum rate of rise was also reduced, as was the overshoot (Table 3.2). The reductions in amplitude, overshoot and maximum rate of rise attained statistical significance in this case ($p<0.001$, $P<0.001$ and $p<0.005$ respectively). No significant effect was seen on the action potential duration in these cells. Returning the cells to a saline containing 10mM Ca^{2+} completely reversed the effects of the 2.5mM Ca^{2+} saline.

Theoretical values for the reduction in amplitude can

Table 3.1

The effect of extracellular Ca^{2+} concentration on action potentials in skeletal muscle fibres from larval Plutella xylostella.

	Resting Potential (mV)	Amplitude (mV)	Overshoot (mV)	Maximum Rate of Rise (Vs^{-1})	Duration of ½ amplitude (ms)	Number of muscle fibres
10mM	-41.8±2.7	58.8±5.0	17.5±4.1	9.7±2.1	70±26	8
5mM	-40.3±2.3	48.7±2.4	9.1±3.0	5.0±0.4*	90±24	8

Values shown are the mean ± standard error for the number of fibres shown. The same cells were exposed to 10mM and 5mM Ca^{2+} in each case. *; $p < 0.005$, students paired t-test.

Table 3.2

Effect of Ca^{2+} concentration on action potentials in skeletal muscle fibres from larvae of Plutella xylostella.

	Resting Potential (mV)	Amplitude (mV)	Overshoot (mV)	Maximum Rate of Rise (Vs^{-1})	Duration (ms)	Number of muscle fibres
10mM Ca^{2+}	-41.4±1.3	62.4±2.5	21.4±1.9	13.8±2.5	51.3±9.0	8
2.5mM Ca^{2+}	-41.2±1.5	48.9±2.9 **	8.0±2.2 **	5.6±0.7 *	76±19	8
Wash (10mM Ca^{2+})	-41.8±1.4	62.5±2.9	20.7±3.3	13.8±2.7	81±26	8

As for Table 3.1 but with different muscle fibres. Values following wash with 10mM Ca^{2+} are also shown. Values given are mean ± standard error of the mean. *, $p<0.005$, **$p<0.001$, as compared with both control and wash values, students paired t-test.
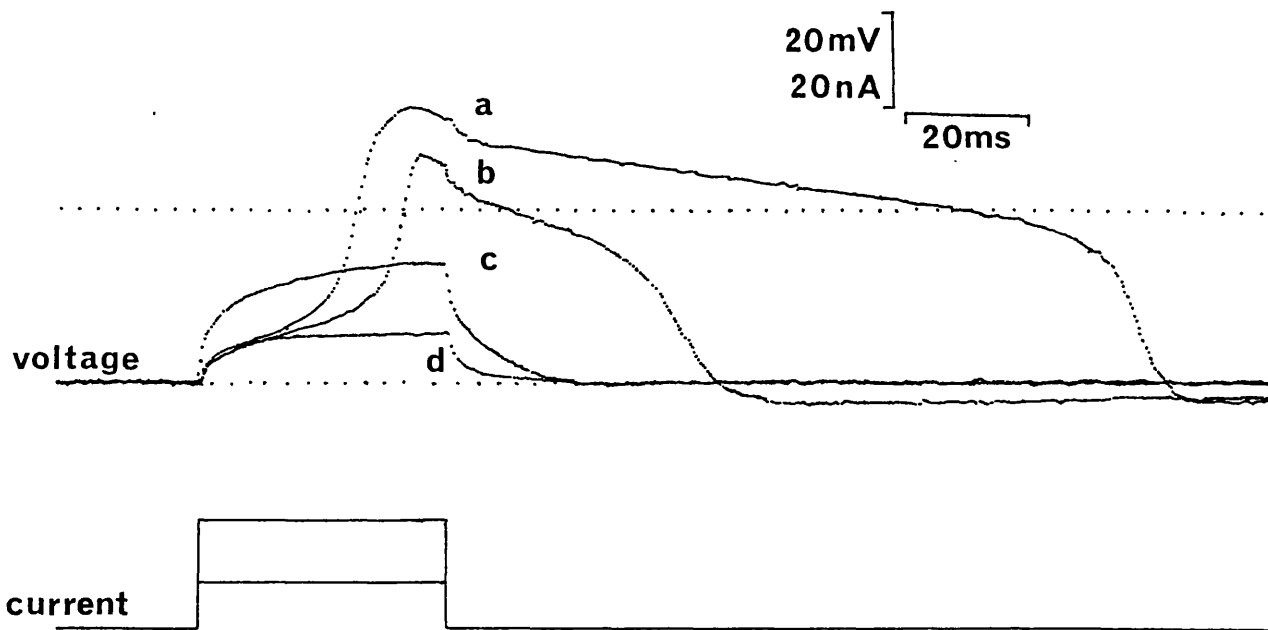
Figure 3.1   Effect of Ca^{2+} concentration on action

potentials in Plutella muscle fibres.

Action potentials triggered from the same muscle fibre in;

a. 10mM Ca^{2+}, b. 5mM Ca^{2+}, c. and d. 0mM Ca^{2+}.   Increasing

the current pulse had no effect on triggering the action

potential in 0mM Ca^{2+} (c.).   Similar effects were seen in

all other cells tested.

71

be calculated using the Nernst equilibrium equation for calcium in this preparation. The equation defines the equilibrium reversal potential (E) of a given ion to be given by;

$$E = \frac{RT}{ZF} \log 10 \frac{[Ca^{2+}]o}{[Ca^{2+}]i}$$

where R is the universal gas constant, T is the absolute temperature (°K), Z is the valency of the ion (in this case, 2), F is the Farraday constant, $[Ca^{2+}]o$ is the external calcium concentration and $[Ca^{2+}]i$ is the intracellular calcium concentration. It can be seen that the equilibrium potential will change with the logarithm of external calcium concentration and thus it can be calculated that, if Ca^{2+} is the major permeant ion during the action potential, the action potential amplitude should be reduced by 8.7mV with 5mM Ca^{2+} and 17.5mV in 2.5mM Ca^{2+}. These values compare reasonably well with the experimental values of 11.2 ± 5.0mV and 13.5 ± 2.1mV that were obtained for the 5mM and 2.5mM Ca^{2+} salines respectively.

The maximum rate of rise is also related to $[Ca^{2+}]o$, but in this case the relationship is direct. The current flow (I) across a membrane with a membrane capacitance C, will give rise to a potential that changes with time (dV/dt), the relationship being;

$$I = C \frac{dV}{dt}$$

Since the size of the current during pure calcium-dependent action potentials will be directly proportional to $[Ca^{2+}]o$ then we would expect the maximum rate of rise of these action potentials to be directly proportional to $[Ca^{2+}]o$ if

72

they are indeed calcium-dependent.

When the $[Ca^{2+}]o$ was changed from 10mM to 5mM the maximum rate of rise was reduced by 42.9 ± 8.9% close to the expected 50% and from 10mM to 2.5mM by 56.1 ± 4.9% (expected=75%).

The theoretical values for both the changes in amplitude and maximum rate of rise assume that at the peak amplitude of the action potential the cell membrane is freely permeable to Ca^{2+} ions and that all other conductances are blocked.

These experiments therefore suggest that action potentials in these muscle fibres are based on the movement of Ca^{2+} ions through voltage-sensitive Ca^{2+} channels.

d) Effect of inorganic calcium channel antagonists on action potentials.

Experiments described in this section were designed to investigate the effects of inorganic Ca^{2+} channel antagonists (Co^{2+}, Cd^{2+} and La^{3+}) on action potentials and so further confirm the role of Ca^{2+} in action potentials.

Action potentials were repetitively stimulated and groups of 20-30 were recorded in control saline, in the presence of the blocking ion and following washout of the test solution. The chosen concentrations of blocking ion were those which are known in other systems to cause a high degree of block of Ca^{2+} channels but which are not high enough to have non-specific effects.

The effects of perfusing muscles with these substances is shown in Figure 3.2. Co^{2+} at a concentration of 20mM

73

Figure 3.2

CONTROL   TEST   RECOVERY

Co²⁺ (20 mM)

Cd²⁺ (1 mM)

La³⁺ (1 mM)

20mV

20mV

20mV

20ms

see over for legend

74
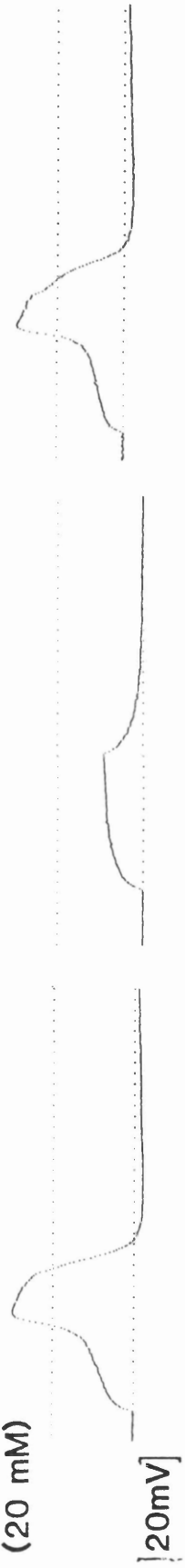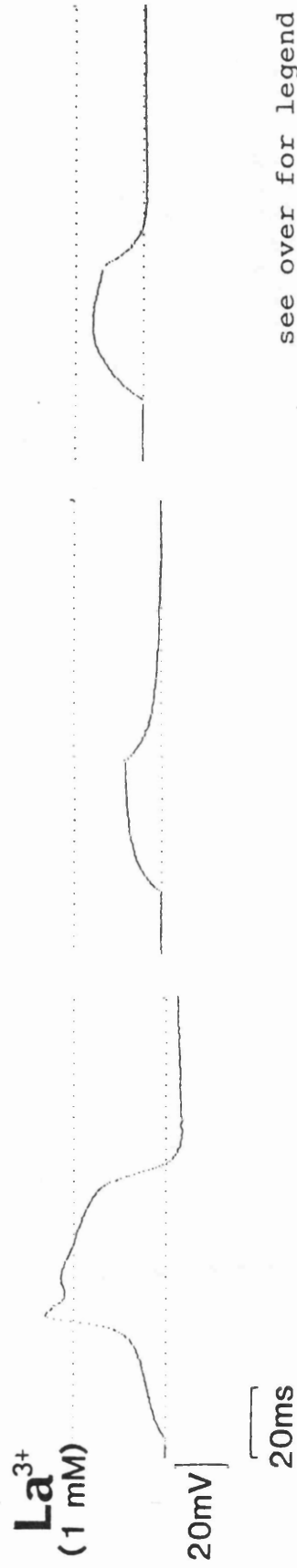
Legend for Figure 3.2   Effect of inorganic Ca^{2+} channel antagonists on action potentials in Plutella muscle fibres. Each row shows action potentials triggered in the same muscle fibre in control saline (left), in the presence of a blocking ion (middle), and following washout in control saline (right). Dotted lines on each trace represent the cell resting membrane potential (bottom line) and the 0mV level (top line).

rapidly (4-5 mins) blocked the action potential. This effect was fully reversible on washing (n=3). Cd^{2+} (1mM) also blocked the action potential (n=3), this effect was again fully and rapidly reversed by washing. La^{3+} (1mM) also produced a rapid block of the action potential (n=3). This block however was almost completely irreversible even after 20 minutes of perfusion with the control saline. Increasing the amplitude of the current pulse to produce stronger depolarisation of the muscle membrane did not overcome the block of these substances to any degree.

These results for Co^{2+}, Cd^{2+} and La^{3+} are what would be expected if the action potential is dependent on Ca^{2+} influx through Ca^{2+} channels.

e) Effect of organic Ca^{2+} antagonists on action potentials.

The organic calcium channel antagonists used were chosen from three chemical classes, 1,4-dihydropyridines (nitrendipine), phenylalkylamines (verapamil) and benzothiazepines (diltiazem). All are thought to block the 'L'-type calcium channel (see Introduction) and were applied to the Plutella muscle fibres in order to test for the involvement of such channels in the action potential.

As with the inorganic antagonists, the concentrations of drug used were those which were as high as possible but which do not give non-specific effects in other preparations (Godfraind et.al., 1986). Action potentials were recorded in the control saline just prior to perfusion of the test saline and after 10-15 minutes in the presence of the drug (see Methods). The tissues were then washed by perfusion

76

Table 3.3

Effect of organic Ca^{2+} channel antagonists on action potentials in larval Plutella muscle fibres.

	Resting Potential (mV)	Amplitude (mV)	Overshoot (mV)	Maximum Rate of Rise (Vs^{-1})	Duration (ms)	Number of muscle fibres
Control	-46.3±1.4	57.5±3.1	11.4±4.1	10.4±1.1	30.5±3.4	
Diltiazem (5µM)	-46.8±1.8	59.2±2.2	12.8±2.6	9.2±1.4	42±11	4
Wash	-44.8±1.2	58.7±2.9	13.5±2.9	10.06±0.81	90±59	
Control	-33.3±4.9	49.6±3.7	15.6±2.1	13.2±2.4	17.5±3.1	
Nitrendipine (1µM)	-33.3±6.6	48.5±6.7	15.8±2.7	11.7±3.4	19.3±2.3	3
Wash	-34.8±9.1	42.9±7.6	8.3±7.7	10.5±3.9	26.6±6.0	
Control	-38.3±4.2	61.2±5.2	23.1±2.0	14.4±2.8	43±19	
Verapamil (1µM)	-37.7±4.0	64.6±6.1	26.5±2.8	14.6±3.0	53±22	6
Wash	-37.3±4.1	62.1±5.3	25.1±2.1	13.1±3.1	43±20	

Values obtained in control saline, saline containing the drug and following wash with control saline from the same muscle fibre in each case. Values given are mean ± s.e.m. No significant differences were found (student's paired t-test).

with the control saline for 15-20 minutes and further action potentials were recorded (Table 3.3).

Verapamil (1μM) had no significant effect on action potential amplitude, overshoot, duration or maximum rate of rise as compared with either control saline or following wash of the muscles. Neither were wash values significantly different from controls.

A similar lack of significant effect on the above action potential parameters was also obtained from cells bathed with either 5μM diltiazem or 1μM nitrendipine (see Table 3.3).

In summary, therefore, the results presented in this section show that the Ca^{2+} channels which appear to underly action potentials in the muscle fibres of larval Plutella xylostella are insensitive to block by all 3 classes of organic Ca^{2+} channel antagonist at the concentrations used, suggesting the absence of L-type channels.

f)   Effects of tetrodotoxin on action potentials.

In vertebrate tissues the skeletal muscle action potential is based mainly on an influx of Na^+ through voltage sensitive sodium channels (see Introduction). To investigate whether Na^+ ion movements were involved in action potentials in Plutella muscle, tetrodotoxin (TTx), which blocks voltage-sensitive Na^+ channels was applied. Action potentials were again stimulated in muscle fibres and recorded in control saline, 5-10 minutes after perfusion with TTx (2.5μM), and 10-15 minutes after wash with control saline. There was no significant effect of TTx on resting

Table 3.4

Effect of tetrodotoxin on action potentials in larval Plutella muscle fibres.

	Resting Potential (mV)	Amplitude (mV)	Overshoot (mV)	Maximum Rate of Rise (Vs^{-1})	Duration (ms)	Number of muscle fibres
Control	-41.7±2.8	62.6±4.9	20.8±4.5	13.1±1.8	39±13	7
Tetrodotoxin (5µM)	-41.1±3.0	64.3±5.1	22.9±4.7	13.6±1.6	36.8±8.2	7
Wash	-41.0±3.4	67.2±4.8	26.1±4.5	13.9±2.3	39.5±5.5	7

Values shown (mean ± standard error of the mean) are from the same fibre in control saline, following application of 2.5µM TTX and after washing in control saline. No significant differences were found between control, TTX-tested and wash values (students paired t-test).

potential or on the amplitude, overshoot, duration or maximum rate of rise of action potentials as compared with control or wash values (Table 3.4). Control and wash values were also not significantly different from each other.

This lack of effect of TTx on the action potentials in Plutella muscle fibres suggests that voltage-sensitive sodium channels play no clear part in action potential propagation.

g) Effect of reducing or removing Cl$^-$ on action potentials.

Many (but not all) of the muscle fibres in this preparation showed an after-hyperpolarisation following the action potential (see Figs. 2.2, 3.1, 3.2). Since a large proportion of the (hyperpolarising) potassium conductance should be blocked by the presence of TEA in the recording medium, the basis of this hyperpolarising potential could be due to inward chloride ion movements. Thus it might be expected that removing Cl$^-$ from the recording saline would abolish the after-hyperpolarisation and possibly alter the measured parameters of the action potential. This was investigated in these experiments.

As in other experiments, action potentials were stimulated repetitively (0.1Hz) by passing current pulses through the recording electrode and action potentials were recorded continuously from the same muscle fibre during perfusion with control (98mM Cl$^-$) saline, Cl$^-$-free saline, and after washing. The Ca^{2+} concentration in both control and test salines for these experiments was adjusted to 5mM since the poor solubility of the CaSO$_4$ used in the Cl$^-$-free

Table 3.5

Effect of removing Cl⁻ on action potentials in muscle fibres from larval Plutella.

	Resting Potential (mV)	Amplitude (mV)	Overshoot (mV)	Maximum Rate of Rise (Vs^{-1})	Duration (ms)	After hyper-polarisation amplitude (mV)	Number of muscle fibres
Control (98mM Cl⁻)	−43.5±2.2	58.9±3.5	15.6±2.5	9.1±1.7	26.4±3.0	1.0±0.4	6
Zero Cl⁻	−43.5±2.1	56.7±4.8	12.9±3.2	6.4±1.7 *	32.7±5.2	1.4±0.3	6
Wash (98mM Cl⁻)	−43.9±2.2	62.7±3.4	19.1±2.1	9.1±1.7	39.0±6.9	1.0±0.4	6

Values given are mean ± s.e.m. for the same cells in control saline followed by test saline after which cells were washed in control saline. *; $p < 0.01$, students paired t-test. No significance differences between control and wash values were found.

saline (see Methods) made it impossible to use higher concentrations.

The results of applying Cl^--free saline to the muscle fibres are given in Table 3.5. Values for amplitude, overshoot or duration measured after 10-15 minutes perfusion with Cl^--free saline were not significantly different from either control values or after 10-15 minutes wash. However, the maximum rate of rise in Cl^--free saline was significantly reduced when compared against both control ($p<0.01$) and wash ($p<0.05$) values. None of the above values were significantly different when control and wash values were compared. All 6 cells studied showed after-hyperpolarisations. The amplitude of these after-hyperpolarisations (maximal negative deflection from the baseline) was unchanged by perfusion with the Cl^--free saline.

From these results it would appear that the afterhyperpolarisation often seen after an action potential in these cells is not caused by an influx of Cl^- ions into the muscle cell. Cl^- may have a role in the action potential since Cl^- removal leads to a decrease in the maximum rate of rise of action potentials, but it is unlikely to underly the action potential since it is not blocked by Cl^- removal nor is its amplitude changed.

h) Effect of ethacrynic acid on action potentials.

Ethacrynic acid is reportedly a blocker of Cl^- channels in erythrocytes and algal membranes (Motais & Cousin, 1976, Lunevsky et.al., 1983) and was therefore used to investigate

Table 3.6

Effect of 100µM ethacrynic acid on action potentials in muscle fibres from larval Plutella xylostella.

	Resting Potential (mV)	Amplitude (mV)	Overshoot (mV)	Maximum Rate of Rise (Vs^{-1})	Duration (ms)	After hyper-polarisation amplitude (mV)	Number of muscle fibres
Control (98mM Cl⁻)	-41.2±2.3	66.7±4.0	25.3±3.6	11.9±3.1	63±19	2.5±0.3 (n=3)	5
Ethacrynic Acid (100µM)	-41.6±2.2	64.5±4.1	23.0±2.6	6.7±0.8	44±11	2.0±0.2 (n=3)	5
Wash	-42.4±2.7	64.3±6.0	21.9±4.3	6.2±1.0	66±21	2.1±0.3 (n=3)	5

Values given are mean ± s.e.m. for the same cells in control saline followed by saline containing ethacrynic acid after which they were washed in control saline. There were no significance differences between test and control values, test and wash values or control and wash values (students paired t-test).

the effect of Cl⁻ channel block on action potentials. Muscles were impaled and action potentials were stimulated (0.1Hz) during perfusion with solutions as above. Action potentials were analysed in control saline, after cells had been perfused with ethacrynic acid (100μM) for 30-40 minutes, and after washing the cells for 30-40 minutes in control saline. None of the measured parameters (resting potential, amplitude, overshoot duration and after-hyperpolarisation) were affected significantly by ethacrynic acid, as compared with controls or values after washing. Although the rate of rise was reduced by ethacrynic acid, this did not attain statistical significance.

Consistent with the results of the preceding section, these data indicate that firstly, Cl⁻ ions are not involved in after-hyperpolarisations, and secondly, support the idea that Cl⁻ ions are not required to trigger an action potential. The hint of a decrease in rate of rise by ethacrynic acid is similar to the decrease in rate of rise produced in Cl⁻-free saline. This may again point to a possible role for Cl⁻ ion movements in the action potential, presumably giving rise to inwardly-directed currents.

i) Effect of ryanodine on action potentials.

As well as acting on Ca^{2+} channels in the sarcoplasmic reticulum, the insecticidal compound ryanodine may have effects on calcium channels in the plasma membrane (see Introduction). The aim of experiments described in this section was to investigate the effects of ryanodine on the

84

Table 3.7

Effect of ryanodine on action potentials in muscle fibres from Plutella larvae.

	Resting Potential (mV)	Amplitude (mV)	Overshoot (mV)	Maximum Rate of Rise (Vs⁻¹)	Maximum Rate of fall (Vs⁻¹)	Duration (ms)	Cell input Resistance (kΩ)	Number of muscle fibres
Control	-39.7 ± 1.8	60.2 ± 3.9	20.4 ± 3.2	11.6 ± 2.2	–	51.7 ± 19.1	–	6
1µM Ryanodine	-40.4 ± 2.1	62.7 ± 4.3	22.3 ± 3.0	11.7 ± 2.5	–	75 ± 28	–	6
Wash (30mins)	-40.5 ± 2.0	60.2 ± 5.7	20.0 ± 4.3	9.8 ± 3.0	–	67 ± 25	–	6
Control	-42.1 ± 3.1	67.2 ± 4.0	24.7 ± 2.6	9.4 ± 1.4	5.2 ± 0.3	49 ± 11	687 ± 49	5
10µM Ryanodine	-43.3 ± 2.9	76.1 ± 5.5 *	33.5 ± 3.8 *	16.9 ± 3.7	4.9 ± 0.2	256 ± 35 **	739 ± 44	5
Wash (30mins)	-42.0 ± 3.3	76.3 ± 5.0	34.5 ± 3.5	17.3 ± 3.6	5.0 ± 0.4	222 ± 52	721 ± 53	5

Values given are mean ± s.e.m. for the same fibres perfused with control saline followed by test saline and after wash with control saline. *, $p<0.01$ **, $p<0.005$, students paired t-test. No significant differences between wash and ryanodine-treated values were found.

Ca^{2+}-dependent action potentials in insect skeletal muscle.

Action potentials were stimulated at 0.1Hz as before and continuous recordings from the same muscle fibre were made during perfusion with 1 or 10μM ryanodine for 10-25 minutes and after 30 minutes washing. Data from these cells before, during and after treatment with ryanodine were averaged together and are presented in Table 3.7. Values obtained for resting potential, amplitude, overshoot, maximum rate of rise and duration of action potentials were not significantly affected by 1μM ryanodine as compared with either control or wash values. The most obvious change seen in the action potential during 10μM ryanodine application was a significant ($p<0.005$) increase in duration as compared with controls (Table 3.7). This effect could not be reversed even after 30 minutes washing; values for action potential duration after wash were not significantly different from values in 10μM ryanodine, but were significantly ($p<0.005$) greater than control values. To investigate further this increase in duration the rate of fall of the action potential was also measured; it was found to be not significantly affected by ryanodine (10μM). Action potential amplitude and overshoot were significantly increased ($p<0.01$) after treatment with 10μM ryanodine. Again, values after washing were not significantly different from values in the presence of ryanodine. As compared with controls the maximum rate of rise was also increased in the presence of ryanodine, although this increase was not statistically significant. Resting cell input resistance was also measured and was not found to be significantly

different between test and control salines.

In summary, 1μM ryanodine had no effect on action
potentials while 10μM ryanodine caused a marked increase in
action potential duration and smaller increases in
amplitude, overshoot and possibly, maximum rate of rise.
These changes could not be reversed by washing. Possible
interpretation of these results are discussed further below.

j)   Effects of avermectin on action potentials and input resistance.

A possible action of antihelminthic agent avermectin on
calcium channels (see Introduction) was investigated here.
The effects of avermectin on cell membrane potential and
input resistance were firstly investigated, since avermectin
application causes changes in membrane potential and an
increase in the conductance of the cell membrane in locust
muscle and nerve (Duce and Scott, 1985, Lacey, 1987). Input
resistance was measured by applying hyerpolarising current
pulses with an amplitude of 10nA and duration of 500ms to
muscle fibres at a frequency of 0.2Hz. The effect of
perfusing Plutella muscle fibres with avermectin at
concentrations of 100nM and 10nM are shown in Figure 3.3 and
mean values are given in Table 3.8. At both 100nM and 10nM,
avermectin produced irreversible depolarisations accompanied
by significant (p<0.001) and irreversible reductions in the
input resistance of the cells. It was found that attempting
to stimulate action potentials following application of
avermectin was very difficult since the increase in
conductance meant that very large current pulses needed to
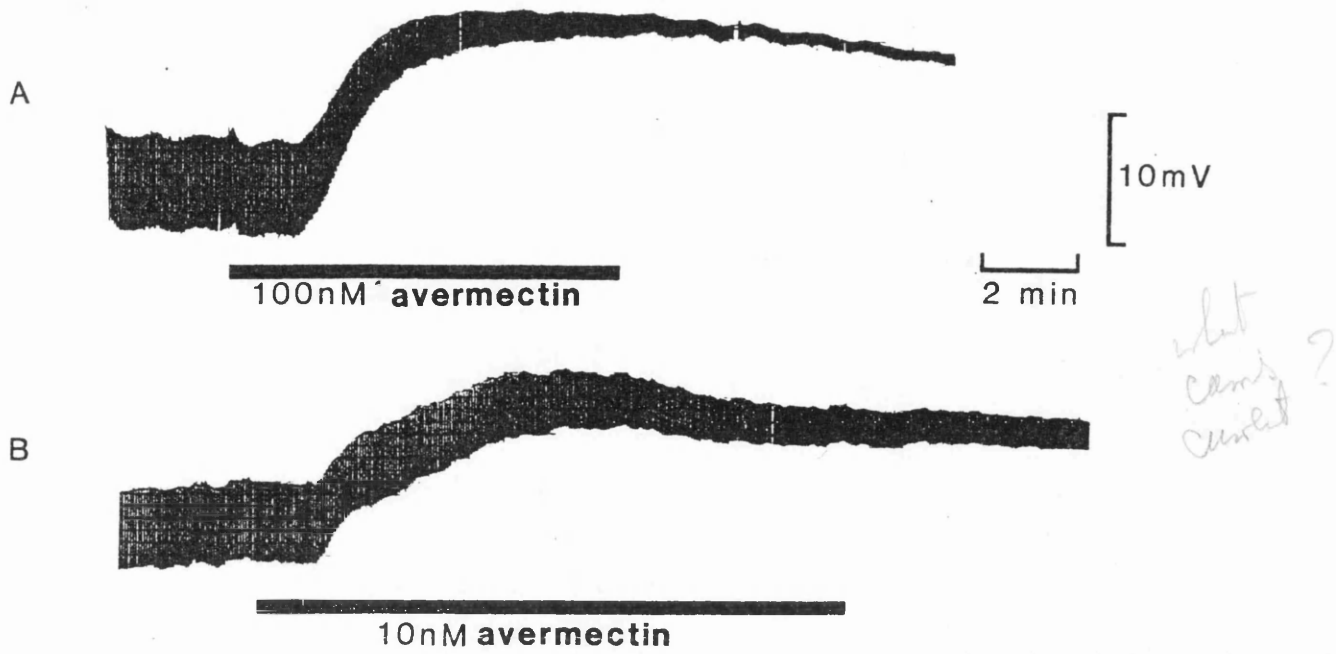
Figure 3.3 Effect of avermectin on muscle fibre membrane potential and input resistance in Plutella larvae. Hyperpolarising current pulses (10nA, 500ms) were passed at a frequency of 0.2Hz. 100nM avermectin (trace A) and 10nM avermectin (trace B) were applied during the bar.

Table 3.8

Effect of avermectin on passive membrane properties of muscle fibres from Plutella larvae.

	Membrane Potential (mV)	Input Resistance (kΩ)	Number of muscle fibres
Control	-47.3±2.6	650±110	4
100nM AVM	-25.8±4.1***	80±21*	4
Control	-41.3±2.8	610±31	3
10nM AVM	-30.9±2·4**	270±33*	3

Values given are means ± s.e.m. for the same fibres during perfusion with control saline and after 30 mins perfusion with saline containing either 100nM or 10nM AVM. *, p<0.02, **, p<0.005, ***, p<0.001, paired t test.

89

Table 3.9

Effect of 10nM avermectin on action potentials in muscle fibres from larval Plutella.

	Holding Potentials (mV)	Amplitude (mV)	Overshoot (mV)	Maximum Rate of Rise (Vs^{-1})	Duration (mS)	Number of muscle fibres
CONTROL	-49.2±1.5 (resting potential)	67.4±2.1	18.5±1.4	11.9±2.1	35.0±7.8	5
AVERMECTIN (10nM) 13mins	-49.8±1.7	64.3±5.7	20.3±7.3	9.8±1.7	29.7±4.6	
23mins	-49.1±1.6	68.2±2.3	20.1±1.8	13.4±2.5	30.4±8.1	5
33mins	-48.9±1.8	66.6±4.7	20.8±3.6	10.7±2.1	32.3±6.2	

Values given are means ± s.e.m. for cells perfused with control saline and following perfusion with 10nM AVM (for 13, 23 and 33 minutes). Cell membrane potential was held at or near the resting potential during perfusion with avermectin by steady passage of appropriate D.C. current. There were no significant differences from controls (paired t-test).

be passed through the intracellular electrode before any regenerative response was seen. At 10nM however, both the depolarisation and the increase in conductance, although irreversible, were small enough to allow recordings of action potentials following avermectin application.

As in previous experiments muscle fibres were impaled and action potentials were repetitively (0.1Hz) stimulated whilst perfusing with control saline and saline containing avermectin (10nM). The resting potential of cells was kept to the same value as that of the cell in control saline by DC current passage so as to reduce possible changes in Ca^{2+} channel activation kinetics and make comparisons more meaningful. The effect of 10nM avermectin on action potential parameters is shown in Table 3.9. Comparison of the values obtained in control saline against values obtained 10, 20 or 30 minutes after avermectin (10nM) was first applied revealed that no significant changes in action potential parameters occured.

Thus, although avermectin caused an increase in membrane conductance at the concentration used it did not appear to affect the Ca^{2+} channels involved in the action potential.

k)   Effect of LEMS IgG on action potentials.

Immunoglobulin (IgG) from patients with the autoimmune muscle weakness disorder Lambert-Eaton Myasthenic syndrome (LEMS) acts on voltage sensitive Ca^{2+} channels at the motor nerve terminal to cause their loss of function (see Introduction). The aim of the study in this section was to

determine whether LEMS IgG had any effect on Ca^{2+} dependent action potentials in Plutella muscles. Dissected specimens of Plutella were incubated for 24 hours in a dissecting saline containing either LEMS or control IgG before recordings of action potentials were made (Table 3.10). There were no significant differences between resting potentials in test and controls although resting potentials in both groups were slightly lower than those obtained in cells which had not been incubated for 24 hours (cf Table 3.6). The measured action potential parameters were not significantly affected by LEMS IgG as compared with controls (Table 3.10), indicating a lack of effect of LEMS IgG on these insect Ca^{2+} channels.

1) Discussion.

In this chapter the results show that the skeletal muscle fibres from larvae of the moth Plutella xylostella exhibit Ca^{2+}-dependent action potentials in the presence of TEA to block K^+ channels. This was shown by the fact that action potentials were reduced in amplitude and maximum rate of rise by a reduction in the external Ca^{2+} concentration and abolished in Ca^{2+}-free solutions or in the presence of inorganic Ca^{2+} channel antagonists. Sodium channels did not seem to be involved since TTX was ineffective on the action potential, and activation of Cl^- channels did not seem to be essential for action potential generation since removal of Cl^- or blockade of Cl^- channels with ethacrynic acid did not affect action potential generation.

The action potentials were found to be insensitive to

Table 3.10

Effect of LEMS antibody on action potentials in muscle fibres of Plutella larvae.

	Resting Potential of cells (mV)	Amplitude (mV)	Overshoot (mV)	Maximum Rate of Rise (Vs^{-1})	Duration (ms)	Number of cells
Control Antibody	-32.4±1.4	65.5±5.1	33.4±5.0	14.4±2.3	42±10	10
LEMS Antibody	-33.4±1.4	70.7±2.5	38.8±2.4	12.8±1.6	24.8±2.4	8

Values given are means ± s.e.m. averaged over muscle fibres incubated with control antibody or (different) muscle fibres incubated with LEMS antibody. There were no significant differences between the two groups (student's two-tailed t-test).

drugs from the three major classes of organic Ca^{2+} channel antagonists in Plutella, suggesting that L-type Ca^{2+} channels are not involved in the response. Neither are these channels antigenically similar to Ca^{2+} channels at the neuromuscular junction or L-type channels in NG108-15 cells as shown by the lack of action of LEMS IgG (which acts on such channels) on the action potential.

The types of Ca^{2+} channel involved in insect muscle action potentials have not so far been determined. Ashcroft (1981) reported that D-600, a derivative of verapamil, blocks action potentials in the muscle fibres of stick insect at micromolar concentrations. The lack of effect of these drugs in Plutella may indicate a difference in drug sensitivity or alternatively a species difference. Those studies where fibres have been voltage clamped suggest that both fast inactivating and slowly inactivating channels may underlie the action potentials (Ashcroft and Stanfield, 1982a,b, Yamamoto et.al., 1981, Yamamoto & Washio, 1981, Salkoff & Wyman, 1983).

TTX was ineffective on the action potentials in Plutella muscle fibres as it is in a number of other insect preparations (Deitmer and Rathmeyer, 1976, Ashcroft, 1981). This possibly indicates a lack of involvement of Na^+ channels in the action potential, indeed a lack of sensitivity to removal of Na^+ has been shown in a number of insect muscle preparations (Fukuda et.al., 1977, Washio, 1972). However, it is possible that TTX-insensitive Na^+ channels may exist in Plutella muscle fibres. The apparent lack of involvement of voltage-sensitive Na^+ channels in the

action potential may be a reflection of the different methods of exerting control over muscles in insects, as compared with vertebrates. In insects, fine control of contraction is produced by having graded, non-propagating 'action potentials' together with multiple inhibitory and multiple excitatory motor inputs which allow an individual muscle fibre to contract in a graded manner. This compares with the all-or-none contractions of individual vertebrate muscle fibres where graded contractions of fibre bundles are produced by changing the number of fibres contracting.

Experiments with Cl^- ion free solutions and the Cl^- channel blocking drug ethacrynic acid indicated that chloride ions were not necessary for triggering action potentials and that the after-hyperpolarisation was not due to chloride shifts. However, these experiments showed that Cl^- movements modified the action potential. The rate of rise of action potentials was larger in the presence of Cl^- ions, indicating larger inward currents. If we assume that the action potentials are based entirely on Ca^{2+} influx then this effect could be explained as a modulatory effect of Cl^- ions on Ca^{2+} channels or, more unlikely as a modulatory effect of the supposedly inactive anions used to substitute for Cl^-.

An alternative hypothesis is that part of the inward current that underlies the action potential is based on a movement of Cl^- out of the cell. Removing external Cl^- is expected to also reduce the internal Cl^- concentration (Rheuben, 1972), and this may account for a reduction in outward Cl^- current and hence maximum rate of rise. This

hypothesis requires that the reversal potential for Cl^- in this preparation lies positive to the resting membrane potential. In many Lepidopteran preparations this is indeed the case (Djamgoz, 1987). In this preparation, the use of 3M KCl in the intracellular microelectrode may give rise to Cl^- (and K^+) loading of the muscle fibres and produce a further shift of the Cl^- reversal potential in the positive direction. Large reductions in the rate of rise of action potentials by ethacrynic acid ($100\mu M$) were seen but these reductions did not attain statistical significance. However, although the results were not statistically significant for ethacrynic acid the rate of rise was markedly reduced and it may be that if further experiments had been done this may have attained statistical significance in which case Cl^- ions may contribute to the total ionic current under the conditions used in this study.

Further evidence for the existence of an additional inward current that is not based on Ca^{2+} in these fibres comes from experiments in which the external Ca^{2+} concentration was reduced from 10mM to 2.5mM. The expected change in rate of rise of action potentials (75% reduction) was greater than the actual change seen (56.1 ± 4.9%). Although this discrepancy may lie within the bounds of experimental inaccuracy, it nevertheless could be taken as evidence for the existence of channels other than Ca^{2+} channels being involved in the action potential. Since the complete removal of Ca^{2+} abolishes the action potential, this putative Cl^- channel would have to be Ca^{2+} activated. It should also be stressed that the action potential cannot

be abolished by the removal of Cl^-. Thus the action potentials in these fibres are largely dependent on Ca^{2+} influx, but a small contribution from a Ca^{2+}-activated Cl^- current cannot be completely discounted.

The lack of involvement of Cl^- ion movements in the afterhyperpolarisation may indicate that the K^+ currents in this preparation were not completely eliminated. In Carausius muscle fibres an 80% block of the delayed K^+ current is achieved with 120mM TEA (Ashcroft & Stanfield, 1982a) while in Drosophila 128mM TEA totally blocks this current (Salkoff & Wyman, 1983). In larval Tenebrio skeletal muscle fibres Yamamoto et.al. (1981) report that 50mM TEA is sufficient to block all outward currents. It is possible that in this preparation the K^+ currents have not been completely eliminated by the 25mM TEA used, although this concentration is sufficient to give an all-or-none response to depolarisation.

In Plutella muscles it was found that $10\mu M$ ryanodine greatly increased the duration of action potentials. Furthermore, the amplitude and overshoot of action potentials were also slightly increased and these effects on the action potential could be explained by direct actions to block K^+ currents or increase Ca^{2+} currents, or an indirect action on these currents by an alteration of intracellular calcium levels. An action of ryanodine to block the repolarising effects of K^+ currents in a locust skeletal muscle preparation was suggested by Usherwood (1962). However, no significant effect of ryanodine at this concentration was seen on the rate of fall of the action

potential as might have been expected if the K^+ current was blocked rendering the above explanation unlikely. The action of ryanodine in crab muscle fibres has been investigated by Goblet & Mournier (1981). In voltage clamped muscle fibres ryanodine was found to increase the calcium current at a given test potential, to inhibit the fast transient outward ('I_{K1}') current and to increase the delayed outward ('I_{K2}') current. It was established that the changes seen in the calcium current with ryanodine were due to changes in the activation/inactivation characteristics in the current. In the presence of ryanodine the Ca^{2+} channels underlying the current open at more negative potentials and are slower to inactivate (i.e. remain open for longer). Since crab muscle fibres undergo a prolonged contracture in the presence of ryanodine it was proposed that these changes (and those associated with the K^+ currents) were secondary to an increased intracellular Ca^{2+} concentration which will give rise to a 'surface charge effect' (Hille, 1984). This shifts the intramembrane potential seen by the putative voltage sensor of the Ca^{2+} channel in the depolarising direction. In Plutella muscle we see an increase in action potential duration and amplitude. This could also be explained in terms of an increase in Ca^{2+} current amplitude and duration. In rat cardiac muscle, ryanodine also prolongs action potentials (Mitchell et.al., 1984a, 1984b). This prolongation of the action potential was ascribed to a reduction in the intracellular Ca^{2+} concentration (by an inhibition of Ca^{2+} release from intracellular stores) reducing the degree of

Ca^{2+}-dependent inactivation of the calcium current (Eckert & Chad, 1984). This theory of reduced intracellular Ca^{2+} could also be applied to the changes seen in Plutella muscle fibre action potentials. Which of the two possible actions of ryanodine (i.e. either an increase or a decrease in release of Ca^{2+} from intracellular stores - see Introduction) are occurring in Plutella muscle fibres cannot be determined directly from the experiments reported here.

No evidence could be found for an action of avermectin on the Ca^{2+} channels underlying action potentials in Plutella at a concentration of 10nM. At this concentration significant changes in both input resistance and resting membrane potential occurred which indicates that AVM would have affected the action potentials if its main action were on insect Ca^{2+} channels. The findings reported by Hart et.al (1986) in locust neurones show that AVM and GABA appear to act on different postsynaptic ion channels. The channels activated by AVM in the neuronal preparation show characteristics one might expect of Ca^{2+} channels (Lacey, 1987), but our experiments clearly show that AVM has no effect on the voltage-activated Ca^{2+} channels underlying Plutella action potentials.

In summary, we have presented evidence that indicates that Ca^{2+} channels underlie the action potential in skeletal muscle fibres of larval Plutella. Ryanodine appears to delay the inactivation of Ca^{2+} channels possibly via its action on intracellular Ca^{2+} channels. Avermectin had no effect on these Ca^{2+} channels, and neither did LEMS IgG

which acts on certain vertebrate Ca^{2+} channels.

CHAPTER4

RESULTS

a) Introduction.

In this chapter, experiments were designed to investigate the physiology of calcium channels in insect neuronal cell bodies and to study their pharmacology. To do this, dissociated cells from the thoracic ganglia of the desert locust <u>Schistocerca gregaria</u> were voltage clamped using the whole cell patch clamp technique. Ba^{2+} was used as the charge carrier, and currents were elicited by step depolarisations. The types of calcium channels present were investigated by changing the holding potential and size of the depolarising steps. The effects on these calcium channels of inorganic and organic Ca^{2+} channel antagonists, ryanodine, pyrethroid insecticides and avermectin were investigated.

b) Properties of whole cell currents in locust neuronal somata.

The first priority in this study was to determine whether calcium currents exist in locust neuronal cell bodies and to identify their general characteristics. In this section the properties of inward currents seen in these cells under whole cell patch clamp are described.
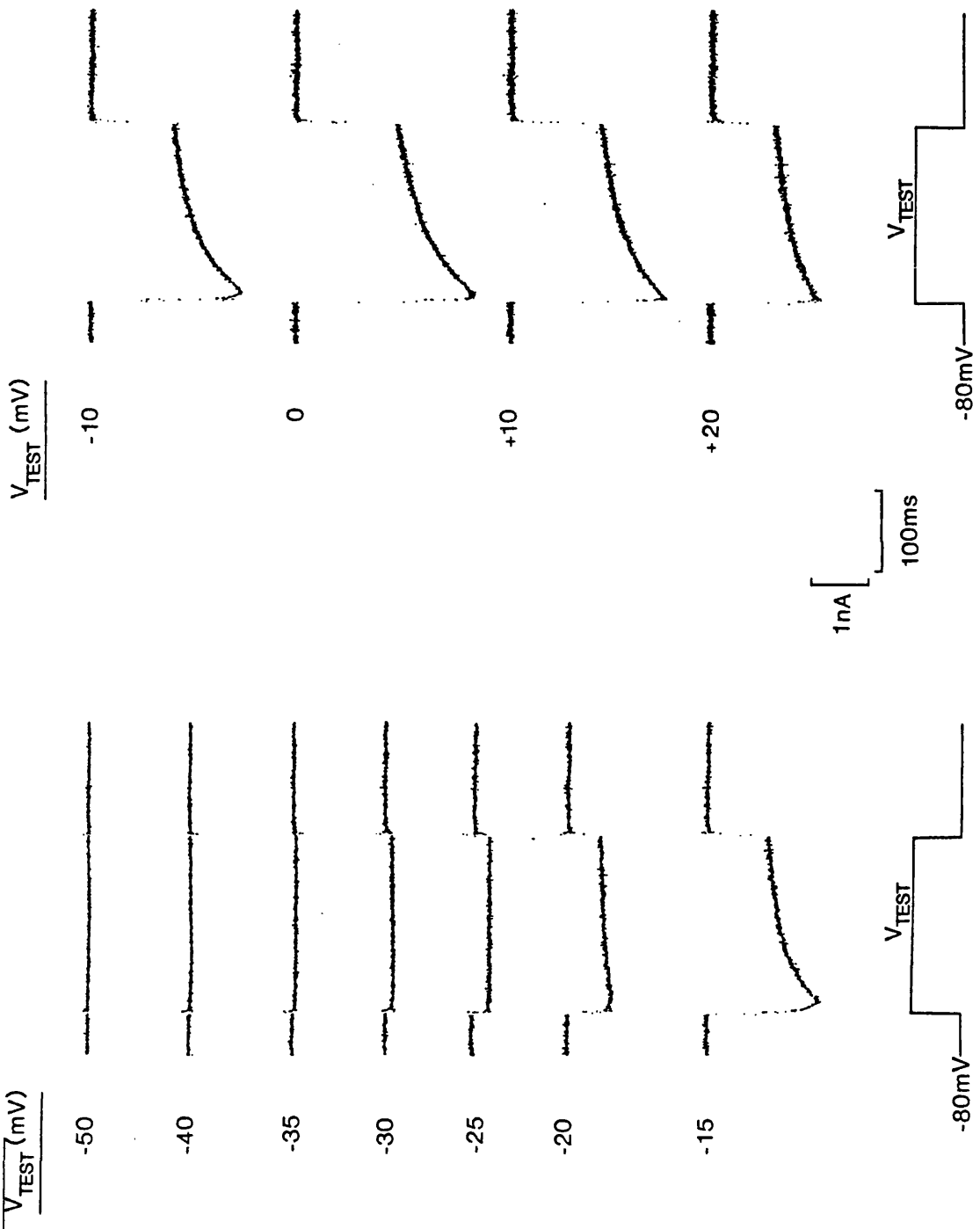
Whole cell patch clamp of dissociated cell bodies from thoracic ganglia of locust using salines designed to isolate the calcium channel current (see Methods) revealed the

presence of large inward currents activated by depolarisation of the cell. Figure 4.1 shows currents seen in a typical cell held at -80mV and with 10mM Ba^{2+} being used as the charge carrying ion and Figure 4.2 shows the I-V relationships for the currents in the same cell. In this cell an inward current was first seen when the cell was depolarised to test potentials equal to or greater than -35mV. At this test potential the current was small and sustained, being only very slowly inactivated throughout the step. Further depolarisiation to test potentials of -30 and -25mV resulted in larger inward currents which were also sustained in nature. With stronger depolarisation to test potentials of -20 to -10mV a rapidly inactivating phase of current was present together with the sustained current.

In most cells a similar current was seen. In three of the cells however, the sustained current was extremely small and only a transient current could be readily seen. The current seen in one of these cells is shown in Figure 4.3. In this cell an inward current was activated by a step to a test potential of -30mV from a -80mV holding potential. The current measured at the end of the depolarising step was very small in all cases (less than 0.06nA) and at all test potentials was less than 10% of the peak inward current.

Currents in these cells varied greatly in amplitude leading to large standard errors when IV curves from a group of cells were averaged together. More importantly, the presence of a cell with a larger inward current in a group leads to a weighting of the averaged IV curve in favour of that cell. In order to try to give cells of different sizes

Figure 4.1

V_{TEST} (mV)

-50

-40

-35

-30

-25

-20

-15

V_{TEST}

-80mV

V_{TEST} (mV)

-10

0

+10

+20

V_{TEST}

-80mV

1nA

100ms

see over for legend

103

<u>Legend for Figure 4.1</u>   Example of whole cell calcium currents in a locust neuronal cell.

Typical currents seen in a locust neuronal cell body under whole cell voltage clamp. The cell was held at a potential of -80mV and step depolarised to the test potentials as indicated next to each current trace. All records are leak and capacitance subtracted and were recorded sequentially from the same cell. The IV relationships for the peak and sustained current measurements from these traces are shown in figure 4.2.
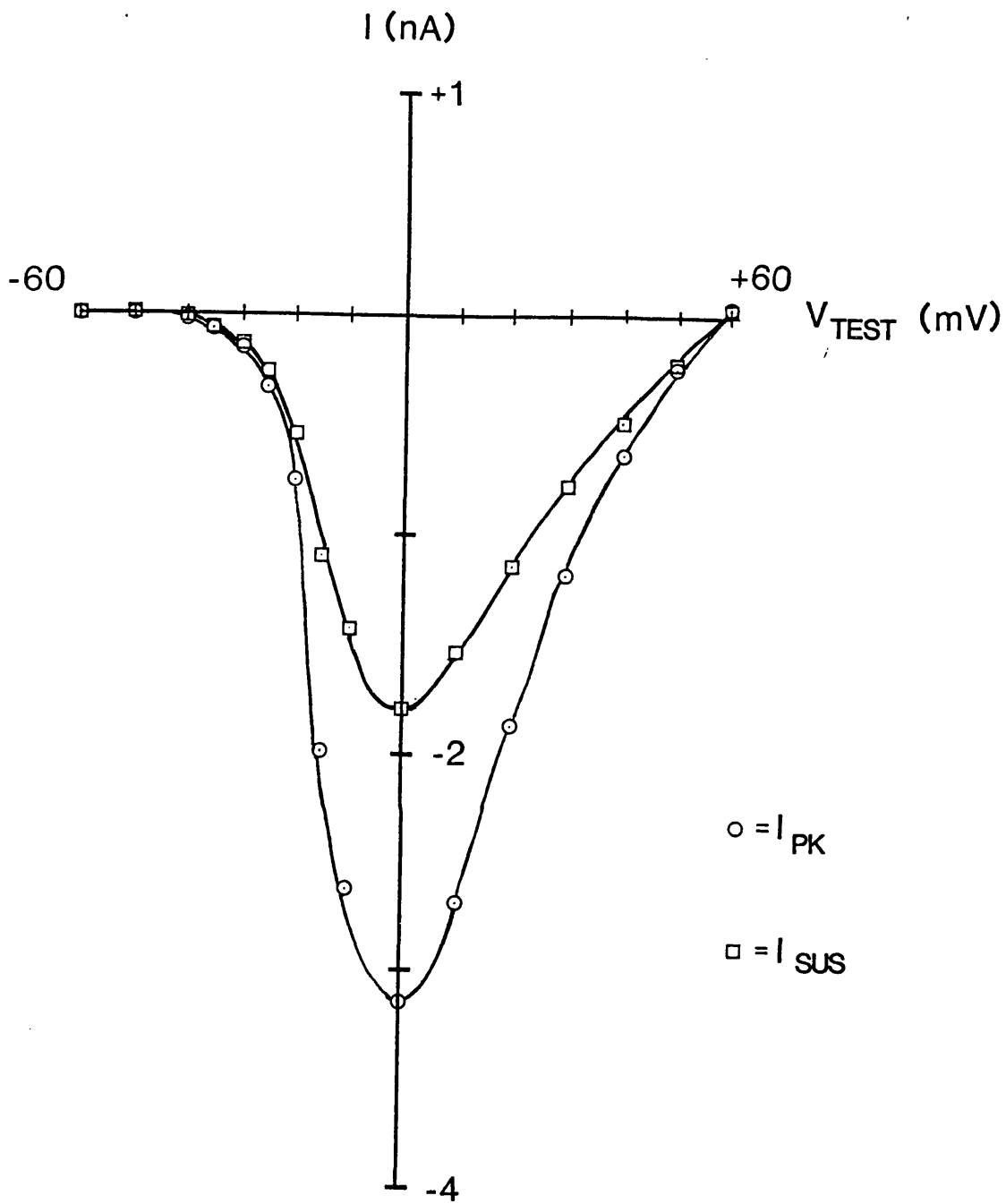
Figure 4.2 Current-voltage relationships for peak and sustained current measurements in a locust neuronal cell. I-V relationship for the peak (I_{PK}) and sustained (I_{SUS}) measurements from the same cell shown in figure 4.1.
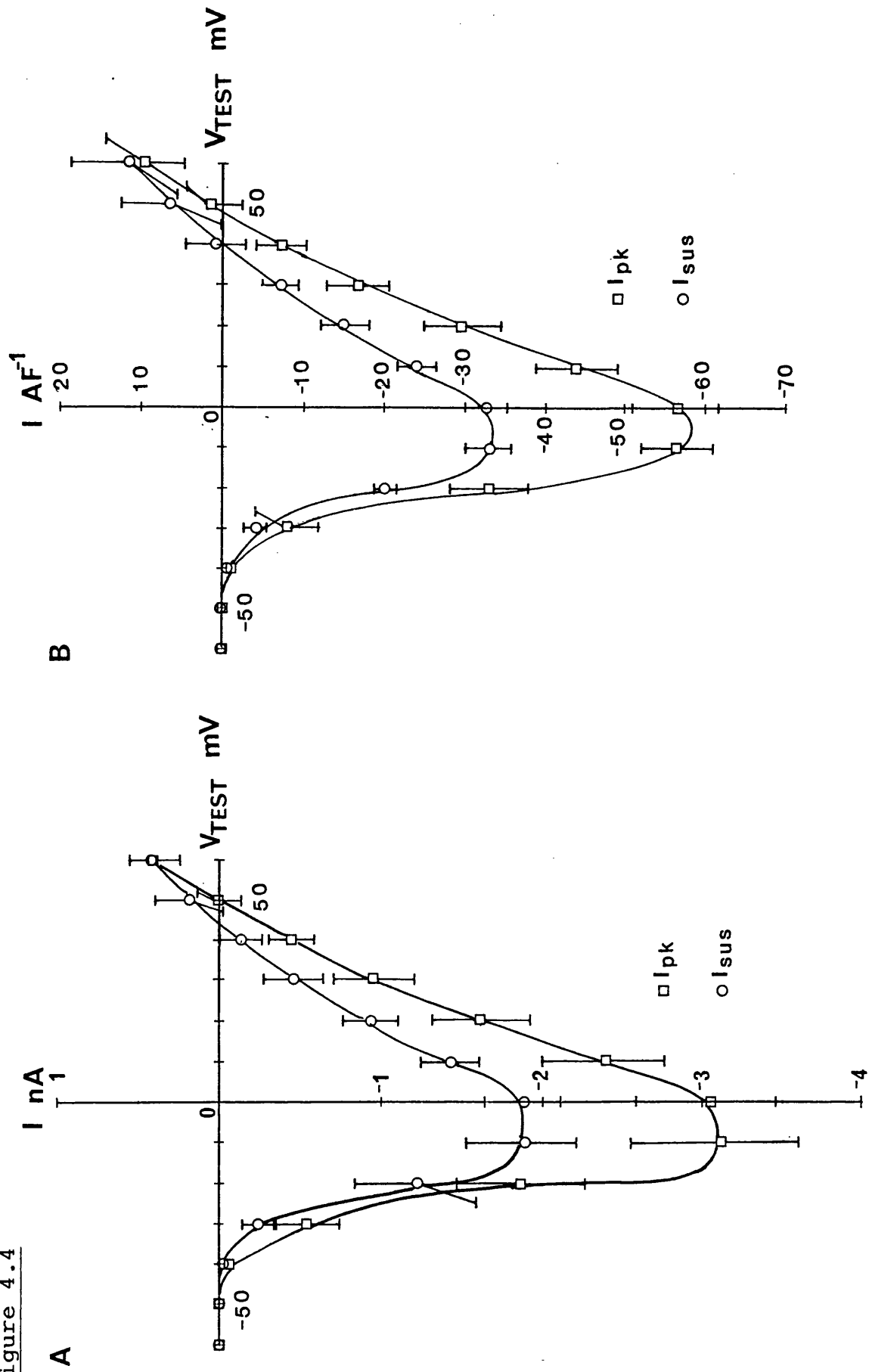
Figure 4.3

-40

-10

-30

·0

1 nA

100ms

-20

+10

I(nA)

+0.5

-60

V_{TEST}(mV)

+60

-0.5

-1.0
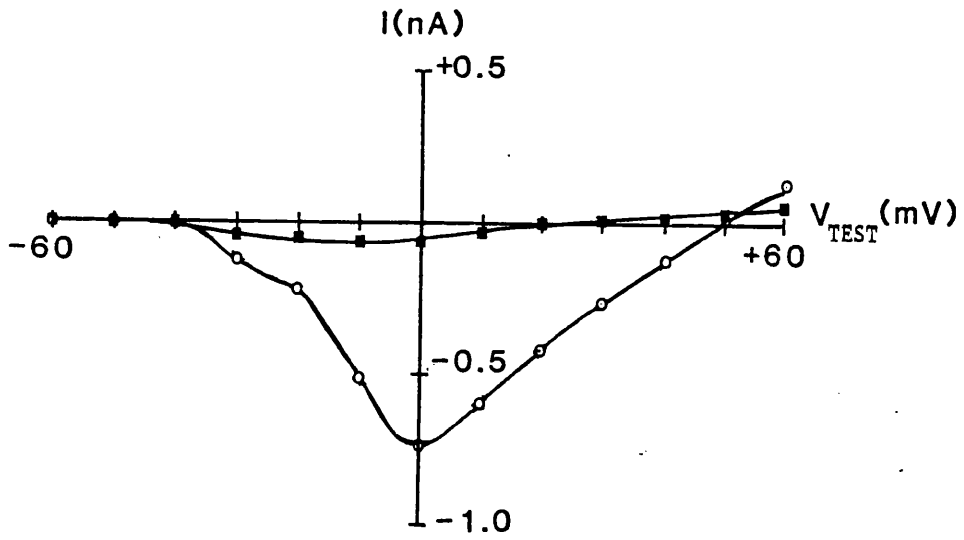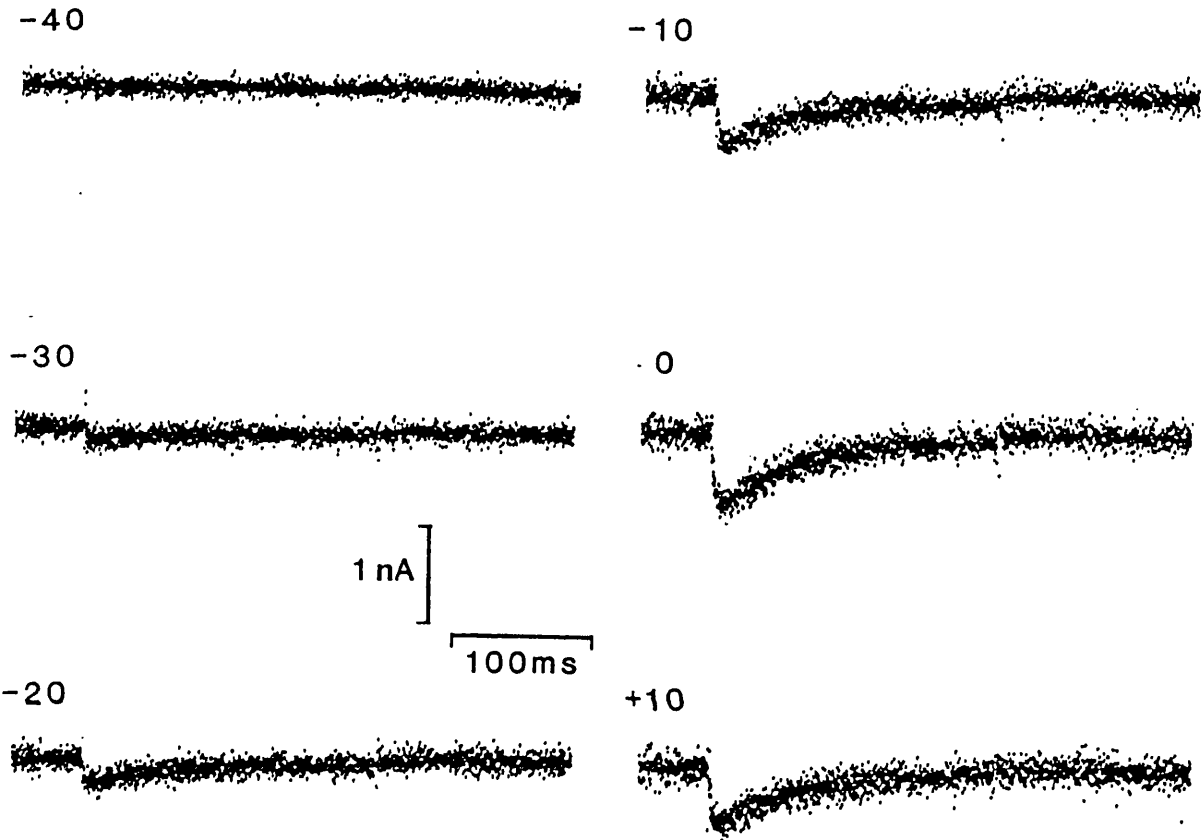
see over for legend

Legend for Figure 4.3   Currents and I-V relationship from a cell showing only transient currents.

This figure shows currents evoked in a cell (above) by stepping from a holding potential of -80mV to the test potentials (in mV) shown by each current trace. Below is the I-V relationships for the peak (open circles) and sustained (filled squares) current measurements made from the same cell.

equal weighting when IV curves were averaged together, currents in each cell were normalised by dividing by the capacitance of that cell, since this should correct for variations in cell surface area. The value obtained by this normalisation procedure indicates the density of current per unit area of cell membrane assuming that cell capacitance is directly proportional to membrane surface area. Figure 4.4 shows averaged IV relationships for 58 cells before normalisation (graph A), and after normalising (graph B) by dividing the current in each cell by the cell's capacitance before averaging IV curves together for the same group of cells. This gives smaller standard errors in the points of the IV curve after normalisation and this reduction may indicate that the current is indeed proportionally related to the cell capacitance. A scatter diagram showing the relationship between the peak inward calcium channel current at 0mV test potential, -80mV holding potential, to the capacitance in each cell is plotted in Figure 4.5. This indicates that there is indeed a roughly linear relationship between cell capacitance and the size of the inward current seen in these cells. There is of course, still some scatter about this line. The slope of the line fitted for the data in Figure 4.5 was 57.1pA/pF. At the test potential used for this graph inward currents were maximal (see fig.4.4). If we assume that the membrane of these cells has a capacitance of $1\mu F$ per cm^2 (Katz, 1966), then this represents a current density of $57.1\mu A/cm^2$ or $0.571pA/\mu m^2$

In summary, freshly dissociated neuronal cell bodies from the thoracic ganglia of locust show large inward
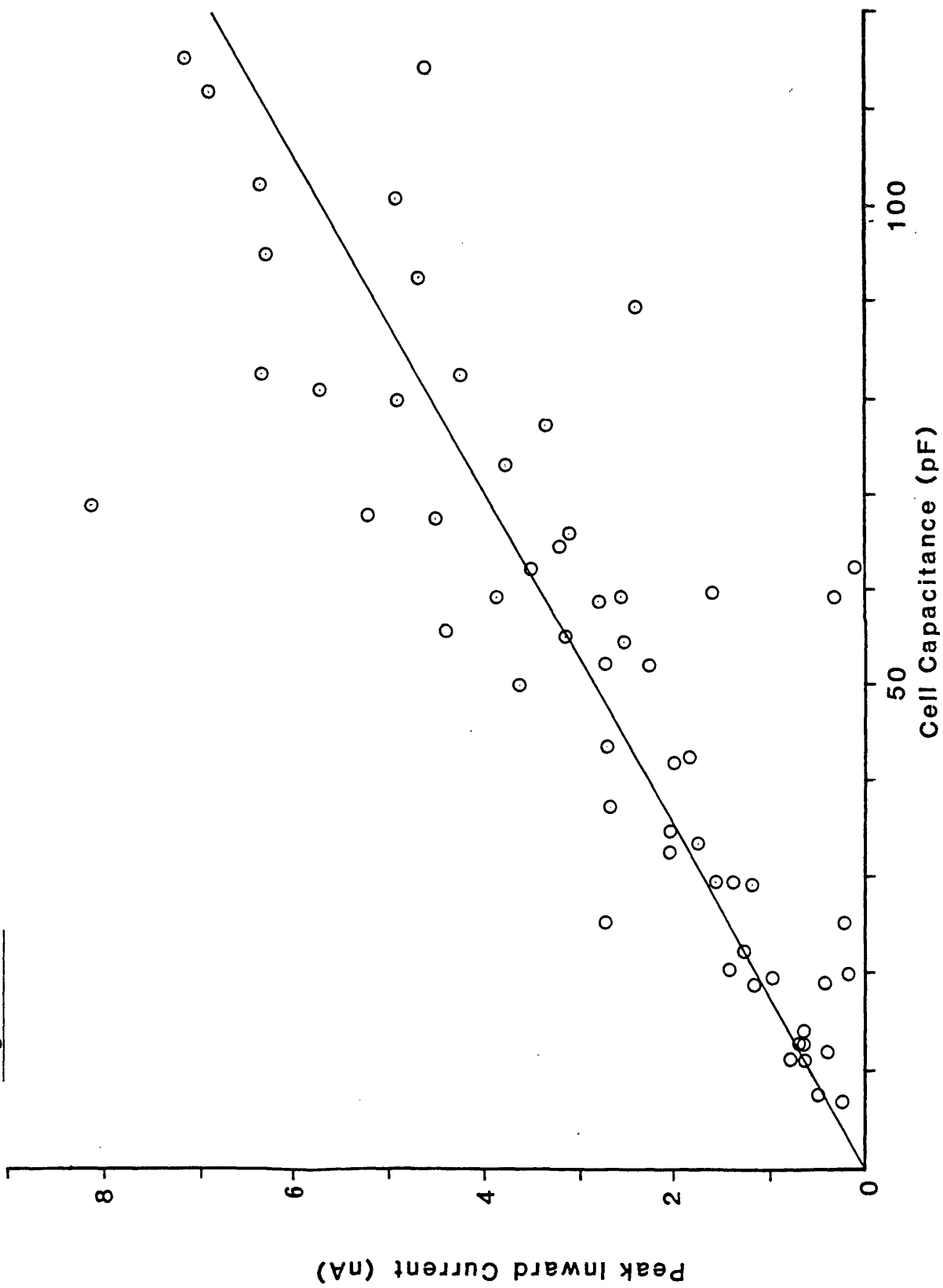
Figure 4.4

A

B

see over for legend

<u>Legend for Figure 4.4</u> Averaged IV relationships before and after normalisation.

Mean IV relationships from control cells. In graph A, peak (I_{PK}) and sustained (I_{SUS}) currents are shown. In graph B, these currents for the same cells as in graph A were first normalised by dividing by the cell capacitance before being averaged. The holding potential was −80mV and leak and capacitance artefacts have been subtracted. Values shown are means ± s.e.m. averaged over 58 cells.

Figure 4.5

see over for legend

111

<u>Legend for Figure 4.5</u>   Relationship between inward current and cell capacitance.

Graph of peak inward current plotted against cell capacitance. Each point is for a different cell. Peak inward current (I_{PK}) was measured usng a holding potential of -80mV and a test potential of 0mV. The straight line is a linear regression fit to the data and has a slope of 57.1AF^{-1}.

currents. These Ca^{2+} channel currents usually showed two phases, one inactivating and the other sustained. Current amplitude was roughly proportional to cell size, indicating a similar current density between cells and allowing the normalisation of currents between individual cells.

c) Run-down of calcium channel currents

Calcium currents in many neuronal preparations under whole cell patch clamp are notoriously labile and will rapidly decrease ('run down') due to exchange ('dialysis')of intracellular factors with the pipette solution. Run-down was present in the locust neuronal cells and although a variety of phosphorylating agents and protease inhibitor 'cocktails' were used, none appeared to markedly prevent the gradual disappearance of the current.

In subsequent experiments however, it was observed that rundown varied markedly between batches of cells and seemed to depend to a certain degree on seal resistance after rupture of the membrane patch to achieve the whole cell configuration. In all experiments in this thesis, cells were therefore chosen in which the seal resistance was better than 5 GΩ and in which 3-4 depolarising steps to -10 mV did not initially show marked rundown. An average experiment required 10-15 minutes, so that potentially rundown could be important. However, this was controlled for by; (i) the above choice of cells which showed little or no rundown, (ii) calculating the rundown by also measuring currents after washing off drugs (where possible) at the end of every experiment.

d)   Effect of holding potential on calcium currents.

In many neuronal cell types it has been found that different components of the calcium channel current can be isolated by imposing more depolarised holding potentials on the cell.   The 'T'-type component is largely inactivated at holding potentials of -40 to -30mV leaving mainly the 'L'-type current.   In these experiments 14 cells were held at a range of holding potentials and test depolarisations applied.   The IV curves at each holding potential are shown in Figure 4.6 for the peak current.   From a holding potential of -80mV, activation of the inward current started to occurr at approximately -40mV and reached a maximum at around -10mV.   At holding potentials of -60mV to -30mV, the current was significantly reduced in amplitude but the maximum (-10mV) and activation voltage (-40mV) were largely unchanged.   At -20mV holding potential no inward current was seen, the mean current from this group of cells being always outwardly directed.   Apparent reversal potentials were found to become more negative as the holding potential became more positive.   This change however may be due to incomplete block of background outward currents in these cells.   When the inward current is large any outwardly directed currents would be masked, but at the more depolarised holding potentials, where the calcium channel current is inactivated, the effect of the outward current in shifting the apparent reversal potential in the more negative direction would dominate.   This effect is most obvious at the -20mV holding potential where the calcium channel
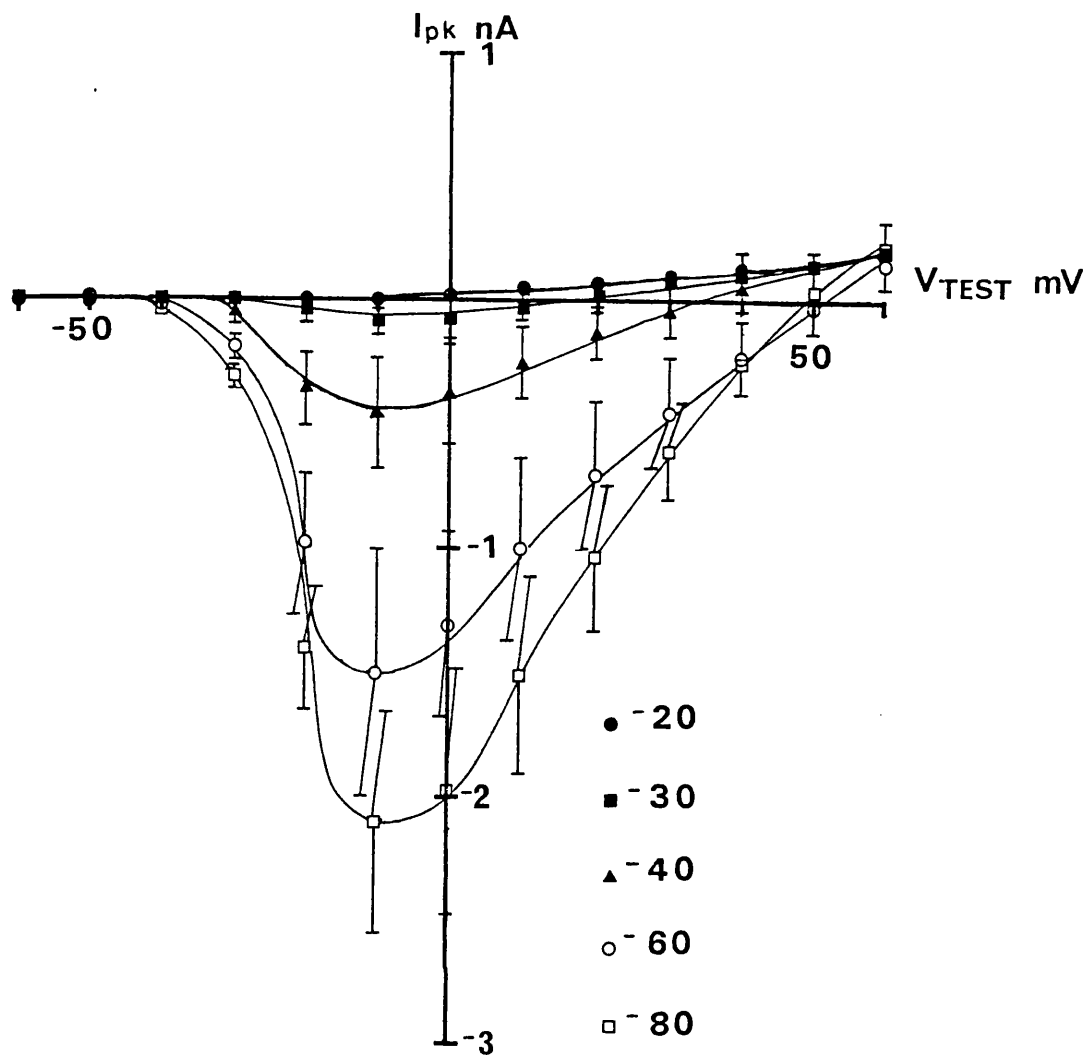
114

Figure 4.6 Effect of holding potential on peak current.
I-V relationships at different holding potentials (shown on
graph in mV) for the peak inward current. Cells were held
successively at each holding potential while I-V
relationships were constructed. Values shown are means ±
s.e.m. of the peak inward current averaged over 14 cells at
each holding and test potential. Values were leak and
capacitance subtracted but not normalised and are from the
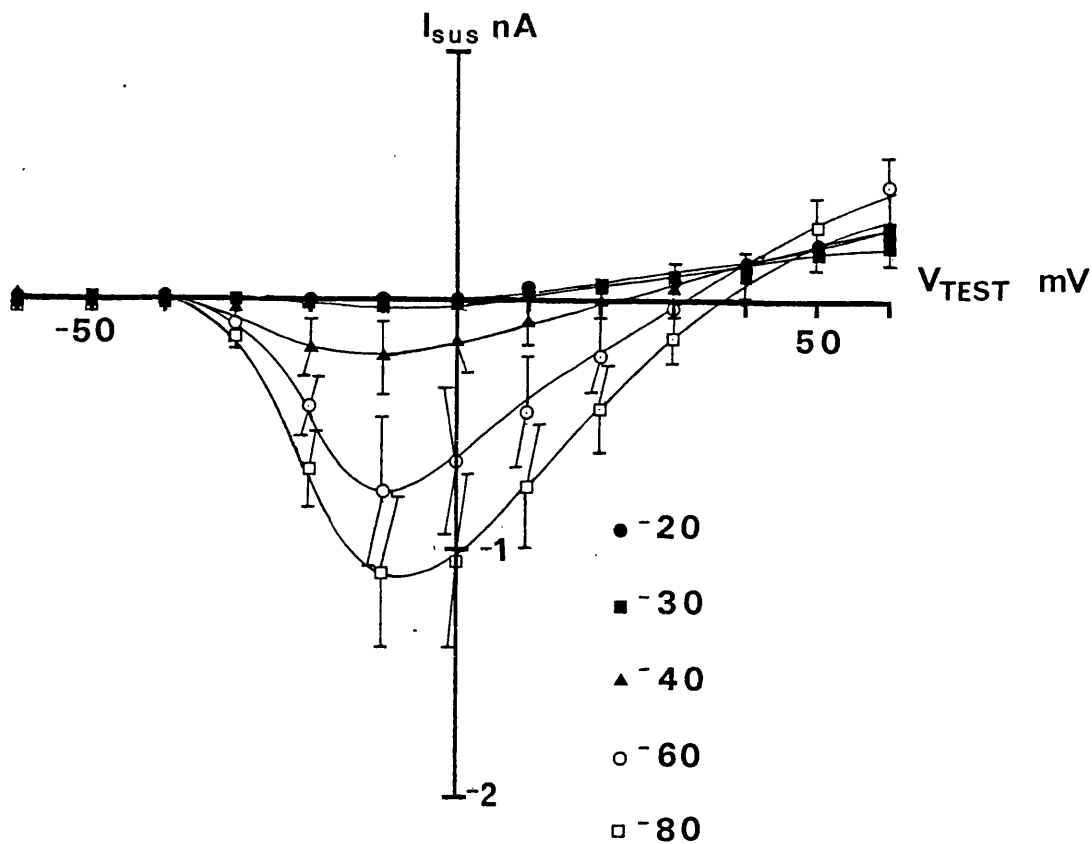same cells shown in figure 4.7.

Figure 4.7   Effect of holding potential on sustained current.

I-V relationships at different holding potentials (shown on graph in mV) for the current measured at the end of a voltage step (sustained current).   Cells were held successively at each holding potential while I-V relationships were constructed.   Values shown are means ± s.e.m. of the sustained current averaged over 14 cells at each holding and test potential. Values were leak and capacitance subtracted but not normalised and are from the same cells shown in figure 4.6.
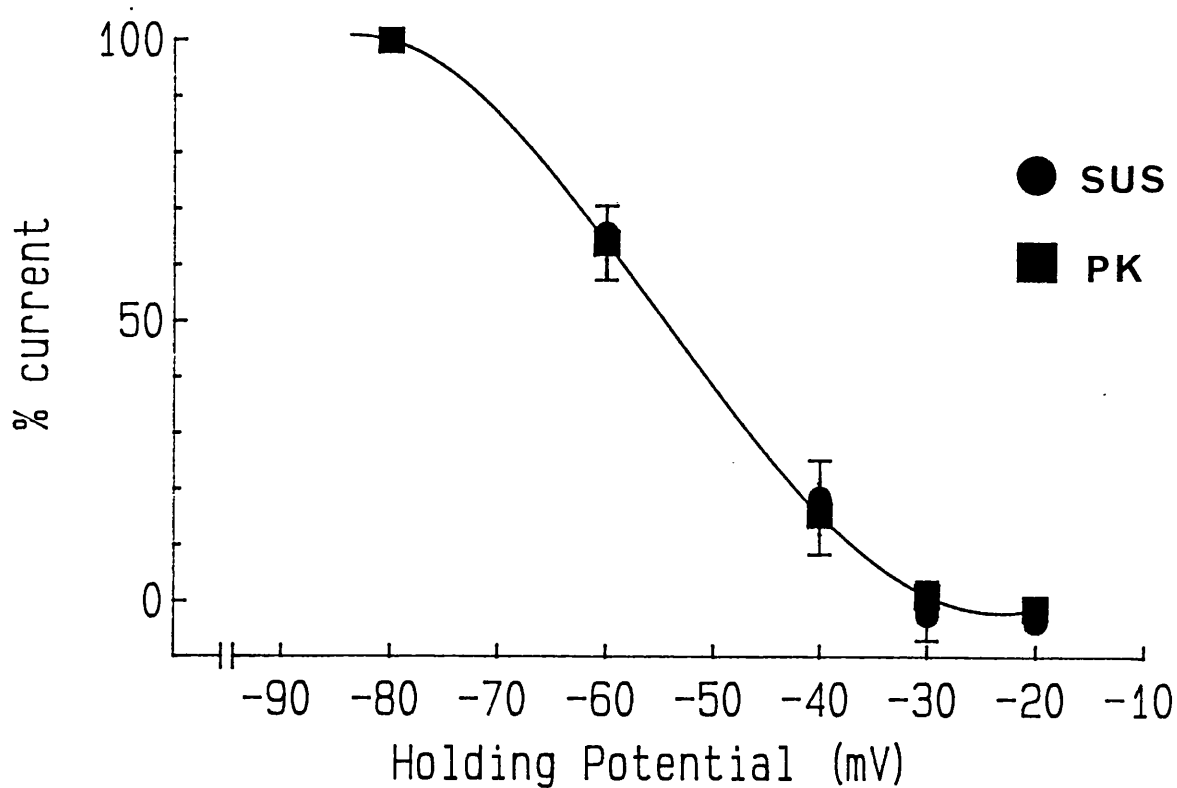
Figure 4.8 Comparison of steady state inactivation kinetics of peak and sustained currents.

Peak (PK) and sustained (SUS) currents are shown here expressed as a percentage of the peak and sustained currents at a holding potential of -80mV and plotted against the holding potential from which they were measured. Individual cells were held successively at each holding potential for 90 seconds before an I-V relationship at that test potential was constructed. Current values at each holding potential and the test potentials between -20mV and +20mV for each cell were then expressed as percentages of the current at-80mV and averaged over the 14 cells used. No significant differences between peak and sustained values at each holding potential were found (paired t-test).

current is completely inactivated and hence only the outward current is seen.

For the sustained current (I_{SUS}) similar results were observed (Figure 4.7) as for peak currents, except that currents were of course smaller. To investigate the relative extent of inactivation of peak and sustained currents at different holding potentials, the curves shown in Figures 4.6 and 4.7 at different holding potentials were expressed as percentages of the values at -80mV (Figure 4.8). There were no significant differences between the peak and sustained measurements at each test potential and holding potential. Thus the degree of steady state inactivation was the same for both peak and sustained currents. As expected, percentage currents were similar at the same holding potential but at different test potentials showing that the steady state inactivation for I_{PK} and I_{SUS} currents was the same throughout the test potential range. In summary, both peak and sustained currents are maximal at a holding potential of -80mV and have similar steady state inactivation characteristics. Thus there could be two types of channel (transient and sustained) with similar steady state inactivation kinetics or simply one type of channel displaying both transient and sustained characteristics.

e) Effect of calcium substitution and choline substitution on calcium channel currents.

The experiments described in this section were performed to test whether the inward current was carried by Ca^{2+} as well as Ba^{2+} and also to determine any possible

Table 4.1   Effect of charge carrier (Ca^{2+} or Ba^{2+}) and choline substitution on inward currents in locust neuronal cell bodies.

Extracellular solution	Mean maximum inward current amplitude (nA)	Mean normalised maximum inward current amplitude (AF^{-1})	Reversal Potential (mV)	Number of cells	Mean cell capacitance (pF)
10mM Ba^{2+}, Na^+, K^+, Mg^+	3.11±0.48	56.5±5.5	49.5±4.4	58	55.1±8.9
10mM Ca^{2+}, choline	2.32±0.41	40.3±2.3*	45.9±2.4	19	70±12*
10mM Ba^{2+}, choline	2.13±0.30**	48.3±6.5	48.1±6.2	17	44±13

Normalised currents were calculated by dividing current values from each cell at each test potential by the cells capacitance. The normalised and un-unormalised maximum inward current for each cell was obtained from the IV relationship to which a curve passing through all the points had been fitted by eye. These values for each cell were then averaged together. Reversal potentials were also obtained from this curve. *, $p<0.02$, **, $p<0.01$, students two-tailed t-test.

119

involvement of Na^+ in the inward current.

In early experiments a saline containing Ca^{2+} as the charge carrier and with choline substituting for Na^+ and K^+ was used to bathe the cells during recordings (see Methods, Table 2.2). A similar saline, containing 10mM Ba^{2+} and choline was also used on some cells. The currents obtained when locust neuronal cell bodies were bathed in these salines are compared against control currents from cells bathed in the standard recording saline in Table 4.1. Currents measured in cells bathed in the saline containing 10mM Ba^{2+} and in the presence of Na^+, K^+ and Mg^{2+} were significantly ($p<0.01$) larger than those measured in 10mM Ba^{2+} but with choline substituting for all other cations. This is perhaps a reflection of the size of cells used, since after the normalisation procedure which corrects for variations in cell size between groups of cells (see above) no significant differences between the amplitude of currents in these two groups of cells could be found.

On the other hand, the absolute values of currents measured using Ca^{2+} as the charge carrier showed no statistically significant differences from those in cells bathed in either of the Ba^{2+} salines, but normalised values were significantly lower (see Table 4.1). Again, the size of the cells sampled in each group may be important. The cells bathed in Ca^{2+} saline were significantly bigger than those in either of the Ba^{2+} salines (if we assume that cell capacitance is a reliable indicator of cell size) which might explain this apparent anomaly. Thus it would appear that the Ca^{2+} channels underlying the inward current in

120

these cells are more permeable to Ba^{2+} than Ca^{2+}. The mean apparent reversal potentials of these currents in all three of the bathing salines did not significantly differ from each other, suggesting that $Ba+$ and Ca^{2+} (but little, if any, Na^+) permeates the Ca^{2+} channel in these cells.

f) Effect of cadmium on calcium currents.

In order to ensure that the inward current seen in these cells is indeed based on the influx of Ba^{2+} through voltage sensitive Ca^{2+} channels, the inorganic Ca^{2+} channel blocking agent Cd^{2+} was applied to cells.

To obtain the control IV curve, neuronal cell bodies were voltage clamped at a holding potential of -80mV and step depolarised (200ms, 0.1Hz) to test potentials ranging from -60 to +60mV under perfusion in the bath with control saline. Repetitive (0.1Hz) steps of 200ms duration to a test potential of -10mV were then performed continuously before and during perfusion with saline containing Cd^{2+}, and during washout of Cd^{2+} with the control saline. In some experiments, IV curves were also obtained before, during and after treatment with Cd^{2+} using a range of test potentials as above.

Figure 4.9 shows the effect of 1mM Cd^{2+} on the inward current in one of these cells. As Cd^{2+} was applied, the amplitude of the current rapidly decreased until after 4-5 minutes the current had disappeared altogether. This effect could be reversed by washing the cell in control saline. In all 3 cells tested Cd^{2+} at a concentration of 1mM was found to completely abolish the inward current, and in each case

Figure 4.9

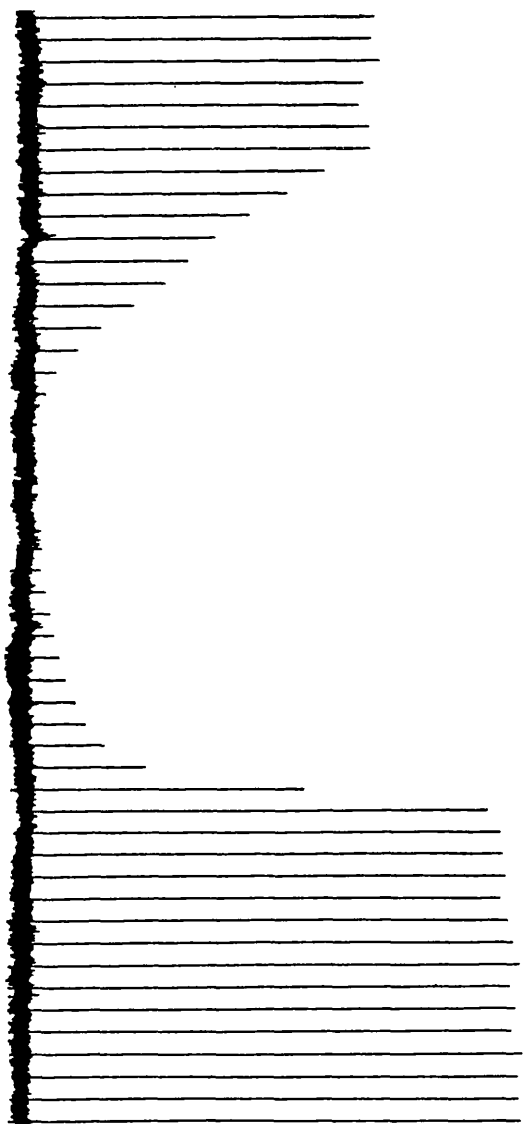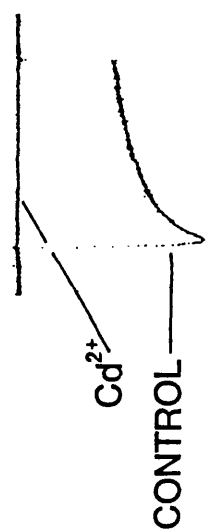VOLTAGE

−10mV
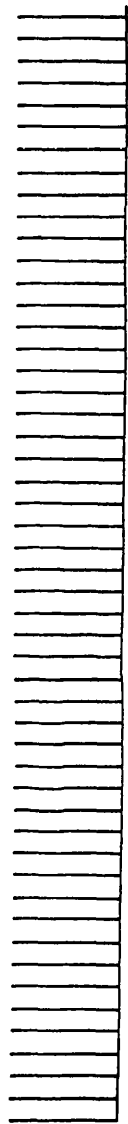
−80mV

CURRENT

1nA

1min

Cd²⁺

Cd²⁺

CONTROL

2nA

200ms

see over for legend

122

Legend for Figure 4.9 Effect of 1mM Cd^{2+} on calcium channel
current.

Block of inward current by 1mM Cd^{2+}. Cd^{2+} was added by
perfusion to the saline bathing a cell held at a potential
of -80mV and repeatedly stepped to a potential of -10mV
(0.1Hz for 200ms). The inset shows the current before and
during perfusion with Cd^{2+} on an expanded timescale.

Figure 4.10

4 mins

1 nA

10 µM Cd²⁺

1 min

DIFFERENCE

10 µM Cd²⁺

CONTROL

1 nA

200 ms
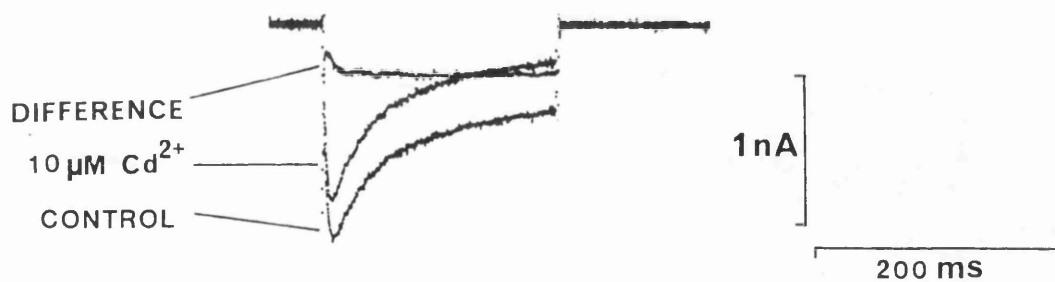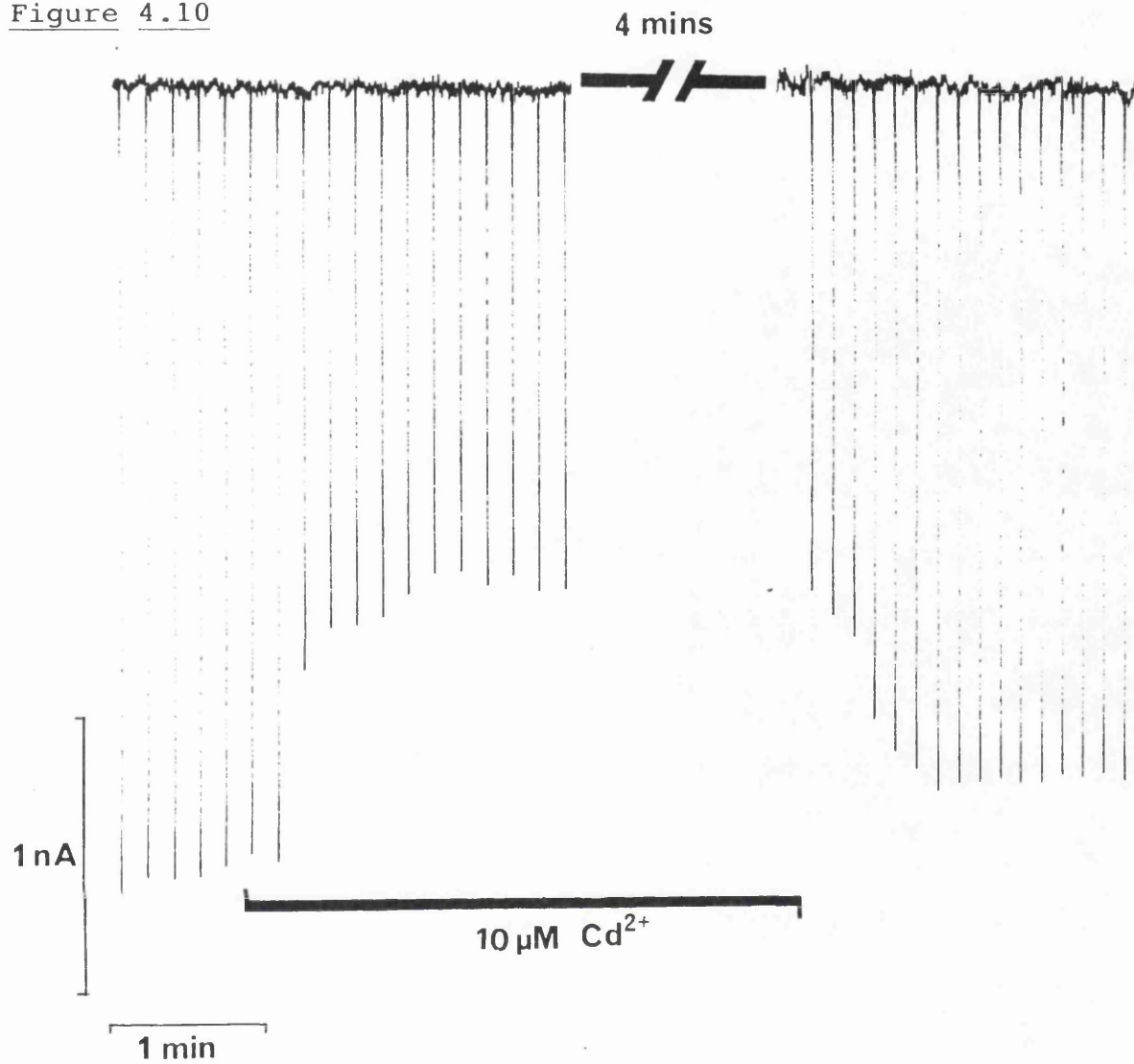
see over for legend

Legend for Figure 4.10   Effect of $10\mu M$ Cd^{2+} on calcium channel current.

Cd^{2+} was applied by perfusion during the bar. The holding potential of the cell was -80mV and the cell was repeatedly stepped to a test potential of -10mV (0.1Hz for 200ms). The inset shows this effect on the current on an expanded timescale. Also shown in the inset is the difference current which was obtained by subtracting the current evoked in the presence of $10\mu M$ Cd^{2+} from the control current. This difference current represents the current component blocked by $10\mu M$ Cd^{2+}. During the 4 minute gap before wash of the cell an I-V relationship was constructed and leak and capacitance subtraction steps were made.

was found to be readily reversible by washing. Thus it is clear that Ca^{2+} channels are involved in the inward current.

Lower concentrations of Cd^{2+} selectively inhibit L- and N-type (but not T-type channels) in vertebrates, so experiments were performed here to investigate the channel types involved using a concentration of $10\mu M$ Cd^{2+} (Figures 4.10 and 4.11). It can be seen in Figure 4.10 that only a partial block of the calcium current occurs. The inset shows the extent of this block more clearly, together with the difference current, obtained by subtracting the current obtained in the presence of $10\mu M$ Cd^{2+} from the control current. This difference current, which represents the blocked component of current, can be seen to be only very slowly inactivating. The IV relationships in control saline and following treatment with $10\mu M$ Cd^{2+} are given for the same cell in Figure 4.11. It can be clearly seen that there was a marked reduction in the sustained component (I_{SUS}) together with a negligible effect on the transient component (I_{DIFF}). The small reduction in I_{PK} appears to come about via the underlying reduction in the sustained component rather than a change in the transient component. This was confirmed by averaging values of the percentage changes in each current measurement for 3 cells, mean values being reduced by; 46 ± 14 % (I_{PK}), 70.5 ± 6.6 % (I_{SUS}) and 19 ± 12 % (I_{DIFF}). This action on the sustained component can also be clearly seen when IV relationships for the difference in current in the presence or absence of Cd^{2+} are studied (Figure 4.12). The IV curves show that the blocked component of current is indeed sustained in nature since
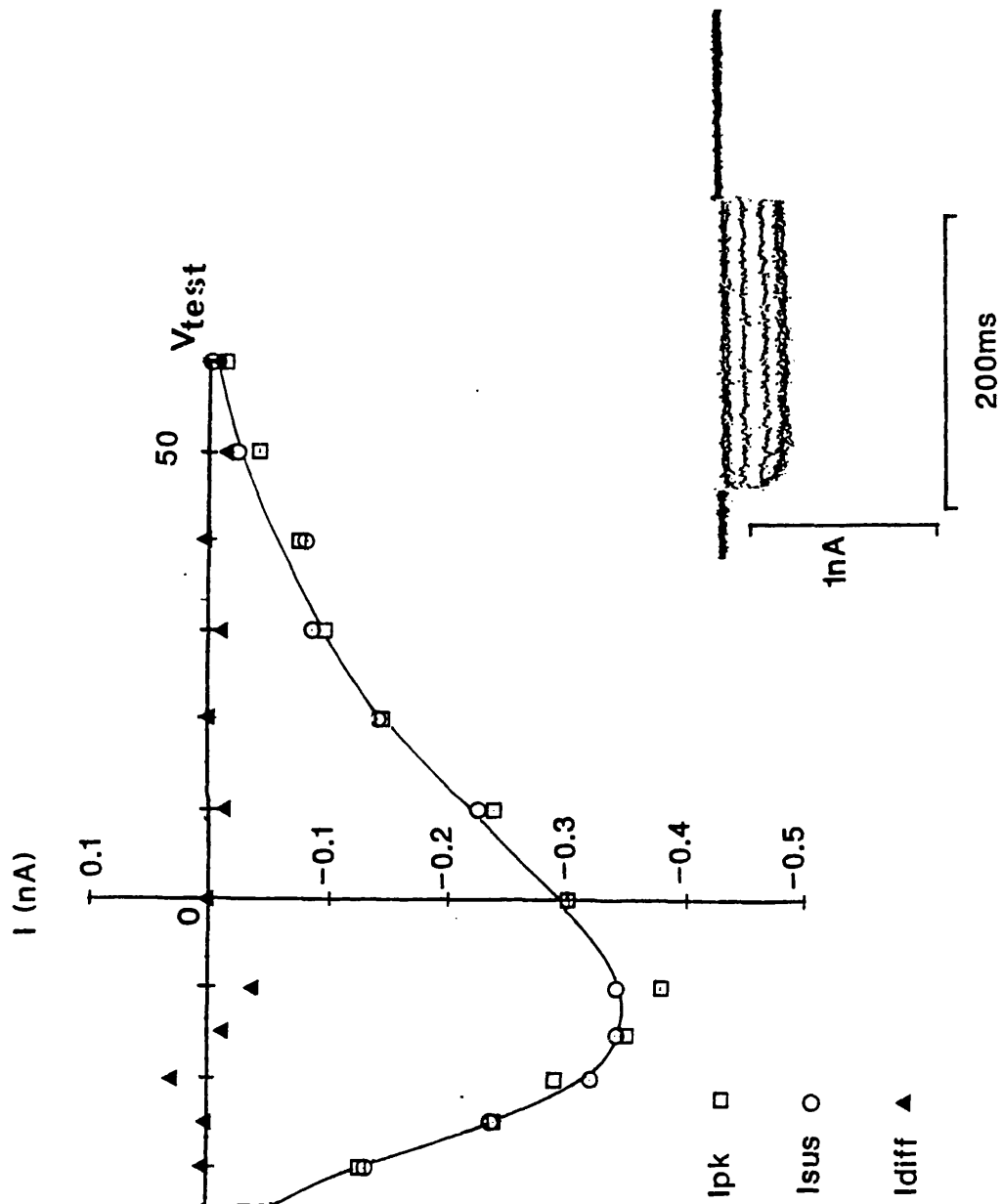
Figure 4.11

127
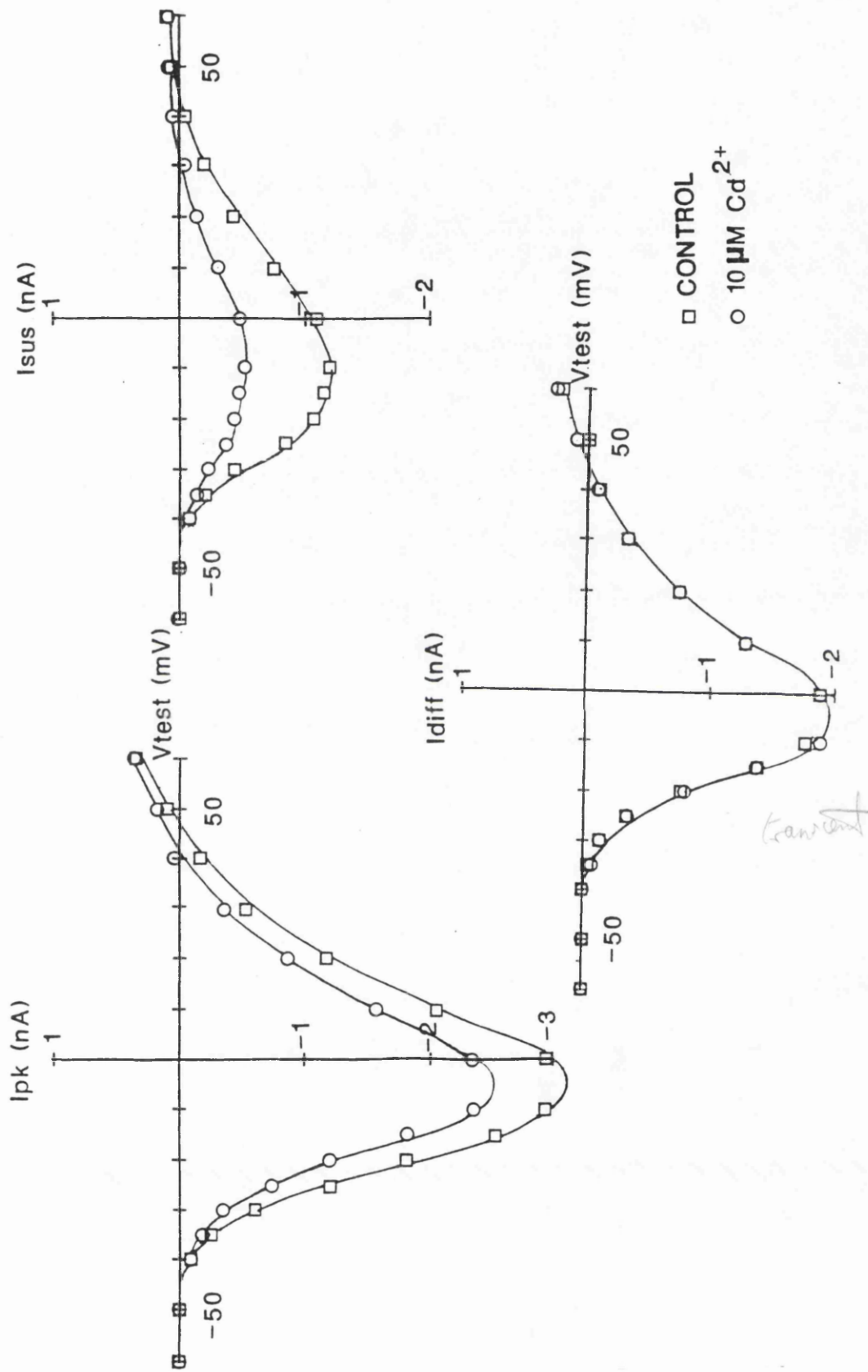
<u>Legend for Figure 4.11</u>   Effect of $10\mu M$ Cd^{2+} on I-V relationships.

I-V relationships for I_{PK} (top left), I_{SUS} (top right) and I_{DIFF} (bottom) before and during perfusion with $10\mu M$ Cd^{2+}. Values were leak and capacitance subtracted and were obtained from the same cell shown in fig 4.8 and 4.10.

Figure 4.12

see over for legend

129

Legend for Figure 4.12   I-V relationship for the current
component blocked by 10μM Cd^{2+}.

Values for each parameter (I_{PK}, I_{SUS} and I_{DIFF}) were
obtained by subtracting the current measured at each test
potential in the presence of Cd^{2+} from the control current
measurement at the same test potential. Currents were leak
and capacitance subtracted before measurement. The inset
shows the equivalent current traces for the component of
current blocked by 10μM Cd^{2+} at test potentials ranging from
-40mV to -10mV. These were obtained by subtracting the
current trace obtained in the presence of 10μM Cd^{2+} from the
control current trace at the same test potential. Data are
from the same cell shown in figures 4.8 and 4.9.

I_{DIFF} is near zero (ie both I_{PK} and IRLX values are almost exactly equal) throughout the range of test potentials studied (see also inset). It is also apparent that this Cd^{2+} sensitive component is activated at a test potential of approximately -45mV and reaches a peak at approximately -10mV. These values are similar to those seen in control cells.

In summary therefore, these results demonstrate firstly that Ca^{2+} channel currents underly the inward current, and that two components of the calcium current exist in these cells. One is blocked by $10\mu M$ Cd^{2+} and is sustained (slowly inactivating) in nature, the other is transient in nature and is completely abolished only by application of 1mM Cd^{2+}.
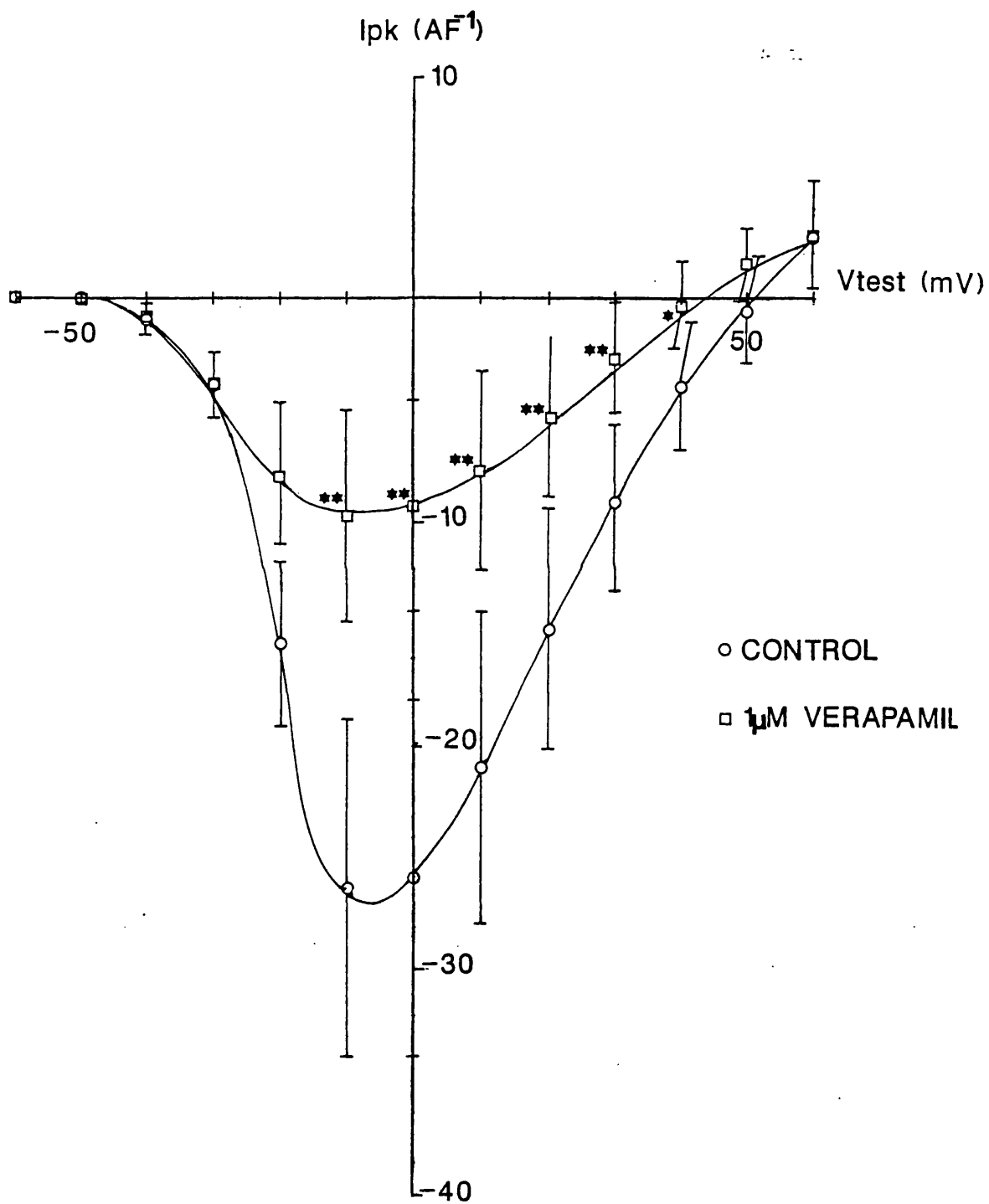
g) Effect of verapamil on calcium currents.

Organic calcium channel antagonists act on L-type channels in vertebrates (see Introduction), and in this section the action of verapamil was tested on the calcium channel currents in cells from locust ganglia in an attempt to pharmacologically classify the channel types present.

Neuronal cell bodies were voltage clamped at a holding potential of -80mV, again using the whole cell patch clamp technique. Whilst being perfused in the bath with control saline (5-10ml/min) cells were depolarised from the holding potential to test potentials ranging from -60 to +60mV (duration 200ms, at 0.1Hz) to allow construction of IV relationships. Following this the cells were then repetitively (0.1Hz) stepped to a test potential of -10mV and perfusion after 3-4 minutes was switched to a saline

131

containing 1μM verapamil. After 8-10 minutes with verapamil the test potential was again ranged from -60 to +60 mV to allow construction of the IV relationship in the presence of verapamil. Verapamil caused significant reductions in amplitude of the peak current in the range of test potentials between -10 and +40mV as compared with controls (Figure 4.13). The maximal inward I_{PK} currents for the 5 cells occured at a mean test potential of -3.4±0.87mV in control saline and were not significantly different from those in verapamil (-8.4±2.0 mV). The IV curve for sustained current (Figure 4.14) was also altered by the application of verapamil, the current being again significantly reduced in the test potential range between -10 and +40mV. The maximal inward current was found to occur at -5.0±1.6mV in the control saline, but with verapamil was shifted significantly (p<0.01) in the hyperpolarising direction to -14.2±0.9mV. The transient component, I_{DIFF} ($I_{PK}-I_{SUS}$) was also significantly reduced by verapamil in the test potential range from -10 to +50 mV (Figure 4.15). The maximal inward current in control cells occured at a mean of -6.8±1.4mV and was not significantly affected by verapamil (-4.6±3.5mV). Figure 4.16 shows the mean percentage reduction in current seen with verapamil at each test potential for the I_{PK}, I_{SUS} and I_{DIFF} measurements in the 5 cells. The reduction in current observed at each test potential was compared statistically and it was found that at the test potentials of 0 and +10mV significantly different (p<0.02 and p<0.01 respectively) degrees of current block occurred between sustained current and
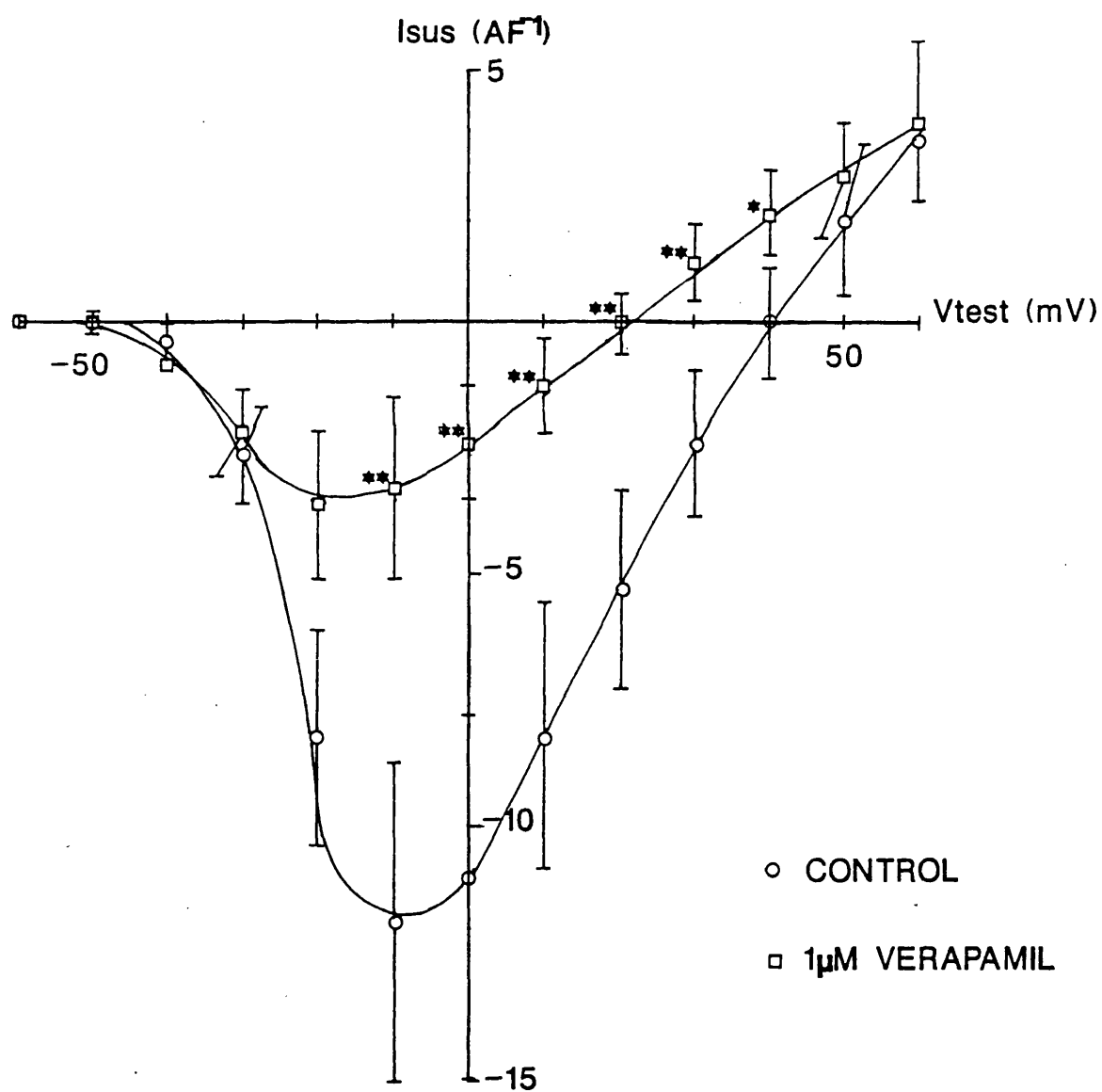
132

Figure 4.13

see over for legend

Legend for Figure 4.13 Effect of verapamil on peak current. Mean I-V relationships for peak current (I_{PK}) of cells in the control saline and following application of $1\mu M$ verapamil. Values for leak and capacitance subtracted current measurements in either control saline or saline containing $1\mu M$ verapamil were normalised by dividing by the cell capacitance. Normalised values for each current measurement at each test potential used were then averaged over the 5 cells and are presented as the mean ± s.e.m. Values were obtained from the same cells shown in figures 4.13 and 4.14. *, $p < 0.01$, **, $p < 0.005$, paired t-test.
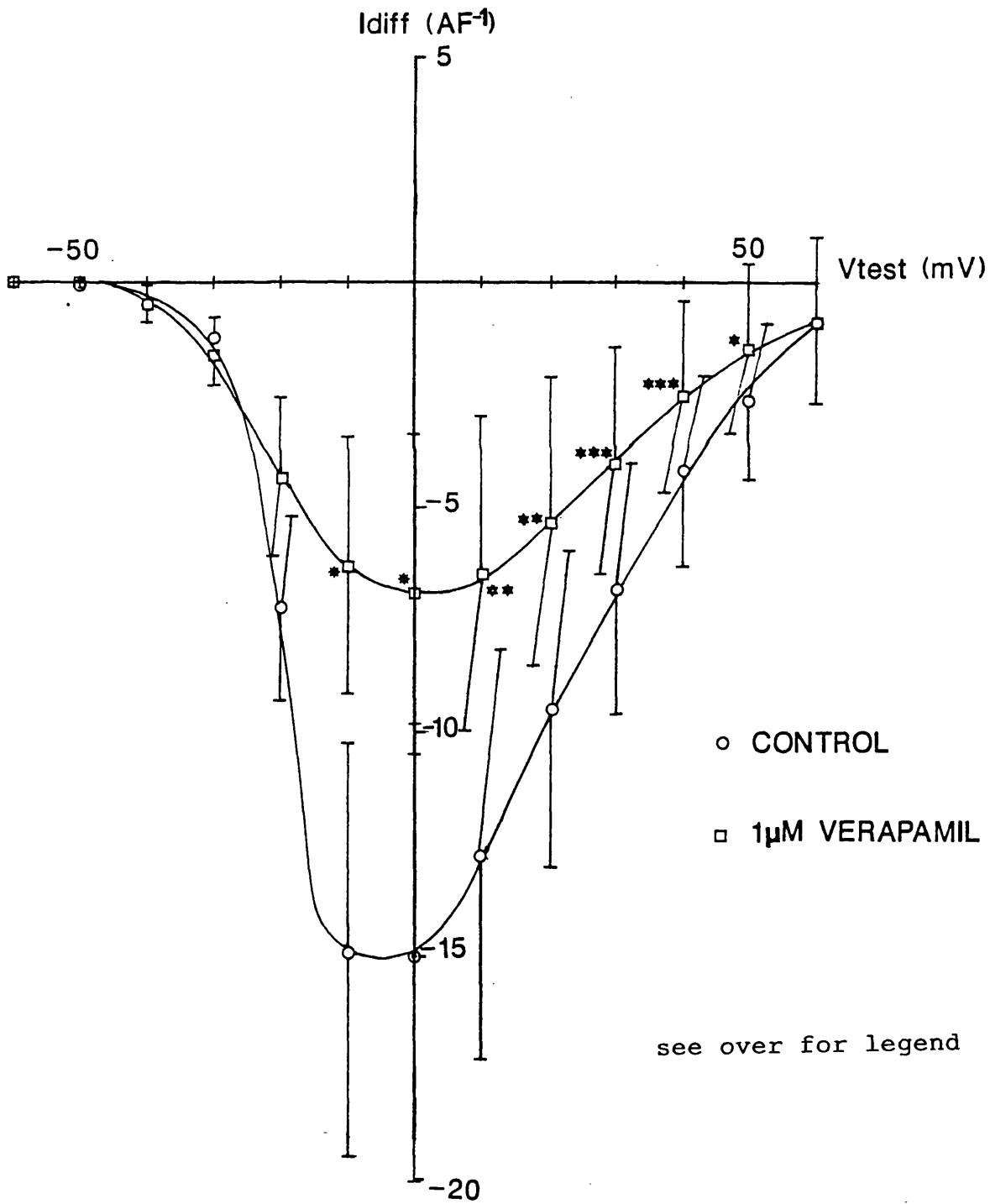
Figure 4.14

see over for legend

Legend for Figure 4.14 Effect of verapamil on sustained current.

Mean I-V relationships for current measured at the end of a voltage step (I_{SUS}) of cells in control saline and following application of $1\mu M$ verapamil. Values for leak and capacitance subtracted current measurements in either control saline or saline containing $1\mu M$ verapamil were normalised by dividing by the cell capacitance. Normalised values for each current measurement at each test potential used were then averaged over the 5 cells and are presented as the mean ± s.e.m. Values were obtained from the same cells shown in figures 4.12 and 4.14. *, $p<0.01$, **, $p<0.005$, paired t-test.

Figure 4.15

<u>**Legend for Figure 4.15**</u> Effect of verapamil on inactivating component of current.

Mean I-V relationships for the inactivating component of current (I_{DIFF}) of cells in control saline and following application of $1\mu M$ verapamil. Values for leak and capacitance subtracted current measurements in either control saline or saline containing $1\mu M$ verapamil were normalised by dividing by the cell capacitance. Normalised values for each current measurement at each test potential used were then averaged over the 5 cells and are presented as the mean ± s.e.m. Values were obtained from the same cells shown in figures 4.12 and 4.13. *, $p<0.01$, **, $p<0.005$, ***, $p<0.001$, paired t-test .
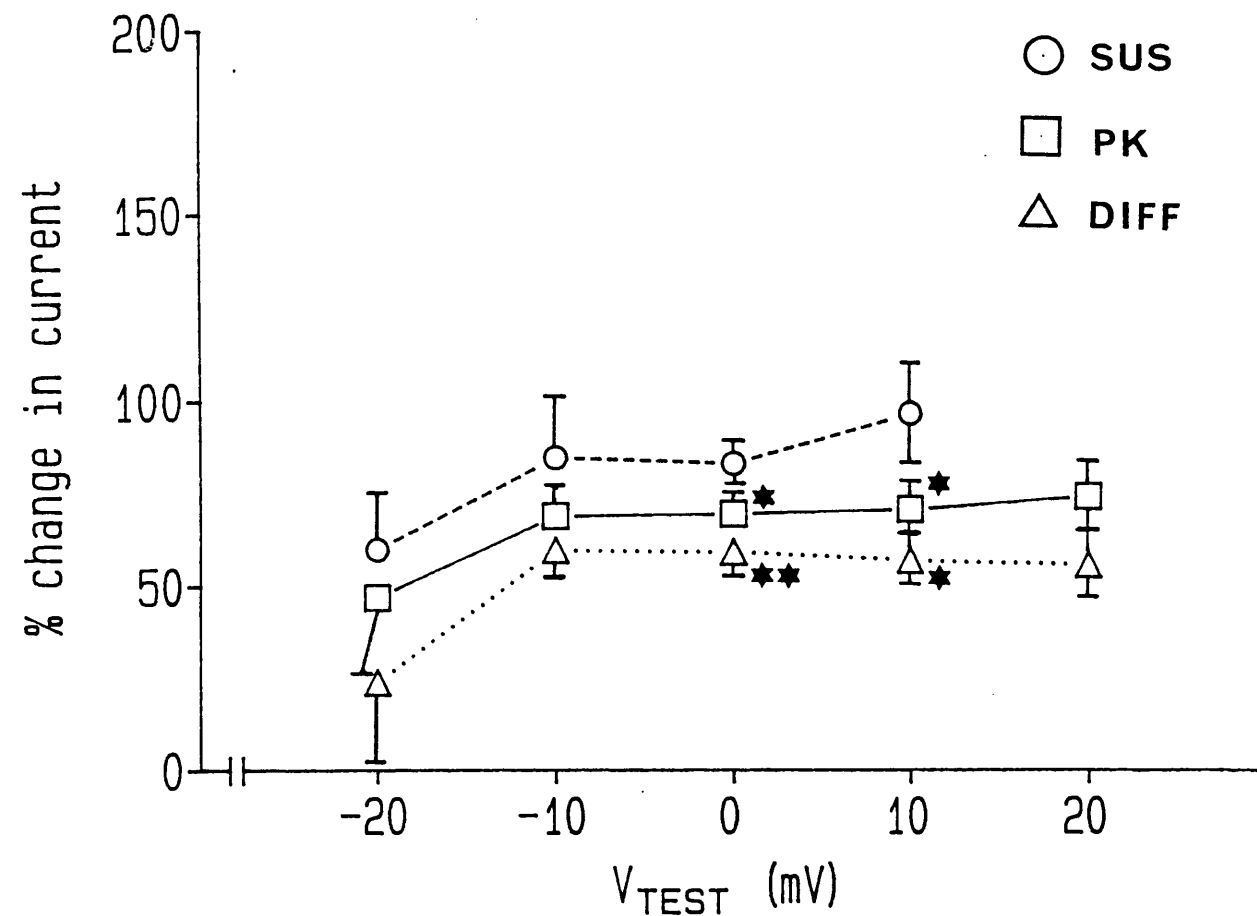
Figure 4.16 Percentage change in components of calcium channel current by verapamil.

The percentage change in current for peak (PK), sustained (SUS) and inactivating (DIFF) components of current after treatment with 1μM verapamil are shown plotted here over the range of test potentials between -20 and +20mV. The percentage change in current values from each cell after treatment with verapamil were calculated for each test potential and were averaged over the 5 cells used. Peak and inactivating current values were compared against sustained values (paired t-test). *, p<0.01, **p<0.002.

transient current with the sustained current being the most affected by verapamil.

To summarise, verapamil ($1\mu M$) caused reductions in the calcium channel currents. The degree of block is greatest at a test potential of 0mV and is also greater in the I_{SUS} measurement than it is in the I_{PK} and I_{DIFF} measurements. Furthermore, the maximal inward current seen in I_{SUS} is shifted in the hyperpolarising direction by verapamil.

h)   Effect of nitrendipine on calcium currents.

The organic Ca^{2+} channel antagonist, nitrendipine was applied to nerve cell bodies to test its effect on Ca^{2+} channel currents.

Initially, the same protocol used for verapamil was followed, i.e. an IV relationship was obtained in control saline, following which cells were depolarised to a test potential of -10mV at a frequency of 0.1Hz in control saline followed by perfusion with saline containing $1\mu M$ nitrendipine and IV curves again obtained. The averaged IV curves for I_{PK} and I_{SUS} in control saline and following treatment with $1\mu M$ nitrendipine are shown in Figure 4.17. There was no significant effect of nitrendipine on peak or sustained currents, whether currents were normalised or not (although the scatter was greater for un-normalised currents). In other experiments, instead of comparing measurements from the same cell before and after nitrendipine, experiments were carried out using a larger group of cells bathed in control saline and a different group of cells bathed in $1\mu M$ nitrendipine. Six 200ms steps

140

Figure 4.17

see over for legend

141
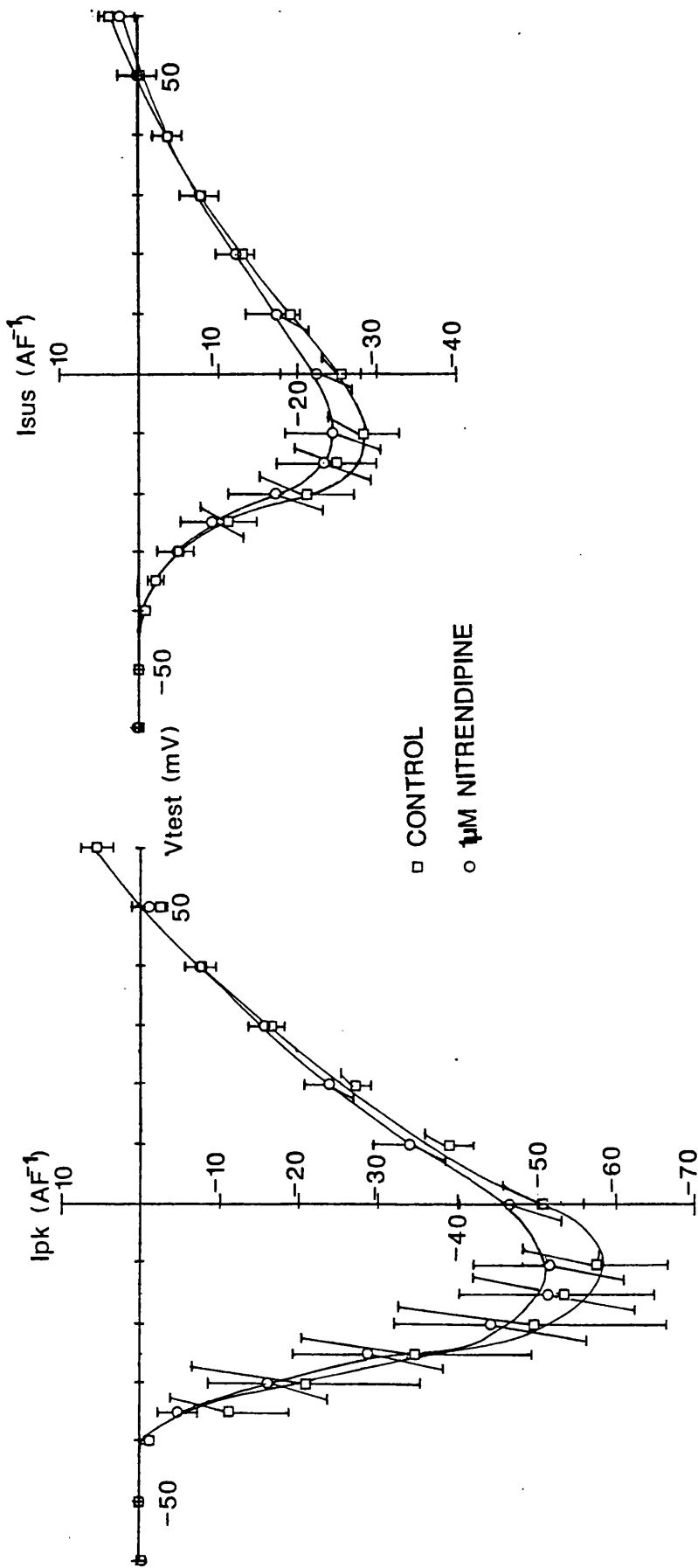
<u>Legend for Figure 4.17</u>   Effect of perfusion with
nitrendipine on peak and sustained currents.

Mean I-V relationships for the peak (I_{PK}, left) and
sustained (I_{SUS}, right) current measurements are shown. The
same cells were recorded from before and during perfusion
with saline containing 1μM nitrendipine.   Values in each
cell were normalised by dividing by the measured cell
capacitance before averaging. Subtraction of leak and
capacitance artefacts was performed before currents were
measured.   Values shown are the mean ± s.e.m. averaged over
the 6 cells used.   No significant differences between
control values and nitrendipine-treated values at each test
potential were found (paired t-test).

Figure 4.18

see over for legend

143
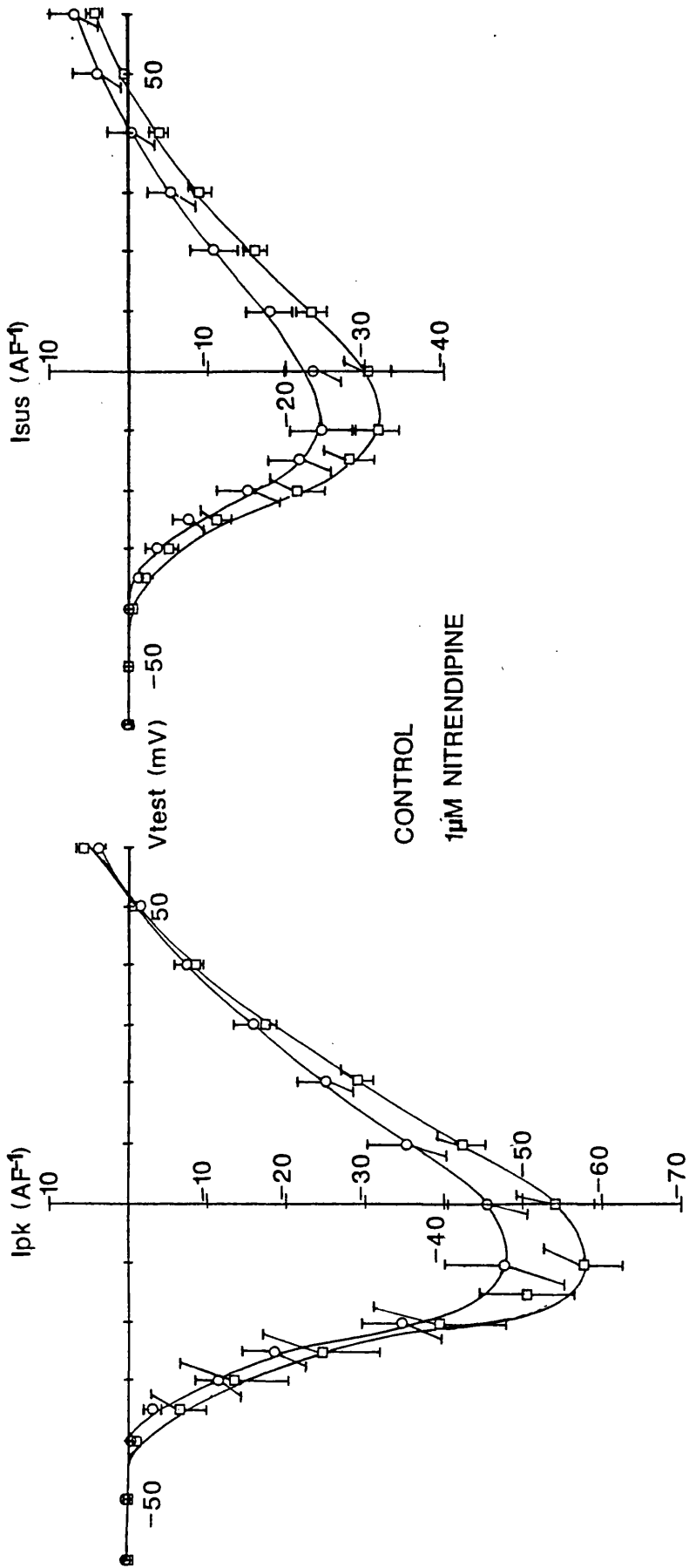
Legend for Figure 4.18   Effect of nitrendipine on peak and
sustained currents in non-perfused cells (-80mV holding
potential).

Mean I-V relationships for the peak (I_{PK}, left) and
sustained (I_{SUS}, right) current measurements elicited from a
holding potential of -80mV are shown for 13 cells bathed in
control saline and 15 different cells treated with $1\mu M$
nitrendipine.   Values in each cell were normalised by
dividing by the measured cell capacitance before averaging.
Subtraction of leak and capacitance artefacts was performed
before currents were measured.   Values shown are the mean ±
s.e.m. averaged over the number of cells used.   No
significant differences between control values and
nitrendipine-treated values at each test potential were
found (paired t-test).   Values were obtained from the same
cells shown in figure 4.19.

Figure 4.19

Isus (AF⁻¹)

Vtest (mV)

Ipk (AF⁻¹)

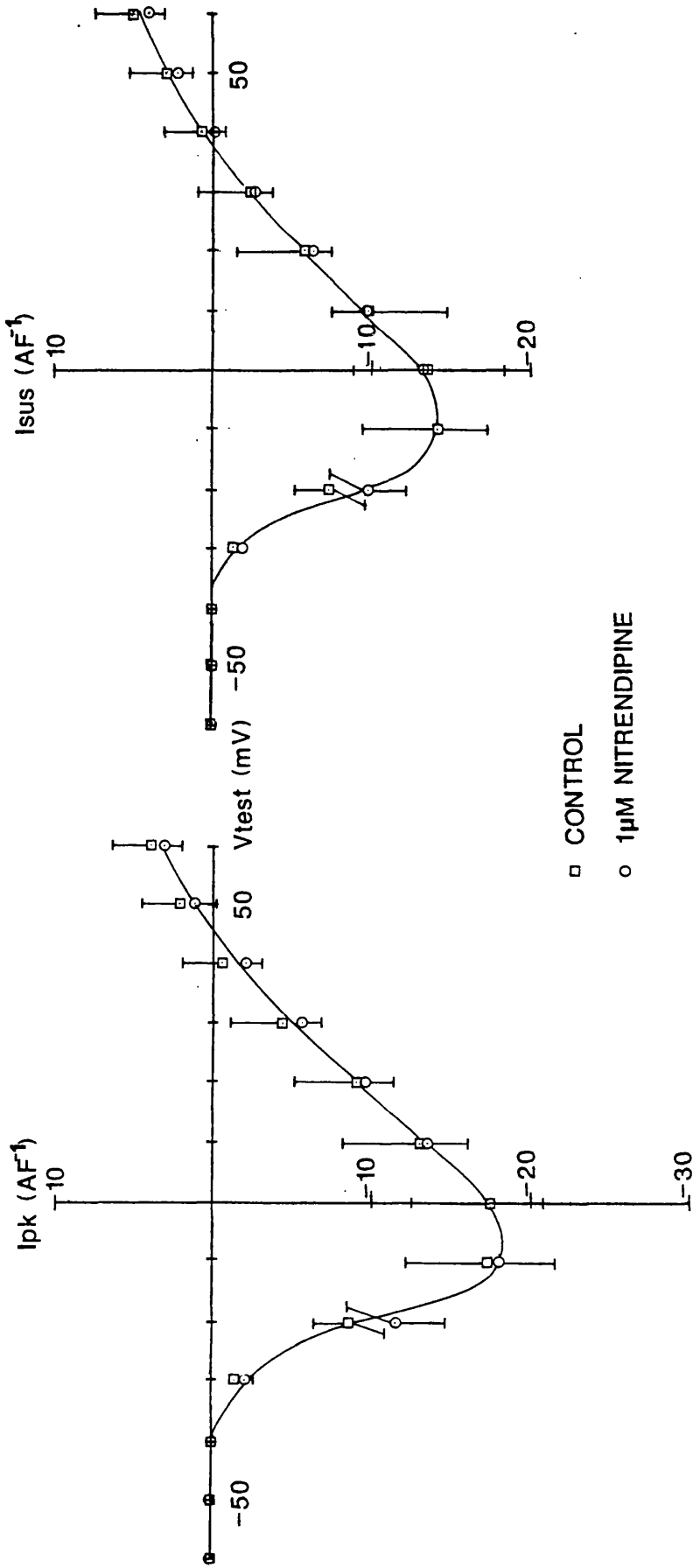□ CONTROL

○ 1μM NITRENDIPINE

see over for legend

145

Legend for Figure 4.19   Effect of nitrendipine on peak and sustained currents in non-perfused cells (-40mV holding potential).

Mean I-V relationships for the peak (I_{PK}, left) and sustained (I_{SUS}, right) current measurements elicited from a holding potential of -40mV are shown for 13 cells bathed in control saline and 15 different cells treated with $1\mu M$ nitrendipine.   Values in each cell were normalised by dividing by the measured cell capacitance before averaging. Subtraction of leak and capacitance artefacts was performed before currents were measured.   Values shown are the mean ± s.e.m. averaged over the number of cells used.   No significant differences between control values and nitrendipine-treated values at each test potential were found (paired t-test).   Values were obtained from the same cells shown in figure 4.18.

to a test potential of -10 mV were performed at a frequency of 0.1Hz before the test potential was ranged from -60 to +60mV to construct an IV relationship. The early steps were imposed so that any use-dependence in the block by nitrendipine could take effect (Lee & Tsien, 1983).

The mean, normalised IV relationships obtained for control (13 cells) and test (15 cells) solutions are plotted in Figure 4.18. Again nitrendipine had no significant effect on peak or sustained currents (similar results were obtained from un-normalised data). These cells were also held at a potential of -40mV and step depolarised as before to give IV curves. The mean, normalised IV relationships obtained from a holding potential of -40mV in control cells and in cells treated with 1μM nitrendipine are shown in Figure 4.19. Again, no significant differences between the currents obtained in the presence of nitrendipine at each test potential as compared with controls were found.

Thus in summary, using both experimental procedures, nitrendipine had no effect on the calcium currents in this preparation.

i) Effect of ryanodine on calcium currents.

In Chapter 3 of this thesis experiments on skeletal muscle fibres of moth larvae were reported in which ryanodine (10μM) was found to produce a marked increase in the duration of electrically stimulated action potentials. The aim of experiments described in this section was to determine whether ryanodine directly affects calcium channels in the cell membrane in addition to its known

Figure 4.20

148
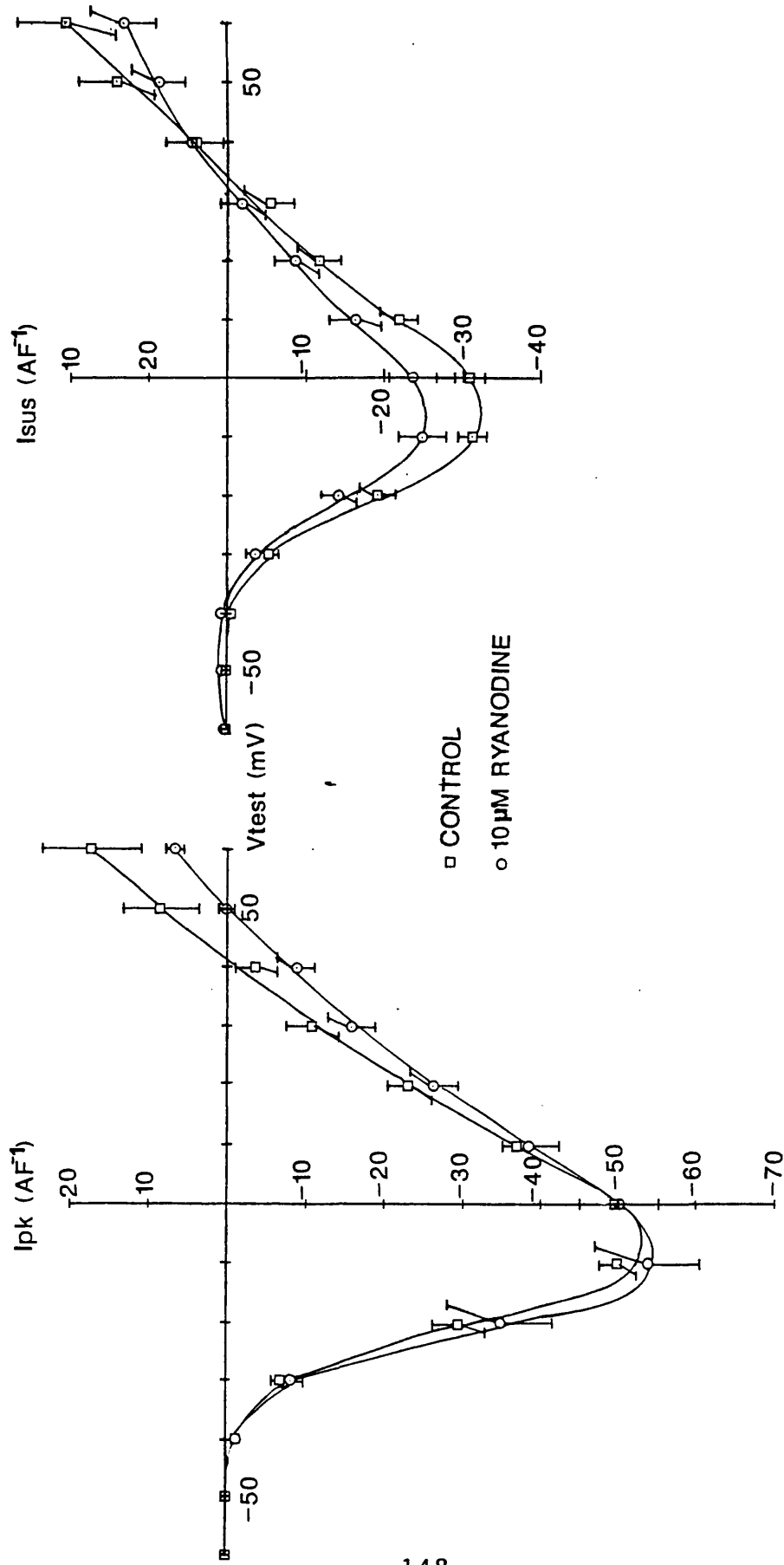
see over for legend

<u>Legend for Figure 4.20</u> Effect of ryanodine on Ca^{2+} channel currents (-80mV holding potential).

I-V curves are shown for the peak (I_{PK}, left) and sustained (I_{SUS}, right) current measurements in cells clamped at -80mV and bathed with either control saline (21 cells) or saline containing $10\mu M$ ryanodine (18 cells). Currents were normalised by dividing by the individual cell capacitance. Leak and capacitance artefacts were subtracted by computer before measurement of currents. Values given are means ± s.e.m. averaged over the number of cells in each group. No statistically significant differences in currents between control or ryanodine-treated cells at each test potential were found (two-tailed t-test).
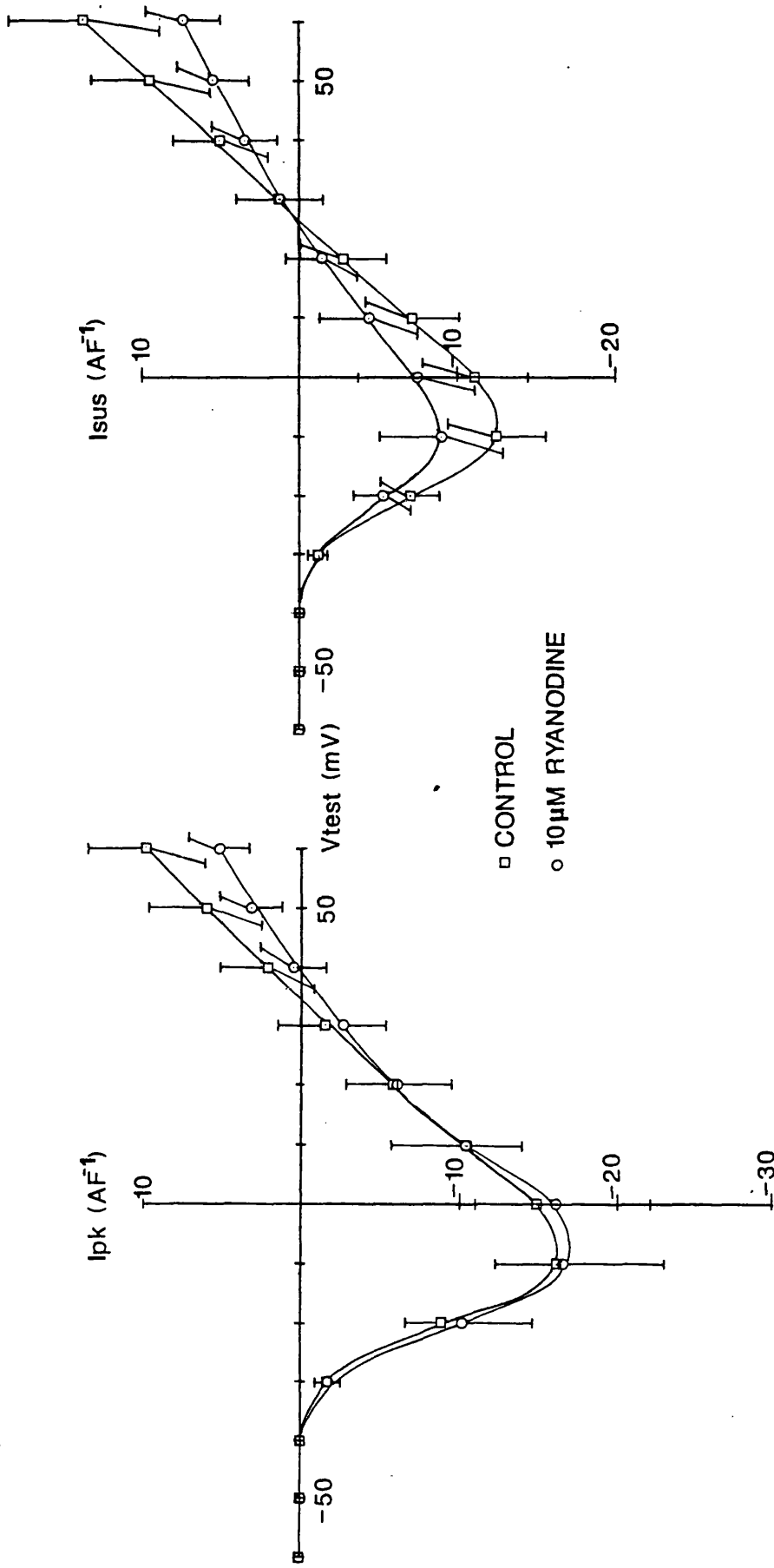
Figure 4.21

see over for legend

150

<u>Legend for Figure 4.21</u> Effect of ryanodine on Ca^{2+} channel currents (-40mV holding potential)

I-V curves are shown for the peak (I_{PK}, left) and sustained (I_{SUS}, right) current measurements in cells clamped at -40mV and bathed with either control saline (21 cells) or saline containing 10μM ryanodine (18 cells). Currents were normalised by dividing by the individual cell capacitance. Leak and capacitance artefacts were subtracted by computer before measurement of currents. Values given are means $\pm$ s.e.m. averaged over the number of cells in each group. No statistically significant differences in currents between control or ryanodine-treated cells at each test potential were found (two-tailed t-test). Currents were measured from the same cells shown in figure 4.20 following a period of 2 minutes at the -40mV holding potential to allow any steady-state inactivation to take place.

effect on calcium release channels in the sarcoplasmic reticulum.

Dissociated cell bodies from locust thoracic ganglia were bathed in either control saline or saline containing 10μM ryanodine. Cells were clamped at a potential of -80mV, again using the whole cell patch clamp technique, and voltage steps (200ms duration at 0.1Hz) to test potentials ranging from -60 to +60mV were performed. Cells were then held at a potential of -40mV for 2 minutes before similar test potential steps were made. Figure 4.20 shows the effect of ryanodine on peak and sustained currents elicited from a holding potential of -80mV.

At all test potentials no significant differences were found between currents (peak or sustained) for ryanodine-treated cells as compared with control cells. This also held true whether normalised or un-normalised values were compared.

The IV relationships for the same cells held at a potential of -40mV are shown in Figure 4.21. Currents evoked from a holding potential of -40mV were smaller than those seen at -80mV, but ryanodine again had no significant effect on either peak or sustained currents. Thus these experiments indicate that ryanodine at a concentration of 10μM had no significant effect on calcium currents in these cells at the holding potentials and test potentials used.

j) Effect of pyrethroids on calcium channel currents.

The pyrethroid class of insecticides act on voltage sensitive sodium channels, prolonging open times of

channels. It has recently been reported that type I pyrethroids also block calcium channels, particularly 'T'-type, and to a lesser extent 'L'-type channels in the N1E-115 cell line (Narahashi, 1986). The aim of experiments reported in this section was to determine the effect of both type I and type II pyrethroids on calcium currents in the insect neuronal preparation used throughout this chapter.

Freshly dissociated cells from locust ganglia were bathed in either control saline or saline containing 1μM of either S-bioallethrin (the active metabolite of a type I compound) or deltamethrin (a type II compound). As before cells were clamped using the whole cell patch technique at a holding potential of -80mV and step depolarised (200ms, 0.1Hz) to a range of test potentials (-60 to +60mV). After this cells were current clamped and their capacitances measured as before (see Methods).

Fifteen cells were treated with 1μM S-bioallethrin and were compared against 12 cells in control saline. IV relationships for peak and sustained currents in both control and treated cells are shown in Figure 4.22. There were no significant differences between control and S-bioallethrin-treated cells for peak or for sustained currents at all test potentials. This was also found to be true whether normalised or un-normalised values were compared.

Thirteen cells were treated with 1μM deltamethrin and were compared against 12 control cells. The IV relationships for both control and test groups are shown in Figure 4.23. Again there were no significant effects of deltamethrin as

Figure 4.22
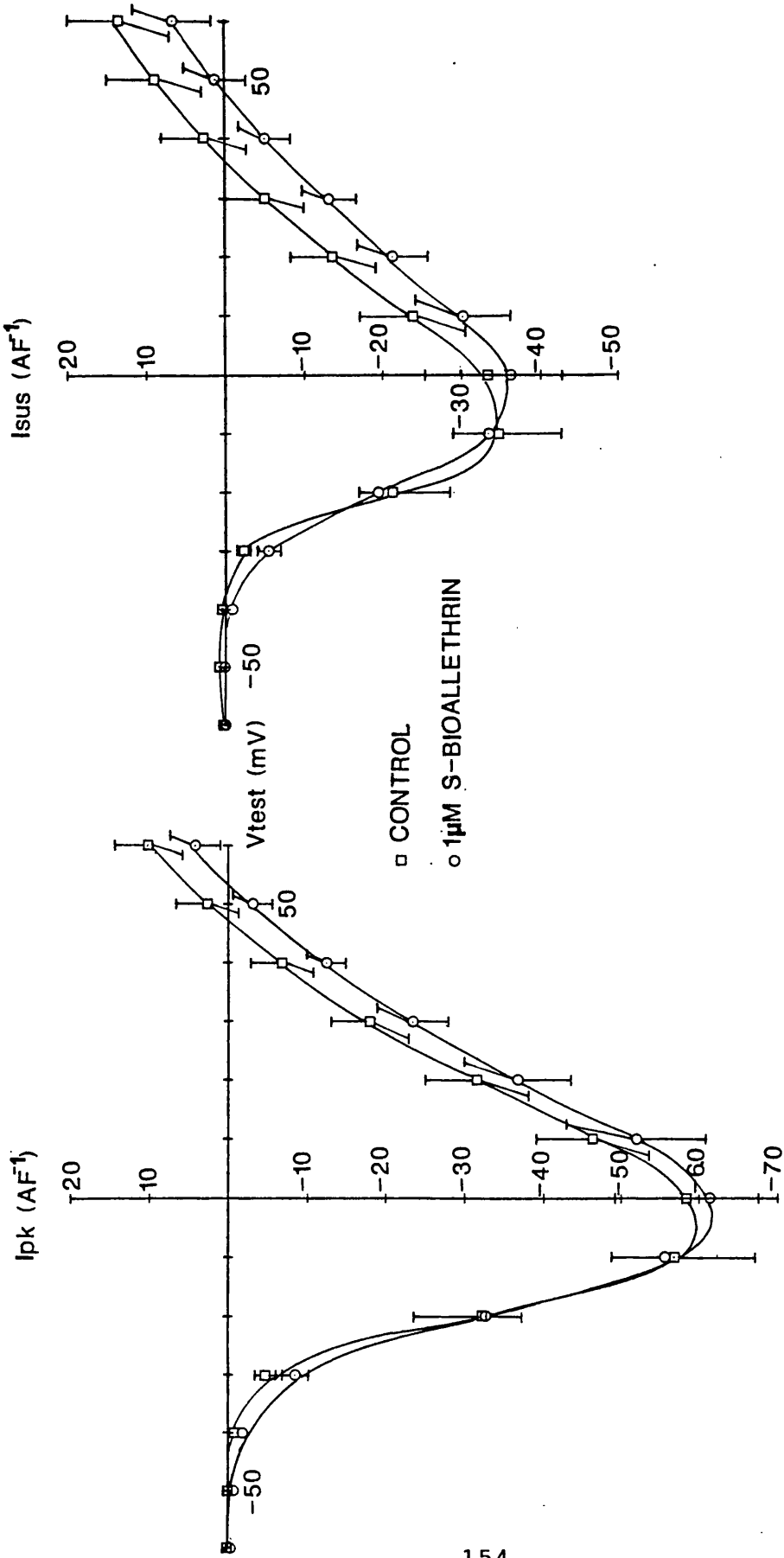
see over for legend

<u>Legend for Figure 4.22</u>   Effect of S-bioallethrin on Ca^{2+} channel currents

I-V curves are shown for the peak (I_{PK}, left) and sustained (I_{SUS}, right) current measurements in cells clamped at -80mV and bathed with either control saline (12 cells) or saline containing $1\mu M$ S-bioallethrin (15 cells). Current values at each test potential from individual cells were normalised by dividing by the cell capacitance.   Leak and capacitance artefacts were subtracted by computer before measurement of currents.   Values given are means ± s.e.m. averaged over the number of cells in each group.   Values obtained at each test potential in control or S-bioallethrin-treated groups were statistically compared (two-tailed t-test) but no significant differences were found.

Figure 4.23

Isus (AF⁻¹)

Vtest (mV)

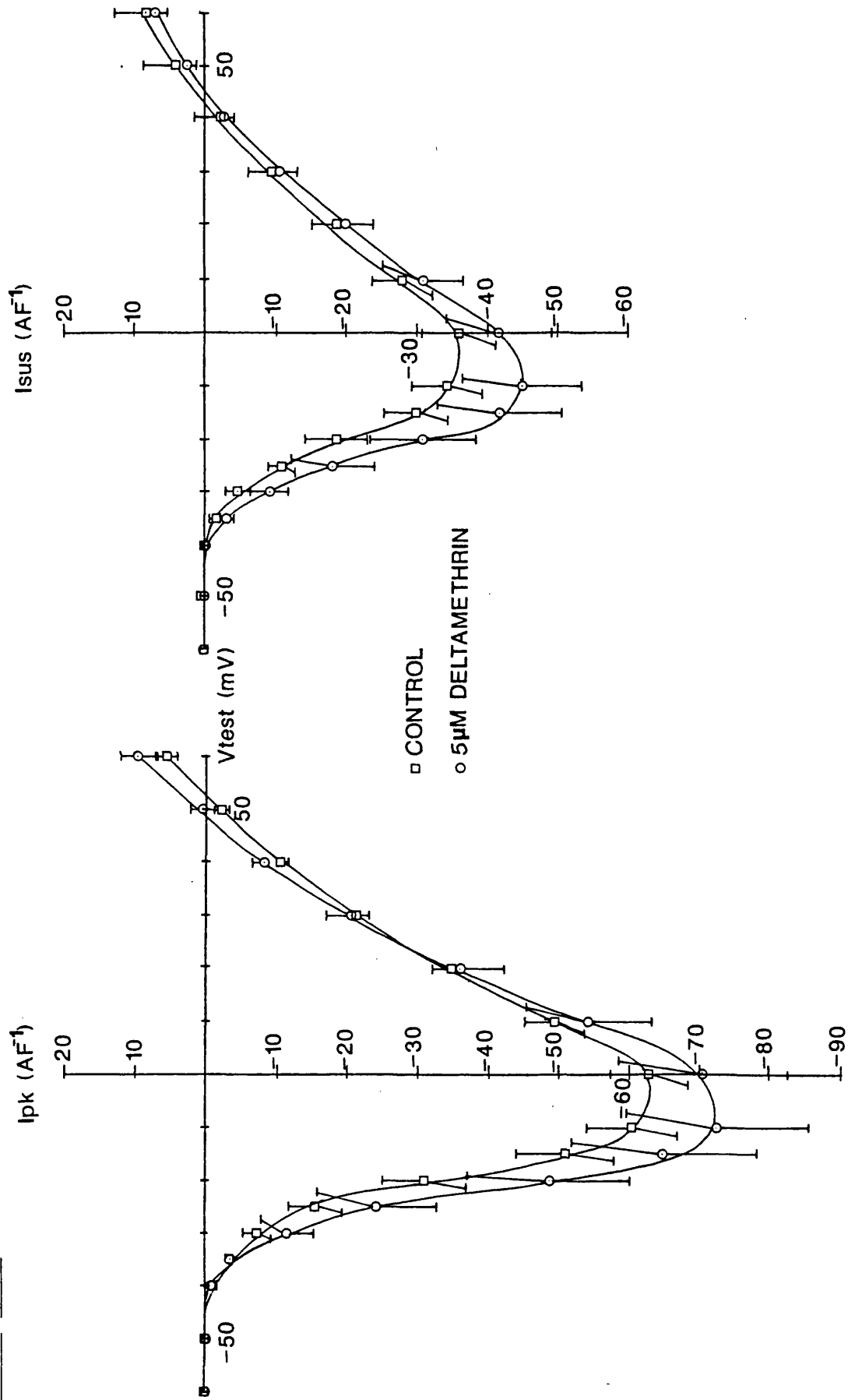□ CONTROL

○ 5μM DELTAMETHRIN

Ipk (AF⁻¹)

see over for legend

156

<u>Legend for Figure 4.23</u>   Effect of deltamethrin on Ca^{2+} channel currents

I-V curves are shown for the peak (I_{PK}, left) and sustained (I_{SUS}, right) current measurements in cells clamped at -80mV and bathed with either control saline (12 cells) or saline containing 1μM deltamethrin (13 cells). Current values at each test potential from individual cells were normalised by dividing by the cell capacitance.   Leak and capacitance artefacts were subtracted by computer before measurement of currents.   Values given are means ± s.e.m. averaged over the number of cells in each group.   Values obtained at each test potential in control or deltamethrin-treated groups were statistically compared (two-tailed t-test) but no significant differences were found.

compared with controls for either peak or sustained currents (normalised or un-normalised) at any of the test potentials used. Thus these results show that at a concentration of 1μM neither S-bioallethrin or deltamethrin had an effect on calcium channel currents in locust neuronal cell bodies.
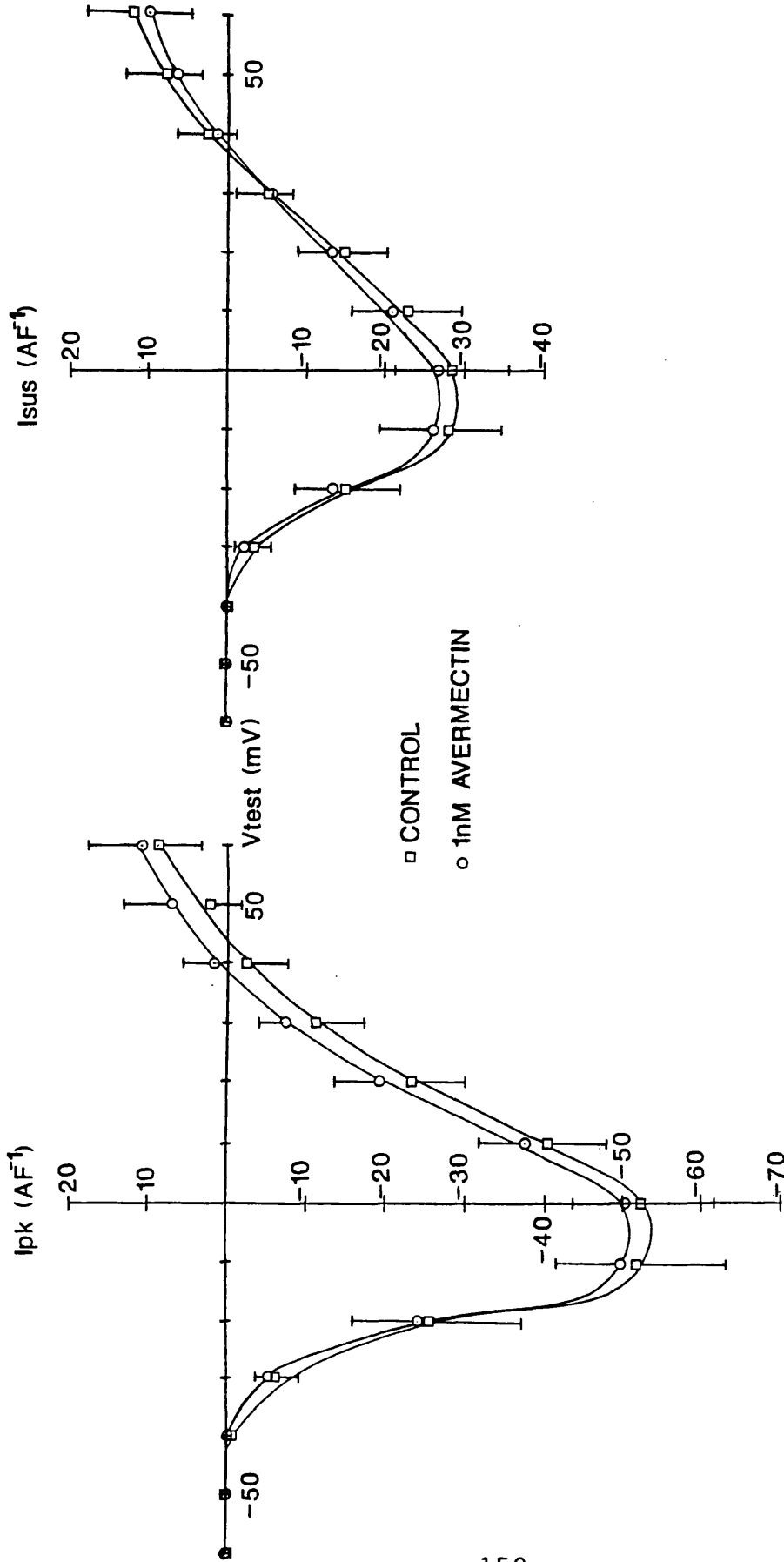
k) Effect of avermectin on cacium channel currents.

Avermectin is believed to act at as a powerful GABA-mimetic but might also act on Ca^{2+} channels (see Introduction). Therefore the experiments described in this section aim to study the effect of avermectin on the calcium currents seen in the locust neuronal preparation used in this chapter.

Cells were patch clamped and held at a potential of -80mV throughout the experiment. Cells were perfused with control saline whilst a range of test potential steps (200ms, 0.1Hz) from -60 to +60 mV were made to allow construction of control IV curves. Following this, cells were repetitively stepped to a test potential of -10mV for 200ms at a frequency of 0.1Hz and such stimulation was continued while the perfusing medium was changed to one containing avermectin. After 5-8 minutes in the presence of avermectin the test potential was again ranged from -60 to +60mV to construct IV curves.

With concentrations of avermectin greater than 1nM, large and irreversible increases in the holding current were observed which made accurate leak subtraction and effective voltage clamping of the cells difficult. When 6 cells were treated with a saline containing 1nM avermectin however, only very small changes in steady state leak were observed,

Figure 4.24

Isus (AF⁻¹)

Vtest (mV)

□ CONTROL

○ 1nM AVERMECTIN

Ipk (AF⁻¹)

see over for legend

159

Legend for Figure 4.24   Effect of avermectin on Ca^{2+} channel currents

I-V curves are shown for the peak (I_{PK}, left) and sustained (I_{SUS}, right) current measurements in cells clamped at -80mV and perfused fistly with control saline and then with saline containing 10nM avermectin B_1 for 5-8 minutes.   Currents were normalised by dividing by the individual cell capacitance.   Leak and capacitance artefacts were subtracted by computer before measurement of currents.   Values given are means ± s.e.m. averaged over the 6 cells tested.   No statistically significant differences in currents obtained after treatment with avermectin as compared with controls were found at any of the test potentials applied (paired t-test).

and it was possible to compare IV relationships obtained in control saline and after avermectin treatment (Figure 4.24). At this concentration there was no significant effect of avermectin on the IV curves whether for peak or sustained currents.

Thus it would appear that avermectin at a concentration of 1nM has no effect on the calcium current in these cells. Effects at higher concentrations of avermectin cannot be ruled out but are impossible to detect using this technique due to the large increases in leak that occur with avermectin application.

1) Single channel recordings of calcium channel currents.

In the experiments described in the earlier sections of this chapter it was only possible to separate components of the calcium current by use of $10\mu M$ Cd^{2+}. The different components appeared to have similar voltage dependence of steady state inactivation and so could not be separated by using more depolarised holding potentials, in contrast to avian dorsal root ganglion cells (Nowycky et al, 1985a). To investigate whether two (or more) different types of channel are present it is necessary to study single channel currents.

The resting potentials of cells bathed in dissecting saline (see Methods) were measured either during the course of the experiment or immediately after the experiment by means of an intracellular microelectrode and mean resting potential values were -39.5 ± 0.7 mV (n=232 cells). After formation of a seal of $10G\Omega$ or better the holding potential of the

pipette was set to near +40mV (as required) so that the transmembrane potential across the patch was exactly 80mV with the intracellular surface negative with respect to the extracellular surface. From this holding potential, to depolarise the patch, the pipette potential was stepped to more negative holding potentials (range, -60 to +60mV) for a duration of 175ms and at a frequency of 0.1Hz. Other holding potentials (-100 to -150mV) and test potentials (+70 to +150mV) were also used when no channel activity was seen. In all, 232 high quality seals (seal resistance > 10GΩ) were made onto cells, and in all but one of these patches no channel activity was detected. These experiments were carried out using 110mM Ba^{2+} in the pipette saline (see Methods), but when the pipette was filled with either a high potassium saline or dissecting saline outward single channel currents were observed; presumably due to K^+ or Cl^- channel activity.

For the one patch where calcium channel activity was seen the resting potential (measured immediately after rupture of the patch) was -40mV. Examples of the inward channel current are shown in Figure 4.25 and the properties of these channels are summarised in Figure 4.26. The number of channel openings in the patch became more frequent with stronger depolarisations (Figure 4.26, A) and the mean duration of each opening also became longer (Figure 4.26, C). The increased channel opening frequency and duration of opening is also reflected in the increase in mean total open time (Figure 4.26, D) during the steps. More depolarised test potentials also gave rise to a reduction in the latency

162

Figure 4.25

-30

-20

-10

0

+20

1pA

50 ms

V_TEST

-80

V_TEST

-80

see over for legend

163
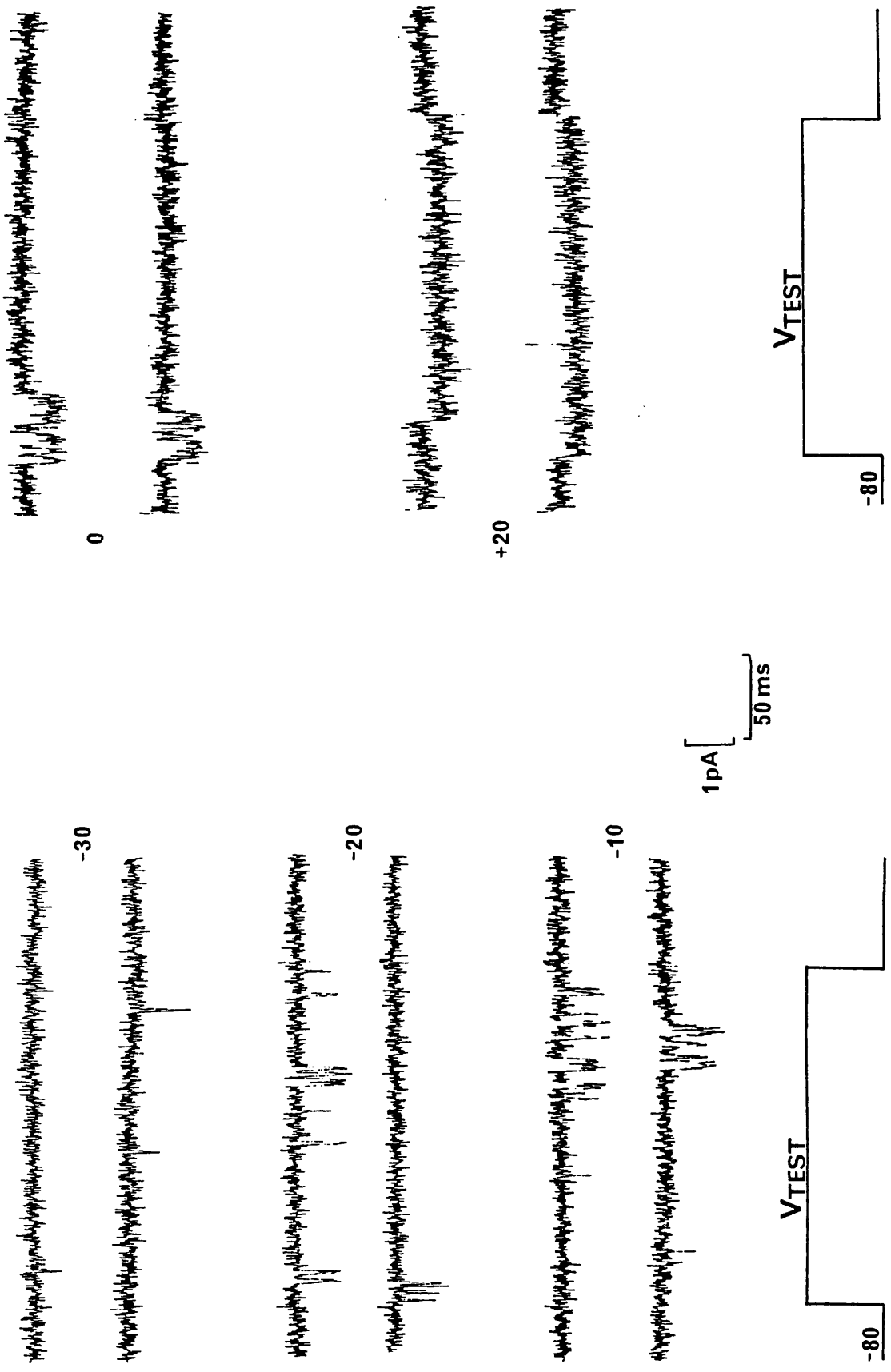
Legend for Figure 4.25   Unitary Ca^{2+} currents in locust

neurones.

Typical current records seen in a cell attached patch held

at a transmembrane potential of -80mV.   Currents were

activated by step depolarisations to the transmembrane test

potentials (V$_{TEST}$) shown by each pair of current traces.

Currents were filtered at 1kHz using an 8-pole Bessel filter

and leak and capacitance artefacts have been subtracted.

Figure 4.26

A   Mean No. openings/step

B   Mean First Latency (ms)

C   Mean Open Duration (ms)

D   Total Open Duration per Step (ms)

Test Potential (mV)
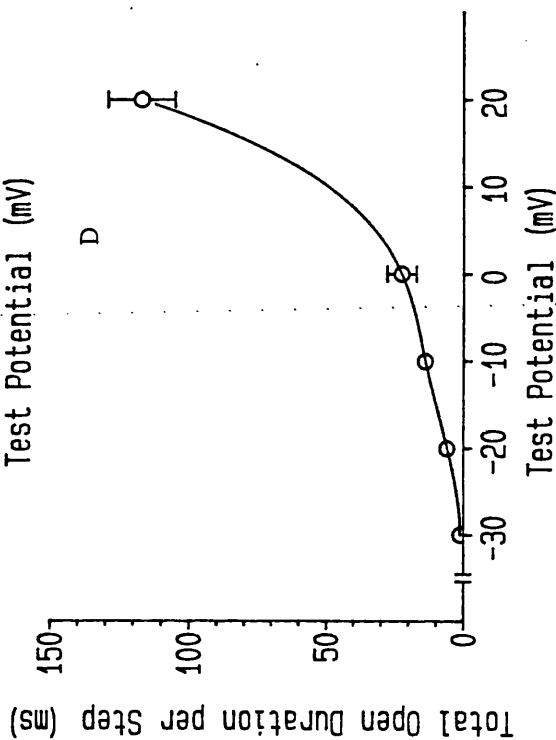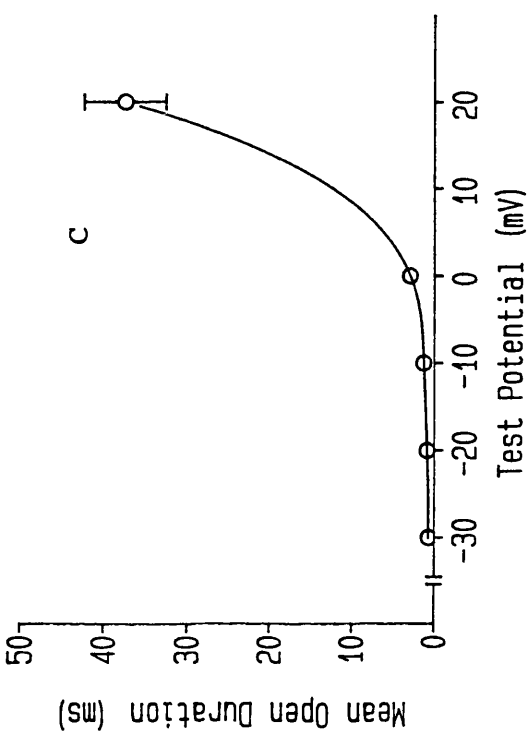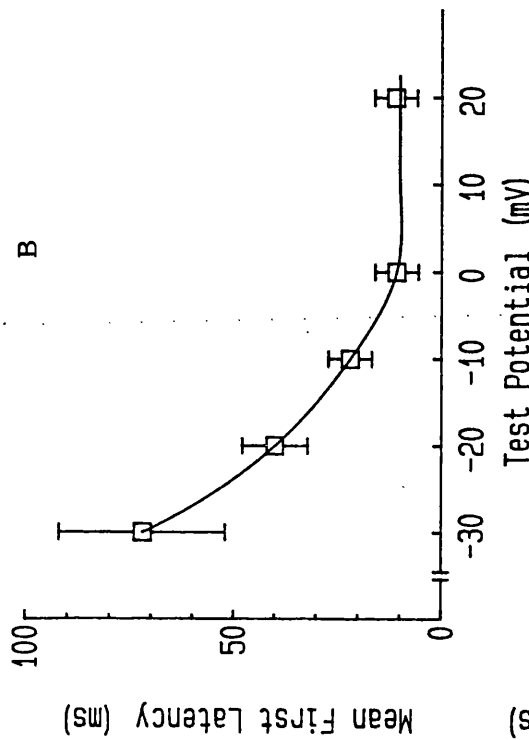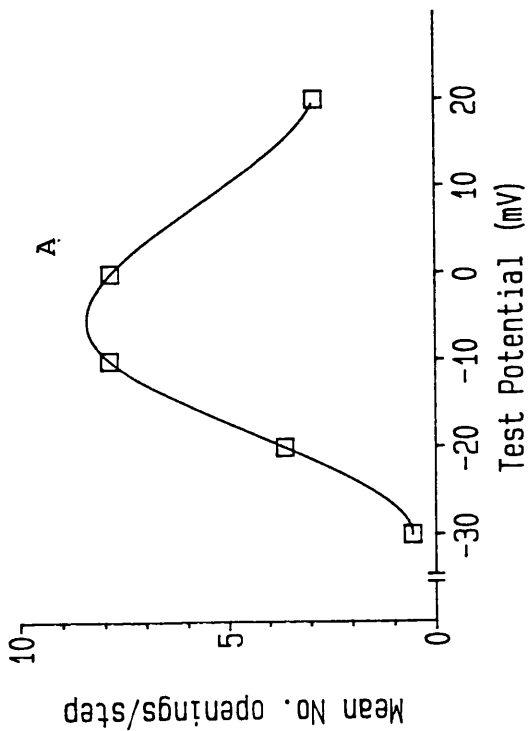
see over for legend

Legend for Figure 4.26   Properties of unitary Ca^{2+} channel currents.

The mean number of openings per voltage step (graph A), mean first latency (graph B), mean open duration of all openings (graph C) and total open duration per voltage step (graph D) are shown plotted against test potential for the cell attached patch shown in figure 4.25.

Figure 4.27 Slope conductance of unitary Ca^{2+} channel currents.

Mean amplitudes of Ca^{2+} channel currents are shown plotted against test potential. Linear regression fit of a straight line to the data gave a slope of 6.9pS and an apparent reversal potential of 81.8mV. Data were obtained from the same membrane patch. Standard error bars for the test potentials above -30mV are smaller than the symbols used here.

to the first channel opening in a step (Figure 4.26, B).
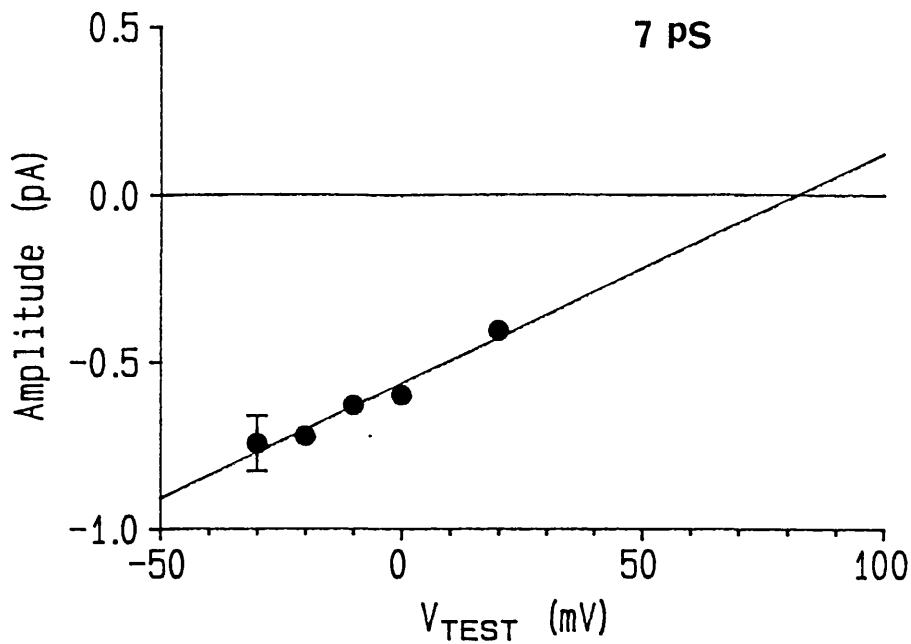
In Figure 4.27 the mean channel amplitude is plotted against test potential and a linear regression fit through the points gave a slope conductance of 6.9pS with a reversal potential of +81.8mV. Figure 4.28 shows frequency histogams of amplitude at given test potentials. The most noticeable feature of all these graphs is the lack of a normal distribution. The wide range of amplitudes with possible multiple peaks may suggest that either there is more than one channel present in the patch or that there is only one channel present with a number of subconductance states. Frequency histograms of channel open time for various depolarising steps are shown in Figure 4.29. Single exponentials fit the data resonably well at the -10 and -20mV test potentials and a multiple exponential fit has been made to the data at the 20mV test potential.

Steps to each test potential which showed channel activity were averaged together by computer and are shown in Figure 4.30. These averaged traces represent the change in probability that the channel is open during the time course of the potential step and show that in the case of steps to test potentials of -10mV and 0mV the probability of channel opening declined throughout the step, i.e. the channel observed in the patch was transient in nature. At a test potential of +20mV however, the channel open probability appeared to remain fairly constant throughout the course of the 175ms step. This may imply that at strongly depolarised potentials the channel does not inactivate and gives rise to sustained currents in the whole cell configuration.
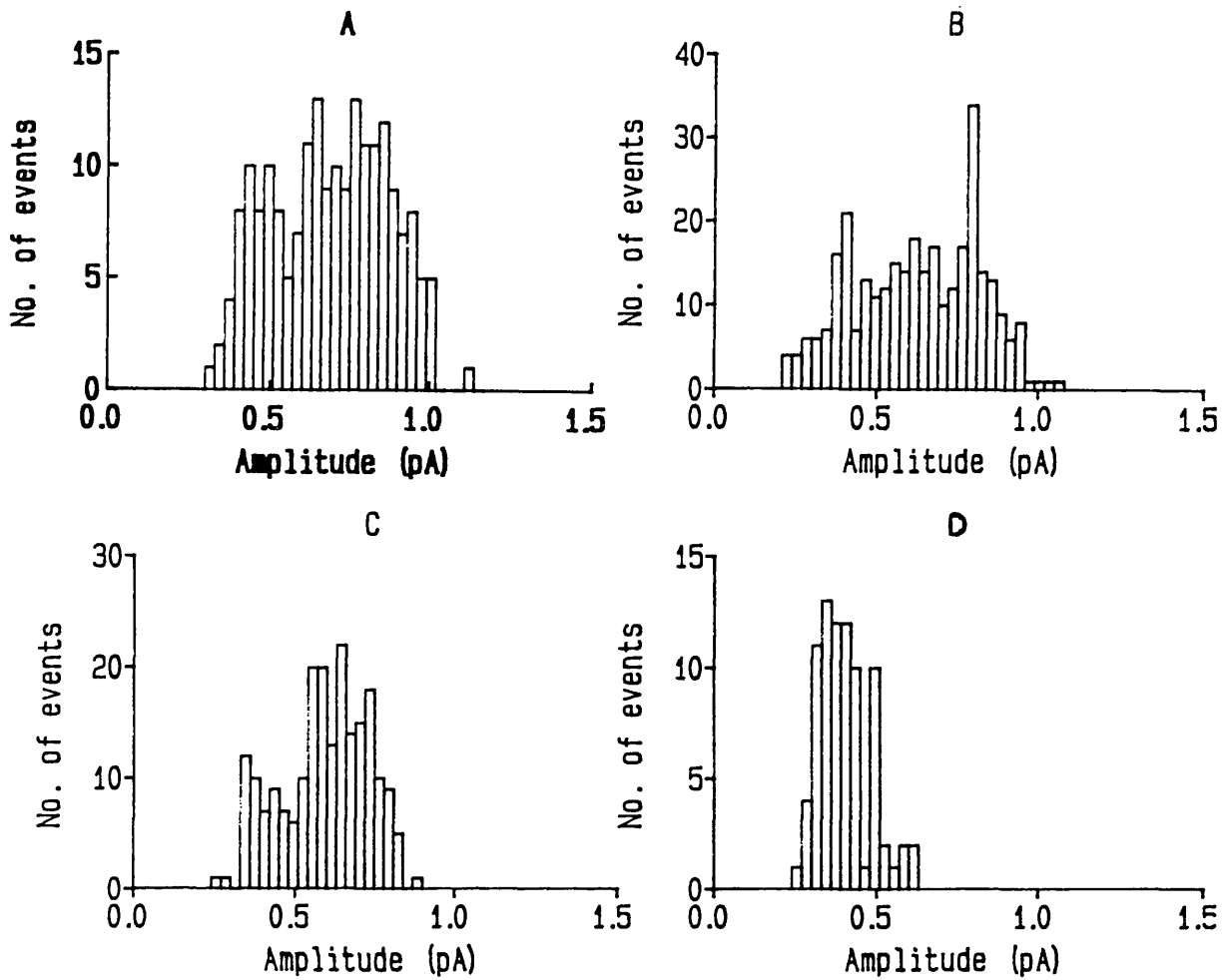
Figure 4.28 Amplitude frequency histograms of unitary Ca^{2+} channel currents.

Frequency is plotted against the amplitude for currents seen at test potentials of -20mV (A), -10mV (B), 0mV (C) and 20mV (D). Amplitude bin width was 0.03pA. Data were obtained from the same membrane patch.

Figure 4.29
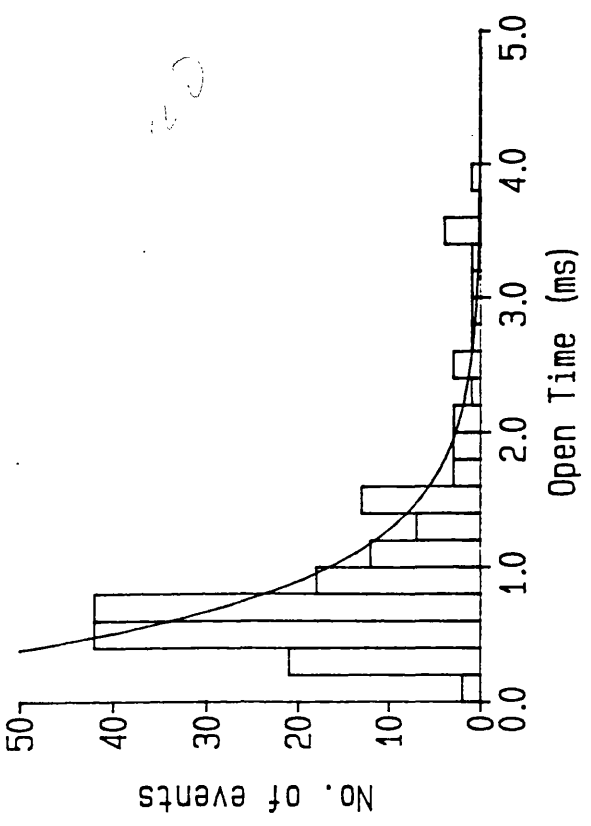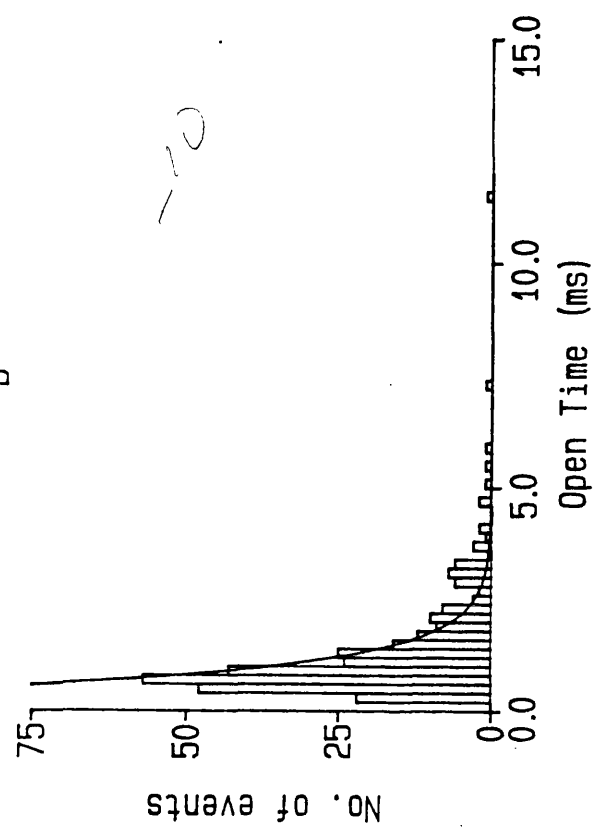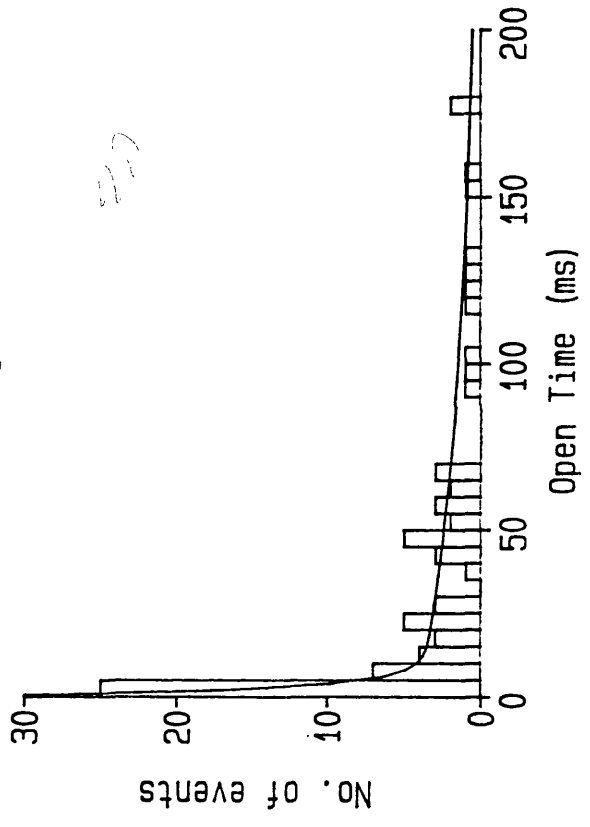
see over for legend

<u>Legend for Figure 4.29</u> Open duration frequency histograms of unitary Ca^{2+} channel currents.

Frequency of open duration times of currents seen at test potentials of -20mV (A), -10mV (B) and 20mV (C). Open time bin width was 0.2ms (graphs A and B) and 5ms (graph C). Exponentials fitted to the data using the sum of squares method gave values for τ of 1.8ms (A), 1.7ms (B) and a double exponential fit with values of 5ms and 100ms (C). Data were obtained from the same membrane patch.

Figure 4.30

-20mV

-10mV

0mV

20mV

see
legend

50ms

Vtest

-80

see over for legend

172

Legend for Figure 4.30 Ensemble average currents obtained from single channel recordings.

Mean current records shown were obtained by averaging together those steps which showed channel activity at each test potential. The amplitude calibration is 0.17pA, 0.25pA, 0.25pA and 0.5pA for the -20, -10, 0 and 20mV traces respectively. Current records were subtracted for capacitance transients and leak before averaging.

Figure 4.31

110 Ba^{2+}

I (AF^{-1})

Vtest (mV)

□ Ipk

o Isus

n=5

see over for legend

174
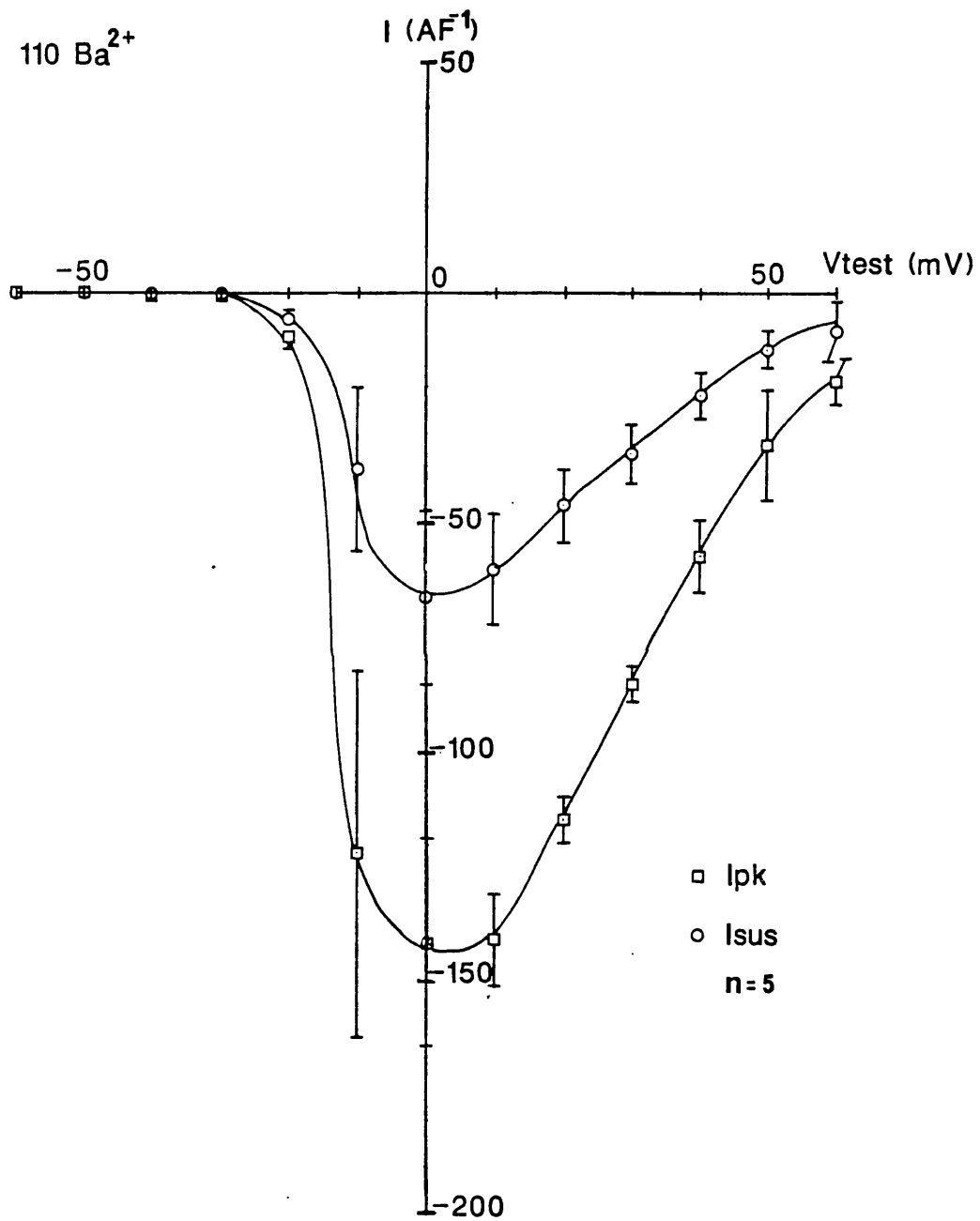
Legend for Figure 4.31 Whole cell Ca^{2+} channel currents in 110mM Ba^{2+}.

I-V curves are shown for the peak and sustained current measurements in cells bathed in a saline containing 110mM Ba^{2+} as the charge carrying ion. Currents from 6 cells were normalised by dividing by the individual cell capacitance before being averaged. Values given are the mean ± s.e.m. Leak and capacitance artefacts were subtracted before measurement.

When the 110mM Ba^{2+} pipette saline was used in the bath and whole cell recordings were made, whole cell calcium channel currents were observed. Mean, normalised current amplitudes were approximately 3 times larger than those seen when 10mM Ba^{2+} was used and displayed similar characteristics (i.e. both transient and sustained components) although the IV curves appeared to be shifted by approximately 10mV in the depolarising direction (Figure 4.31). This therefore shows that Ca^{2+} channel currents do occur in the presence of 110mM Ba^{2+} and the solution used in the cell attatched pipette does not appear to prevent Ca^{2+} channel activity.

In summary, the observation of single Ca^{2+} channel currents in these cells proved to be very difficult. In the one patch where channel activity was observed a low conductance channel was characterised.

m) Discussion.

The experiments described in this chapter were designed to study Ca^{2+} channel currents in the somata of neuronal cells freshly dissociated from the thoracic ganglia of locust, Schistocerca gregaria. Large inward currents were seen when cells were depolarised with Ba^{2+} used as the charge carrying ion. Evidence that these currents were carried through Ca^{2+} channels was provided by a number of different experiments. In the first place, all experiments were carried out under conditions which should prevent currents carried by other ions; TTX was present in the bathing solution to block voltage-dependent Na^+ channels,

TEA was present both inside and outside the cell to block K^+ channels, and the use of Ba^{2+} in the bathing solution and Cs^+ in the pipette solution also reduced K^+ currents. Furthermore, when Na^+ was replaced in the bathing solution with choline, no significant differences in the inward current in cells were seen, again showing a lack of involvement of Na^+ in the inward current. This inward current (which was also carried by Ca^{2+}) was blocked by Cd^{2+}, the inorganic Ca^{2+} channel blocking agent. Taken together, these oservations all suggest that the inward currents are carried by the passage of Ba^{2+} through voltage-dependent Ca^{2+} channels.

The inward Ca^{2+} current amlpitudes in these cells were proportional to the cell capacitance and hence presumably, cell surface membrane area; indicating a roughly constant Ca^{2+} current per unit area for the cells recorded from. This provided a convenient means to normalise Ca^{2+} currents between cells and prevent weightings of unnormalised averaged currents towards those in the larger cells.

Is the calcium channel current carried by more than one type of channel?

The Ca^{2+} channel currents seen in these cells appeared to show two phases. At a holding potential of -80mV a sustained phase, activated at test potentials positive to -40mV and a transient phase activated from test potentials positive to approximately -30mV were seen. In all cases where both phases were seen, the sustained current threshold

was at a more negative potential to the transient current threshold. These two current components could not be separated by imposing more depolarised holding potentials on the cells, since both peak and sustained currents showed the same degree of steady state inactivation at each holding potential. This would suggest that if two different channels underlie the peak and sustained components of the Ca^{2+} channel current, then these channels have similar steady state inactivation properties and very slightly different activation kinetics. If, however, both peak and sustained components of the current are based on a single channel type showing both transient and sustained phases, then this would also be consistent with the above results, with the rate of inactivation simply depending on the test potential.

These currents differ from those in other cell types where both transient and sustained components of current are seen. For instance in cultured neurones from dorsal root ganglia, the transient component is inactivated at more depolarised steady state holding potentials (around -40mV) leaving the sustained component as the only current activated by step depolarisation (e.g. Nowycky et al, 1985a). Furthermore, again in contrast to other cell types, the transient component of the Ca^{2+} current in these locust neurones is activated by slightly larger depolarising steps than those required to activate the sustained component of current. These transient and sustained components of the Ca^{2+} channel current could, however, be separated by their differential sensitivity to block by Cd^{2+}. The block of the

sustained component of current (seen at low concentrations of Cd^{2+}) provides strong evidence that two channel types exist. On its own however, this does not provide conclusive proof of separate Ca^{2+} channel types. If the two phases of current are carried by a single channel type, then it is possible that Cd^{2+} preferentially blocks the channel when it is in a state that favours sustained-type behaviour.

Verapamil, which also might have been expected to block only the (the) sustained component of the Ca^{2+} channel current, appeared to have an effect on both components, although the sustained component was affected to a greater degree than the transient component, possibly supporting the idea of two channel types. Nitrendipine had no effect on the Ca^{2+}channel currents in these cells and therefore proved to be of no use in determining whether more than one channel type existed. Furthermore, type I pyrethroids, which preferentially block T-type channels in the N1E-115 cell line (Narahashi, 1986), had no effect on the Ca^{2+} channel currents in these locust neurones. Conclusive evidence for either one or two channel types might have been expected from the single channel experiments, but only limited data could be obtained. In the only patch in which channel activity was seen, the ensemble average traces showed that at the lower test potentials (-20 to 0mV) the current was transient in nature, but at a test potential of +20mV it became sustained. This dual nature may indicate that both sustained and transient activity may be shown by the same channel. However, it would be expected from the currents seen in whole cell recordings that the sustained current

would be seeen at the more negative test potentials and the more transient current at more positive test potentials. Clearly this experiment is inconclusive and further single channel recordings would be required to clarify this result.

Thus in summary, the experiments reported in this chapter have not shown conclusively that the biphasic nature of the Ca^{2+} channel current in these cells is mediated by more than one channel type. However the balance of evidence probably favours two channel types, one being sustained, activated at more negative potentials and more sensitive to Cd^{2+} than the other, Cd^{2+} resistant, transient current type. If this is the case both channel types would have similar steady state inactivation characteristics and similar sensitivity to verapamil.

Pharmacology of locust neuronal calcium channels.

Pharmacologically the Ca^{2+} channels of locust neurones do not closely resemble those seen in vertebrate systems. As stated above, the Ca^{2+} channels underlying the Ba^{2+} current in this preparation appeared to be blocked by verapamil but not by nitrendipine. This agrees well with the biochemical studies of Pauron et al (1987) and Greenberg et al (1989) on another insect neuronal preparation. Both groups found that in Drosophila head membranes the phenylalkylamines bound to the membranes with a very high affinity but that a very much lower affinity binding was associated with the dihydropyridines. Furthermore, in experiments where these brain membranes were reconstituted into planar lipid bilayers channels were found which were

(as for locust) highly sensitive to phenylalkylamines but insensitive to dihydropyridines. Other channel types were also observed which were sensitive to dihydropyridines but not phenylalkylamines or which were insensitive to both class of compound. Byerley and Leung (1988) have reported that benzothiazepines have no effect on the Ca^{2+} current in cultured neurones from Drosophila embryos, but that a weak, reversible blocking effect could be seen with high concentrations of phenylalkylamines.

It is interesting to note that in our experiments verapamil did not appear to have a significant blocking effect at the lower test potentials which elicited an inward current. Use dependence (Lee and Tsien, 1983) can be ruled out as a factor causing this since the cells were repeatedly depolarised during the run-on of verapamil. It may thus be possible that the sustained component of the Ca^{2+} current consists of a further subdivision of types with one type insensitive to verapamil activated at the lower test potentials and the other type sensitive to verapamil and activated at more positive test potentials.

Although pyrethroids act on mammalian sodium and calcium channels (Narahashi, 1986) and on insect sodium channels (Hart, 1986, see also Introduction), in locust neuronal cell bodies pyrethroids of both classes had no effect on the Ca^{2+} channel current. It would therefore appear that there are further pharmacological differences between vertebrate and insect Ca^{2+} channels.

Ryanodine was found to have no action on locust neuronal Ca^{2+} channels. This is in contrast to its marked

effect on Ca^{2+}-dependent action potentials in moth larval skeletal muscle (Chapter 3). Thus it is possible that ryanodine produces its effect on Ca^{2+} currents in skeletal muscle via an indirect mechanism, probably by its known action to alter Ca^{2+} release from the sarcoplasmic reticulum (see Introduction) which in turn can indirectly affect Ca^{2+} channel kinetics. The lack of action on the locust neuronal Ca^{2+} currents may be due to the fact that cells were dialysed with a solution containing EGTA and any intracellular release of Ca^{2+} would be strongly buffered. Furthermore, no direct action of ryanodine on other neuronal Ca^{2+} currents has yet been shown (see e.g. Nishio et al, 1986), although a recent report has indicated that there exist Ca^{2+} release channels similar in structure to the ryanodine receptor in neuronal endoplasmic reticulum but which are gated by inositol 1,4,5-triphosphate (Mignery et.al., 1989).

Avermectin, at low concentrations (1nM) was not found to have an effect on the Ca^{2+} channel current. At higher concentrations avermectin caused an increase in conductance in the locust neurones and because of this it was not possible to resolve its action on the Ca^{2+} channels. The apparent similarity between the properties of avermectin-operated channels and Ca^{2+} channels (Hart et al, 1986, Lacey, 1987) might therefore be simply coincidental. The recent report that AVM may induce the appearence of non-selective cation channels in cell membranes (Martin and Pennington, 1989) may provide a better explaination for the effects of AVM in this preparation.

182

Table 4.2 Summary of properties of calcium channels in muscle and nerve preparations.

	Plutella muscle	Locust nerve	Vertebrate tissues		
			L	N	T
Activation Threshold	-	-40 to -30mV	-10mV	0mV	-50mV
Steady State Inactivation	-	sus=trans	poor	readily inactivating	
Inorganic Antagonists (Ca^{2+})	block	sus>trans	L,N>T		
Organic Antagonists	no effect	verapamil block / nitrendipine no effect	block	no effect	no effect
LEMS IgG	no effect	-	block	no effect	no effect
Ryanodine	prolongation	no effect	-	-	-
Pyrethroids	-	no effect	no effect	no effect	no effect
Avermectin	no effect	no effect	-	-	-

Summary of the properties of Ca^{2+} channels in insect muscle and nerve investigated in this thesis, together with properties of Ca^{2+} channels in vertebrate tissues for comparison. In the column for locust nerve any differential effects on the sustained component (sus) and the transient component (trans) are also shown. Data for vertebrate channels were obtained from the same sources used in Table 1.1.

183

To summarise this chapter (see also Table 4.2), the results of investigations into the physiological and pharmacological properties of insect neuronal Ca^{2+} channels are reported. Evidence was presented showing that Ca^{2+} channels are present in this preparation. Based on inactivation rate and preferential block by Cd^{2+}, there may be two types of channel present, one transient and the other sustained. These channel types differed from both the physiological (e.g activation and inactivation kinetics) and pharmacological (e.g. actions of Ca^{2+} antagonists and pyrethroids) properties of the L, N and T types of channel described in vertebrate neurones.

REFERENCES

ASHCROFT, F.M. (1981). Calcium action potentials in the skeletal muscle fibres of the stick insect Carausius morosus. J. Exp. Biol. 93: 257-267.

ASHCROFT, F.M. & STANFIELD, P.R. (1982a). Calcium and potassium currents in muscle fibres of an insect (Carausius morosus). J. Physiol. 323: 93-115.

ASHCROFT, F.M. & STANFIELD, P.R. (1982b). Calcium inactivation in skeletal muscle fibres of the stick insect, Carausius morosus. J. Physiol. 330: 349-372.

BARRETT, J.S., PEARSON, H.A. & W.-WRAY, D. (1988). Non-competitive antagonism of calcium by magnesium at the mouse neuromuscular junction in vitro. J. Physiol. 401: 91P.

BEAM, K.G. & KNUDSON, C.M. (1988). Effect of postnatal development on calcium currents and slow charge movement in mammalian skeletal muscle. J. Gen. Physiol. 91: 799-815.

BEAM, K. G., TANABE, T. & NUMA, S. (1989). Structure function and regulation of the skeletal muscle dihydropyridine receptor. Annals N. Y. Acad. Sci. 560: 127-137.

BEAN, B.P. (1984). Nitrendipine block of cardiac calcium
channels: High-affinity binding to the inactivated
state. Proc. Nat. Acad. Sci. USA. 81: 6388-6392.

BEAN, B.P. (1989). Neurotransmitter inhibition of neuronal
calcium currents by changes in channel voltage
dependence. Nature 340: 153-156.

BELTON, P. (1969). Innervation and neural excitation of
ventral muscle fibres of the larva of the waxmoth,
Galleria mellonella. J. Insect. Physiol. 15: 731-741.

BOKISCH, A.J. & WALKER, R.J. (1986). The action of
avermectin (MK936) on identified central neurones from
Helix and its interaction with acetylcholine and
gamma-aminobutyric acid (GABA) responses. Comp.
Biochem. Physiol. 84: 119-125.

BROWN, A.M., KUNZE, D.L. & YATANI, A. (1986). Dual effects
of dihydropyridines on whole cell and unitary calcium
currents in single ventricular cells of guinea-pig. J.
Physiol. 379 495-514.

BURGES, J. & W.-WRAY, D. (1989). Effect of the calcium-
channel agonist CGP 28392 on transmitter release at
mouse neuromuscular junctions. Ann. N.Y. Acad. Sci.
560: 297-300.

BYERLY, L. & LEUNG, H. (1988). Ionic currents of Drosophila

neurons in embryonic cultures. J. Neurosci. 8: 4379-4393.

CACHELIN, A.B., DEPEYER, J.E., KOKUBUN, S. & REUTER, H. (1983). Ca^{2+} channel modulation by 8-bromocyclic AMP in cultured heart cells. Nature 304: 462-464.

CARBONE, E. & LUX, H.D. (1984). A low voltage-activated, fully inactivating Ca channel in vertebrate sensory neurones. Nature 310: 501-502.

CARBONE, E. & LUX, H.D. (1987a). Kinetics and selectivity of a low-voltage-activated calcium current in chick and rat sensory neurones. J. Physiol 386: 547-570.

CARBONE, E. & LUX, H.D. (1987b). Single low-voltage-activated calcium channels in chick and rat sensory neurones. J. Physiol 386: 571-601.

CATTERALL, W.A., SEAGAR, M.J., TAKAHASHI, M. & NUNOKI, K. (1989). Molecular properties of dihydropyridine-sensitive calcium channels. An. N.Y. Acad. Sci. 560: 1-14.

CHAD, J.E. & ECKERT, R. (1986). An enzymatic mechanism for calcium current inactivation in dialysed Helix neurones. J. Physiol. 378: 31-51.

COCHRANE,D.G., ELDER,H.Y. & USHERWOOD, P.N.R.

(1972).Physiology and ultrastructure of phasic and tonic skeletal muscle fibres in the locust, Schistocerca gregaria. J. Cell Sci. 10: 419-441.

CONSTANTIN, L.L. (1975). Contractile activation in skeletal muscle. Prog. Biophys. Molec. Biol. 29: 197-224.

DEISZ, R.A. & LUX, H.D. (1988). γ-aminobutyric acid-induced depression of calcium current of chick neurones. Neurosci. Lett. 56: 205-210.

DEITMER, J.W. & RATHMAYER, W. (1976). Calcium action potentials in larval muscle fibres of the moth Ephestia kuhniella (lepidoptera). J. Comp. Physiol. 112: 123-132.

DEITMER, J.W. (1977). effects of cobalt and manganese on the calcium-action potentials in larval insect muscle fibres (Ephestia kuhniella). Comp. Biochem. Physiol. 58A: 1-4

DEITMER, J.W. (1977). Electrical properties of skeletal muscle fibres of the flour moth larve Ephestia kuhniella. J. Insect. Physiol. 23: 33-38.

DJAMGOZ, M.B.A. (1987). Insect muscle: Inracellular ion concentrations and mechanisms of resting potential generation. J. Insect Physiol. 33: 287-314.

DOCHERTY, R.J. (1988). Gadolinium selectively blocks a component of calcium current in rodent neuroblastoma x glioma hybrid (NG108-15) cells. J. Physiol. 398: 33-47.

DOCHERTY, R.J. & BROWN, D.A. (1986). Interaction of 1,4-dihydropyridines with somatic Ca currents in hippocampal CA1 neurones of the guinea pig in vitro. Neurosci. Lett. 70: 110-115.

DOCHERTY, R.J. & MCFADZEAN, I. (1989). Noradrenaline-induced inhibition of voltage-sensitive calcium currents in NG 108-15 hybrid cells. Eu. J. Neurosci. 1: 132-140.

DOLPHIN, A.C. (1987). Nucleotide binding proteins in signal transduction and disease. TINS 10: 53-57.

DOLPHIN, A.C., FORDA, S.R. & SCOTT, R.H. (1986). Calcium dependent currents in cultured rat dorsal root ganglion neurones are inhibited by an adenosine analogue. J. Physiol. 373: 47-61.

DOLPHIN, A.C. & SCOTT, R.H. (1987). Calcium channel currents and their inhibition by (-)-baclofen in rat sensory neurones: modulation by guanine nucleotides. J. Physiol. 394: 1-17.

DUCE, I.R. & SCOTT, R.H. (1985). Actions of dihydroavermectin B_{1a} on insect muscle. Br. J.

Pharmacol. 85: 395-401.

DUNLAP, K., HOLZ, G.G. & RANE, S.G. (1987). G proteins as regulators of ion channel function. TINS 6: 241-244.

ECKERT, R. & CHAD, J.E. (1984). Inactivation of calcium channels. Prog. Biophys. Molec. Biol. 44: 215-267.

ELLIS, S.B., WILLIAMS, M.E., WAYS, N.R., BRENNER, R., SHARP, A.H., LEUNG, A.T., CAMPBELL, K.P., McKENNA, E., KOCH, W.J., HUI, A., SCHWARTZ, A. & HARPOLD, M.M. (1987). Sequence and expression of mRNAs encoding the α_1 and α_2 subunits of a DHP-sensitive calcium channel. Science 241: 1661-1664.

FABIATO,A. & FABIATO,F. (1979). Calcium and cardiac excitation-contraction coupling. Ann. Rev. Physiol. 41: 473-484.

FEDULOVA, S.A, KOSTYUK, P.G., VESELOVSKY, N.S. (1981). Calcium channels in the somatic membrane of rat dorsal root ganglion neurones: effect of cAMP. Brain Res. 214: 210-214.

FEDULOVA, S.A, KOSTYUK, P.G., VESELOVSKY, N.S. (1985). Two types of calcium channels in the somatic membrane of new-born rat dorsal root ganglion neurones. J. Physiol. 359: 599-635.

FILL, M. & CORONADO, R. (1988). Ryanodine receptor channel of sarcoplasmic reticulum. TINS 11: 453-457.

FORSCHER,P. & OXFORD, G.S. (1985). Modulation of calcium channels by norepinephrine in internally dialyzed avian sensory neurons. J. Gen. Physiol. 85: 743-763.

FRITZ, L.C., WANG, C.C. & GORIO, A. (1979). Avermectin B_{1a} irreversibly blocks postsynaptic potentials at the locust neuromuscular junction by reducing muscle membrane resistance. Proc. Nat. Acad. Sci. USA. 76: 2062-2066.

FUKUDA, J. & KAWA, K. (1977). Permeation of manganese, cadmium, zinc and beryllium through calcium channels of an insect membrane. Science 196: 309-311.

GANITKEVITCH, V.Y., SHUBA, M.F. & SMIRNOV, S.V. (1987). Calcium-dependent inactivation of potential-dependent calcium inward current in an isolated guinea-pig smooth muscle cell. J. Physiol. 392: 431-449.

GOBLET, C. & MOUNIER, Y. (1981). Effects of ryanodine on the ionic currents and the calcium conductance in crab muscle fibres. J. Pharmacol. Exp. Ther. 219: 526-533.

GODFRAIND, T., MILLER, R. & WIBO, M. (1986). Calcium antagonism and calcium entry blockade. Pharm. Rev. 38: 321-415.

GONZALEZ-SERRATOS, H., VALLE-AGUILERA, R., LATHROP, D. A. & DEL CARMEN GARCIA, M. (1982). Slow inward calcium currents have no obvious role in excitation-contraction coupling. Nature 298: 292-294.

GOODMAN, C.S. & HEITLER, W.J. (1979). Electrical properties of insect neurones with spiking and non-spiking somata: normal, axotomised, and colchicine-treated neurones. J. exp. Biol. 83: 95-121.

GREENBERG, R.M., STRIESSNIG, J., KOZA, A., DEVAY, P., GLOSSMAN, H. & HALL, L.M. (1989). Native and detergent-solubilized membrane extracts from Drosophila heads contain binding sites for phenylalkylamine calcium channel blockers. Insect Biochem. 19: 309-322.

HAGIWARA, S. & BYERLY, L. (1981). Calcium channel. Ann. Rev. Neurosci. 4: 69-125.

HAMILL, O.P., MARTY, A., NEHER, E., SAKMANN, B. & SIGWORTH, F.J. (1981). Improved patch-clamp techniques for high-resolution current recording from cells and cell-free membrane patches. Pflugers Archiv 391: 85-100.

HART, R.J. (1986). Mode of action of agents used against arthropod parasites. in 'Chemotherapy of parasitic diseases. Eds. W.C. Campbell and R.S. Rew. Plenum publishing Corp.

HART, R.J., LACEY, G.R. & W.-WRAY, D. (1986). The postsynaptic actions of avermectin at locust thoracic ganglia. J. Physiol. 376: 43P.

HESCHELER, J., ROSENTHAL, W., TRAUTWEIN, W. & SCHULTZ, G. (1987). The GTP-binding protein Go, regulates neuronal calcium channels. Nature 325: 445-446.

HESS, P., LANSMAN, J.B. & TSIEN, R.W. (1984). Different modes of Ca channel gating behaviour favoured by dihydropyridine Ca agonists and antagonists. Nature 311: 538-544.

HESS, P., LANSMAN, J.B. & TSIEN, R.W. (1986). Calcium channel selectivity for divalent and monovalent cations. J. Gen. Physiol. 88: 293-319.

HESS, P. & TSIEN, R.W. (1984). Mechanism of ion permeation through calcium channels. Nature 309: 453-456.

HILLE, B. (1984). Ionic channels of excitable membranes. Sinauer Associates inc.

HODGKIN, A.L. & HOROWICZ, P. (1957). The differential action of hypertonic solutions on the twitch and action potential of a muscle fibre. J. Physiol. 136: 17P.

HOREJSI, J. & SMETANA, R. (1956). The isolation of gamma globulin from blood-serum by rivanol. Acta med. scand.

155: 65-70.

HOWARTH, J.V. (1958). The behaviour of frog muscle in hypertonic solutions. J. Physiol. 144: 167-175.

IMAGAWA, T., SMITH, J. S., CORONADO, R. & CAMPBELL, K. P. (1987). Purified ryanodine receptor from skeletal muscle sarcoplasmic reticulum is the Ca^{2+}-permeable pore of the calcium release channel. J. Biol. Chem. 262: 16636-16643.

ITO, K., TAKAKURA, S., SATO, K. & SUTKO, J. L. (1986). Ryanodine inhibits the release of calcium from intracellular stores in guinea pig aortic smooth muscle. Circ. Res. 58: 730-734.

JENDEN, D. J. & FAIRHURST, A. S. (1969). The pharmacology of ryanodine. Pharm. Rev. 21: 1-25.

KAMEYAMA, M., KAMEYAMA, A., NAKAYAMA, T. & KAIBARA, M. (1988). Tissue extract recovers cardiac calcium channels from 'run-down'. Pflugers Arch. 412: 328-330.

KASS, R.S. & SANGUINETTI, M.C. (1984). Calcium channel inactivation in the calf cardiac Purkinje fibre: evidence for voltage- and calcium-mediated mechanisms. J. Gen. Physiol. 84: 705-726.

KATZ, B. (1966). Nerve, muscle, and synapse. McGraw-Hill.

KIM, Y.I. & NEHER, E. (1988). IgG from patients with Lambert-Eaton syndrome blocks voltage-dependent calcium channels. Science 439: 405-408.

KNUDSON, C.M., JAY, S.D. & BEAM, K.G. (1986). Developmental increase in skeletal muscle slow calcium current. Biophys. J. 49: 13a.

KONGASMUT, S., LIPSCOMBE, D. & TSIEN, R.W. (1989). The N-type channel in frog sympathetic neurons and its role in α-adrenergic modulation of transmitter release. An. N.Y. Acad. Sci. 560: 312-333.

KONNERTH, A., LUX, H.D. & MORAD, M. (1987). Proton-induced transformation of calcium channel in chick dorsal root ganglion cells. J. Physiol. 386: 603-633.

KOSTYUK, P.G. (1980). Calcium ionic channels in electrically excitable membrane. Neuroscience 5: 945-959.

LACEY, G.R. (1987). Electrophysiological studies of postsynaptic ion channels in mouse, rat and locust: Cholinergic and GABA-ergic transmission. PhD thesis. University of London.

LAI, F. A., ERICKSON, H. P., ROUSSEAU, E., LIU, Q. & MEISSNER, G. (1988). Purification and reconstitution of the calcium release channel from skeletal muscle.

Nature 331: 315-319.

LANG, B., NEWSOM-DAVIS, J., PEERS, C., PRIOR, C. & W.-WRAY, D. (1987a). The effect of myasthenic syndrome antibody on presynaptic calcium channels in the mouse. J. Physiol. 390: 257-270.

LANG, B., NEWSOM-DAVIS, J., PEERS, C., & W.-WRAY, D. (1987b). Selective action of Lambert-Eaton myasthenic syndrome antibodies on Ca^{2+} channels in the neuroblastoma x glioma hybrid cell line NG 108 15. J. Physiol. 394: 43P.

LANG, B., NEWSOM-DAVIS, J. & W.-WRAY, D. (1988). The effect of Lambert-Eaton myasthenic syndrome antibody on slow action potentials in mouse cardiac ventricle. Proc. Roy. Soc. Lond. B 235: 103-110.

LANSMAN, J.B., HESS, P. & TSIEN, R.W. (1986). Blockade of calcium currents through single calcium channels by Cd^{2+}, Mg^{2+} and Ca^{2+}. J. Gen. Physiol. 88: 321-347.

LEE, K.S., MARBAN, E. & TSIEN, R.W. (1985). Inactivation of calcium channels in mammalian heart cells: joint dependence on membrane potential and intracellular calcium. J. Physiol. 364: 395-411.

LEE, K.S. & TSIEN, R.W. (1983). Mechanism of calcium channel blockade by verapamil, D-600, diltiazem and

nitrendipine in single dialysed heart cells. Nature 302: 790-794.

LEES, G., PEARSON, H.A. & W.-WRAY, D. (1988). Effect of calcium channel antagonists and ryanodine on action potentials in insect muscle fibres. Br. J. Pharmacol. 95: 744P.

LEES, G., PEARSON, H.A. & W.-WRAY, D. (1989). Calcium channels in isolated locust thoracic ganglia. J. Physiol. 410: 13P.

LIPSCOMBE, D., KONGASMUT, S. & TSIEN, R.W. (1989). α-Adrenergic inhibition of sympathetic neurotransmitter release mediated by modulation of N-type calcium-channel gating. Nature 340: 639-642.

LUNEVSKY, V.Z., ZHERELOVA, O.M., VOSTRIKOV, I.Y. & BERESTOVSKY, G.N. (1983). Excitation of Characeae cell membranes as a result of activation of calcium and chloride channels. J. Memb. Biol. 72: 43-58.

MCCLESKEY, E.W., FOX, A.D., FELDMAN, D.H., CRUZ, L., OLIVERA, B.M., TSIEN, R.W. & YOSHIKAMI, D. (1987). w-Conotoxin: Direct and persistent block of specific types of calcium channels in neurons but not in muscle. Proc. Nat. Acad. Sci. 84: 4327-4331.

MCFADZEAN, I. & DOCHERTY, R.J. (1989). Noradrenaline- and

enkephalin-induced inhibition of voltage-sensitive calcium currents in NG 108-15 hybrid cells. Eu. J. Neurosci. 1: 141-147.

MARCHETTI, C., CARBONE, E. & LUX, H.D. (1986). Effects of dopamine and noradrenaline on calcium channels of cultured sensory and sympathetic neurones of chick. Pflugers Arch. 406: 104-111.

MARTIN, R.J. & PENNINGTON, A.J. (1989). Ivermectin induces cation channels in isolated patches of Ascaris muscle. J. Physiol. 410: 83P.

MEISSNER,G. (1984). Adenine nucleotide stimulation of Ca^{2+}-induced release Ca^{2+} release in sarcoplasmic reticulum. J.Biol.Chem. 259: 2365-2374.

MEISSNER, G., DARLING, E., & EVELETH,J., (1986). Kinetics of rapid Ca^{2+} release by sarcoplasmic reticulum. Effects of Ca^{2+}, Mg^{2+} and adenine nucleotides. Biochemistry. 25: 236-244.

MELLIN, T.N, BUSCH,R.D. & WANG, C.C. (1983). Postsynaptic inhibition of invertebrate neuromuscular transmission by avermectin B_{1a}. Neuropharmacol. 22: 89-96.

MIGNERY, G.A., SUDHOF, T.C., TAKEI, K. & DE CAMILLI, P. (1989). Putative receptor for inositol 1,4,5-trisphosphate similar to ryanodine receptor. Nature

342: 192-195.

MIKAMI, A., IMOTO, K., TANABE, T., NIIDOME, T., MORI, Y., TAKESHIMA, H., NARUMIYA, S. & NUMA, S. (1989). Primary structure and functional expression of the cardiac dihydropyridine-sensitive calcium channel. Nature 340: 230-233.

MITCHELL, M.R., POWELL, T., TERRAR, D.A. & TWIST, V.W. (1984a). Ryanodine prolongs Ca-currents while supressing contraction in rat ventricular muscle cells. Brit. J. Pharmacol. 81: 013-015.

MITCHELL, M.R., POWELL, T., TERRAR, D.A. & TWIST, V.W. (1984b). The effects of ryanodine, EGTA and low-sodium on action potentials in rat and guinea-pig ventricular myocytes: evidence for two inward currents during the plateau. Brit. J. Pharmacol. 81: 543-550.

MIYAMOTO, T., OHIZUMI, Y., WASHIO, H. & YASUMOTO, Y. (1984). Potent excitatory effect of maitotoxin on Ca channels in the insect skeletal muscle. Pflugers Arch. 400: 439-441.

MOTAIS, R. & COUSIN, J.L. (1976). Inhibitory effect of ethacrynic acid on chloride permeability. Am. J. Physiol. 231: 1485-1489.

NARAHASHI, T. (1986). Mechanisms of action of pyrethroids on

sodium and calcium channel gating. in 'Neuropharmacology and pesticide action' Eds. Ford, Lunt, Reay and Usherwood. Ellis Horwood and VCH.

NARAHASHI, T., TSUNOO, A. & YOSHII, M. (1987). Characterisation of two types of calcium channels in mouse neuroblastoma cells. J. Physiol. 383: 231-249.

NISHIO, M., KIGOSHI, S. & MURAMATSU, I. (1986). Ryanodine has no effect on the Ca current in single ventricular cells of guinea-pig. Eu. J. Pharmacol. 124: 353-356.

NOWYCKY, M.C., FOX, A.P. & TSIEN, R.W. (1985a). Three types of neuronal calcium channel with different calcium agonist sensitivity. Nature 316: 440-443.

NOWYCKY, M.C., FOX, A.P. & TSIEN, R.W. (1985b). Long-opening mode of gating of neuronal calcium channels and its promotion by the dihydropyridine calcium agonist BAY K 8644. Proc. Nat. Acad. Sci. USA. 82: 2178-2182.

ORCHARD, I. (1976). Calcium dependent action potentials in a peripheral neurosecretory cell of the stick insect. J. Comp. Physiol. 112: 95-102.

OSTERRIEDER, W., BRUM, G., HESCHELER, J., FLOCKERZI, V. & HOFMANN, F. (1982). Injection of subunits of cyclic AMP-dependent protein kinase into cardiac myocytes modulates'Ca^{2+} current. Nature 298: 576-578.

PAUL, S.M., SKOLNICK, P. & ZATZ,M. (1980). Avermectin B_{1a}: an irreversible activator of the γ-amino butyric acid-benzodiazepine-chloride ionophore receptor complex. Biochem. Biophys. Res. Commun. 96: 632-638.

PAURON, D., QAR, J., BARHANIN, J., FOURNIER, D., CUNAY, A., PRALAVORIO, M., BERGE, J-B. & LAZDUNSKI, M. (1987).Identification and affinity labelling of very high affinity binding sites for the phenylalkylamine series of Ca^{2+} channel blockers in the Drosophila nervous system. Biochem. 26: 6311-6315.

PEARSON, H.A, LEES, G. & W.-WRAY, D. (1990). Lack of effect of avermectin on calcium channels in muscle fibres from moth larvae. Brit. J. Pharmacol. 99: 250P.

PEARSON, H.A., NEWSOM-DAVIS, J., LEES, G., & W.-WRAY, D. (1989). Lack of action of Lambert-Eaton myasthenic syndrome antibody on calcium channels in insect muscle. An. N.Y. Acad. Sci. 560: 291-293.

PEERS, C., LANG, B., NEWSOM-DAVIS, J., & W.-WRAY, D. (1990). Selective action of myasthenic syndrome antibodies on calcium channels in a rodent neuroblastoma x glioma cell line. J. Physiol. 421: 293-308.

PELZER, S., BARHANIN, J., PAURON, D., TRAUTWEIN, W., LAZDUNSKI, M. & PELZER, D. (1989a). Diversity and novel

pharmacological properties of Ca^{2+} channels in Drosophila brain membranes. EMBO J. 8: 2365-2371.

PELZER, D., GRANT, G.O., CAVALIE, A., PELZER, S., SIEBER, M., HOFFMAN, F. & TRAUTWEIN, W. (1989b). Calcium channels reconstituted from the skeletal muscle dihydropyridine receptor protein complex and its al peptide subunit in lipid bilayers. An. N.Y. Acad. Sci. 560: 138-154.

PEREZ-REYES, E., KIM, H.S., LACERDA, A.E., HORNE, W., WEI, X., RAMPE, D., CAMPBELL, K.P., BROWN, A.M. & BIRNBAUMER, L. (1989). Induction of calcium currents by the expression of the α_1-subunit of the dihydropyridine receptor from skeletal muscle. Nature 340: 233-236.

PICHON, Y. & ASHCROFT, F.M. (1984). Nerve and muscle: electrical activity. in; 'Comprehensive insect physiology biochemistry and pharmacology'. Eds G.A. Kerkut and L.I. Gilbert. Pergamon press.

PIETROBON, D., PROD'HOM, B. & HESS, P. (1988). Conformational changes associated with ion permeation in L-type calcium channels. Nature 333: 373-376.

PITMAN, R.M. (1979). Intracellular citrate or externaly applied tetraethylammonium ions produce calcium-dependent action potentials in an insect motorneurone cell body. J. Physiol. 291: 327-337.

PONG, S.S. & WANG, C.C. (1980). The specificity of high affinity binding of avermectin B_{1a} to mammalian brain. Neuropharmacology 19: 311-317.

PONG, S.S., WANG, C.C. & FRITZ, L.C. (1980). Studies on the mechanism of action of avermectin B_{1a}: stimulation of release of Y-aminobutyric acid from brain synaptosomes. J. Neurochem. 34: 351-358.

PROD'HOM, B., PIETROBON, D. & HESS, P. (1987). Direct measurement of proton transfer rates to a group controlling the dihydropyridine-sensitive calcium channel. Nature 329: 243-246.

REUTER, H. (1983). Calcium channel modulation by neurotransmitters, enzymes and drugs. Nature 301: 569-574.

REUTER, H. (1987). Calcium channel modulation by β-adrenergic neurotransmitters in the heart. Experientia 43: 1173-1175.

RHEUBEN, M.R. (1972). The resting potential of moth muscle fibre. J. Physiol. 225: 529-554.

ROSENBERG, R.L., HESS, P., REEVES, J.P., SMILOWITZ, H. & TSIEN, R.W. (1986). Calcium channels in planar lipid bilayers: Insights into mechanisms of ion permeation

and gating. Science 231: 1564-1566.

SALKOFF, L. B. & WYMAN, R. J. (1983). Ion currents in drosophila flight muscles. J. Physiol. 337: 687-709.

SCHNEIDER, M.F. & CHANDLER, W.K. (1973). Voltage dependent charge movement in skeletal muscle: a possible step in excitation-contraction coupling. Nature 242: 244-246.

SCHWARTZ,L.M., MCCLESKEY, E.W. & ALMERS,W. (1985). Dihydropyridine receptors in muscle are voltage dependent but most are not functional calcium channels. Nature 314: 747-751.

SCOTT, R.H. & DOLPHIN, A.C. (1986). Regulation of calcium currents by a GTP analogue: potentiation of (-)-baclofen mediated inhibition. Neurosci. Letts. 56: 59-64.

SCOTT, R.H. & DOLPHIN, A.C. (1987). Activation of a G protein promotes agonist responses to calcium channel ligands. Nature 330: 760-762.

SHEPHEARD, P. (1973) Musculature and innervation of the neck of the dessert locust, Schistocerca gregaria. J. Morphol. 139, 439-464.

SMITH, J. S., CORONADO, R. & MEISSNER, G. (1986a). Single channel measurements of the calcium release channel

from skeletal muscle sarcoplasmic reticulum. J. Gen. Physiol. 88: 573-588.

SMITH, J. S., CORONADO, R. & MEISSNER, G. (1986b). Single-channel calcium and barium currents of large and small conductance from sarcoplasmic reticulum. Biophys. J. 50: 921-928.

STANFIELD, P. R. (1983). Tetraethylammonium ions and the potassium permeability of excitable cells. Rev. Physiol. Biochem. Pharmacol. 97: 1-67.

STRIESSNIG,J., GOLL, A., MOOSBURGER, K. & GLOSSMAN, H. (1986). Purified calcium channels have three allosterically coupled drug receptors. FEBS Lett. 197 204-210.

SUTKO, J.L., WILLERSON, J.T., TEMPLETON, G.H., JONES, L.R. & BESCH, JR., H.R. (1979). Ryanodine: Its alterations of cat papillary muscle contractile state and responsiveness to inotropic interventions and a suggested mechanism of action. J. Pharacol. exp. Ther. 209: 37-47.

SUTKO, J. L., ITO, K. & KENYON, J. L. (1985). Ryanodine: a modifier of sarcoplasmic reticulum calcium release in striated muscle. Fed. Proc. 44: 2984-2988.

TAKESHIMA,.H., NISHIMURA, S., MATSUMOTO, T., ISHIDA, H., KANGAWA, K., MINAMINO, N., MATSUO, H., UEDA, M.,

COBLEY, U. T., HANAKOA, M., HIROSE, T. & NUMA, S. (1989). Primary structure and expression from complementary DNA of skeletal muscle ryanodine receptor. Nature 339: 439-445.

TANABE, T., BEAM, K.G., POWELL, J.A. & NUMA, S. (1988). Restoration of excitation-contraction coupling and slow calcium current in dysgenic muscle by dihydropyridine receptor cDNA. Nature 336: 134-139.

TANABE, T., TAKESHIMA, H., MIKAMI, A., FLOCKERZI, V., TAKAHASHI, H., KANGAWA, K., KOJIMA, M., MATSUO, H., HIROSE, T. & NUMA, S. (1987). Primary structure of the receptor for calcium channel blockers from skeletal muscle. Nature 328: 313-318.

TRAUTWEIN, W. (1985). Calcium channels in the membrane of the cardiac myocyte: Physiological and pharmacological control. Triangle 24: 101-114.

TRAUTWEIN, W., CAVALIE, A., FLOCKERZEI, V., HOFMANN, F. & PELZER, D. (1987). Modulation of calcium channel function by phosphorylation in guinea pig ventricular cells and phospholipid bilayer membranes. Circ. Res. 61: I.17-I.23.

TSIEN, R.W. (1986). in Neuromodulation. pp 206-242 Eds. L.K. Kaczmarek and I.B. Levitan. Oxford University Press.

TSIEN, R.W., LIPSCOMBE, D., MADISON, D.V., BLEY, K.R. & FOX, A.P. (1988). Multiple types of neuronal calcium channel and their selective modulation. TINS 11: 431-438.

USHERWOOD, P.N.R. (1962). The action of the alkaloid ryanodine on insect skeletal muscle. Comp. Biochem. Physiol. 6: 181-199.

USHERWOOD, P.N.R. & CULL-CANDY, S.G. (1975) Pharmacology of somatic nerve-muscle synapses. In: Insect Muscle (P.N.R. Usherwood, ed.), Academic Press.

USHERWOOD, P.N.R. & GRUNDFEST, H. (1965) Peripheral inhibition in skeletal muscle of insects. J. Neurophysiol. 28, 497-518.

VILVEN, J. & CORONADO, R. (1988). Opening of dihydropyridine calcium channels in skeletal muscle membranes by inositol triphosphate. Nature 336: 587-589.

WANGENKNECHT, T., GRASSUCCI, R., FRANK, J., SAITO, A., INUI, M. & FLEISCHER, S. (1989). Three-dimensional architecture of the calcium channel/foot structure of sarcoplasmic reticulum. Nature 338: 167-170.

WANKE, E., SARDINI, A. & FERRONI, A. (1989). L and N Ca^{2+} channels coupled to muscarinic receptors in rat sensory neurons. An. N.Y. Acad. Sci. 560: 398-400.

WASHIO, H. (1972). The ionic requirements for the initiation of action potentials in insect muscle fibres. J. Gen. Physiol. 59: 121-134.

WEEVERS, R. DE G. (1966). A lepidopteran saline: effects of inorganic cation concentrations on sensory, reflex and motor responses in a herbivorous insect. J. Exp. Biol. 44: 163-175.

W.-WRAY, D., NORMAN, R.I. & HESS, P. (Eds.) (1989). Calcium channels: structure and function. Ann. N.Y. Acad. Sci. volume 560.

YAMAMOTO, D., FUKAMI, J-I. & WASHIO, H. (1981). Voltage clamp studies on insect skeletal muscle. I. The inward current. J. Exp Biol. 92: 1-12.

YAMAMOTO, D. & WASHIO, H. (1981). Voltage clamp studies on insect skeletal muscle. II. The outward currents. J. Exp. Biol. 92: 13-22.

YAMAMOTO, D. & WASHIO,H. (1980). Ionic selectivity of the calcium channels in insect larval muscle fibres. J. Exp. Biol. 85: 333-335.

YOSHIKAMI, D., BAGABALDO, Z. & OLIVERA, B.M. (1989). The inhibitory effects of omega-conotoxins in Ca channels and synapses. An. N.Y. Acad. Sci. 560: 230-248.